DESIGN AND SYNTHESIS OF 2,4,9-TRITHIAADAMANTANE DERIVATIVES AS ANTI-INFLUENZA A DRUG CANDIDATES

A Dissertation

Presented to

The Graduate Faculty of The University of Akron

In Partial Fulfillment

of the Requirements for the Degree

Doctor of Philosophy

Tracy C. Olin

May, 2014

ProQuest LLC.
789 East Eisenhower Parkway
P.O. Box 1346
Ann Arbor, MI 48106 - 1346

DESIGN AND SYNTHESIS OF 2,4,9-TRITHIAADAMANTANE DERIVATIVES AS ANTI-INFLUENZA A DRUG CANDIDATES

Tracy C. Olin

Dissertation

Approved:	Accepted:
_____	_____
Advisor Dr. David A. Modarelli	Department Chair Dr. Michael Taschner
_____	_____
Advisor Dr. Christopher J. Ziegler	Dean of the College Dr. Chand Midha
_____	_____
Committee Member Dr. Wiley J. Youngs	Dean of the Graduate School Dr. George R. Newkome
_____	_____
Committee Member Dr. Michael J. Taschner	Date
_____	
Committee Member Dr. Richard L. Londraville	

ABSTRACT

The objective of this dissertation is to describe the design, synthesis, and characterization of 7-substituted-2,4,9-trithiaadamantane (tripod) derivatives as new anti-influenza drug candidates, specifically blockers for the M2 ion channel of the influenza A virus. Of the four current FDA-approved anti-influenza chemotherapeutics, only two function by blocking the M2 ion channel of the virus. However, due to the developed mutations of certain amino acid residues lining the interior pore of the ion channel, the two drugs, amantadine and rimantadine, now have little to no effect on the most common virus strains. The recently elucidated structure of the M2 proton channel has provided structural insight and new knowledge leading to the development of these novel drug candidates that may have an enhanced affinity for mutated ion channels and also a shorter biodistribution time, decreasing host toxicity. The drugs described within this work have incorporated sulfur atoms into the base of the molecule accommodating the larger diameter of the mutated pore and allowing an ease of biodegradation.

Chapter 1 of this work gives an introduction to the influenza virus, the ion channel structure and function, as well as new drug developments and previous work with trithiaadamantanes. Also discussed will be some current antiviral drugs used to treat influenza, and possible drug candidates currently being developed by other research groups. The rationale for drug design based on specific mutations believed to occur in

the most abundant influenza strains will be looked at in context of designing new drug candidates.

Chapter 2 of this dissertation describes the multi-step syntheses of the novel 2,4,9-trithiaadamantan-7-amine and 1-(2,4,9-trithiaadamantan-7-yl)ethan-1-amine derivatives as possible influenza A ion channel blockers. Also discussed are attempted synthetic routes to these molecules.

The starting material to the synthesized drug candidates is not commercially available and is made via a six-step route, which yields a mere 10-20% at best, and requires several purification steps. Chapter 3 will focus on several new routes that were explored for the improved synthesis of this starting material, methyl-2,4,9-trithiaadamantan-7- carboxylate, as well as the synthesis of other molecules that could serve as enhanced starting compounds.

DEDICATION

This dissertation is dedicated to my loving family. Without their support and encouragement I would have given up years ago. To my mother who has taught me countless lessons in life, but most importantly to never give up; to push through no matter how tough the situation, and to always look at the positives in this crazy "circle of life." To my father, for providing me with a stable foundation, for putting up with and trying to understand all of my craziness, and for teaching me the value of an education. Words cannot express my gratitude for all you both have done to help me better my life. I look forward to the day I can do the same for my children. I hope I have made you both proud!

To my grandparents, who are the backbone of our family and have helped mold me into the person I am today. You have taught me the meaning of hard work, and have been my role models since I was a child. I aspire to provide for my family as you have so graciously done for yours. Even though you don't quite understand what career I am pursuing and why I needed so many years of "dog-gone" college, you both have stood behind me and given me endless support and inspiration, and for that I am forever thankful.

Most importantly, I want to dedicate this work to my daughters- the loves of my life. To Jaydah, for being the inspiration that began this journey nearly 11 years ago. I

want to thank you for being my little partner throughout my college years, for understanding when I was tired, busy, or any less of a mother than I should have been. For attending your first college lectures with me at the ripe age of 3, and for all the "good luck on your test today mommy!" well-wishings you have given me. I couldn't have done it without you. To Josie, my little sweetheart, who keeps me smiling everyday and gives me the strength and inspiration to finish this work. Forgive me for spending the first year of your life finalizing my work and writing this dissertation. I know it will all be worth it in the end. I love you both so very much and hope that all of this work makes your lives better in so many ways.

To the other love of my life, Jesse Allen, who has been nothing but supportive and encouraging throughout my years in graduate school. Thank you for allowing me to catch up on much needed sleep after many long days in the lab and all-night writing sessions. To Harry Wilson, who has been my greatest ally throughout my entire college career. Without all of your help and support with Jaydah, I would have never had the ability to put in the long hours necessary to accomplish my goals. I am so grateful you are a huge part of our lives! To my dear friends, William Reed and Elizabeth Zell, for all of their insight, support, laughter and love. We began this journey together, and it is truly unfortunate that Bill will not be here when it ends. You are missed often big guy, may you rest peacefully. Finally, to my sister Sharon, my niece Alexis (GO BUCKS!!), my nephews Braydon, Miles and Levi, as well as the rest of my family who has stood strong by my side throughout both my undergraduate and graduate school career. I love you all so much! FINALLY… the light at the end of the tunnel is shining bright!

ACKNOWLEDGEMENTS

First, I would like to thank my advisors, Dr. David Modarelli and Dr. Christopher Ziegler. Without their encouragement, guidance and willingness to help the completion of this graduate project, it would not have been possible. I am truly grateful to have the both of them in my corner. I would also like to thank Dr. Jun Hu for his great ideas and creativity that helped to begin this project.

I would also like to thank my past lab mates who have helped mold me into the chemist I am today. Dr. Jacob Weingart, for spending many hours in the lab teaching me how to master the tripod reaction! You were truly an awesome mentor and I learned so much from working with you. Thank you to Dr. Tejal Deodar and Caroline Davis, for being great friends throughout some frustrating times in the lab! We were all on this crazy ride together and I couldn't have asked for better ladies to go through graduate school along side. A special thank you to the undergraduate students I had the privilege to mentor: Mr. Christopher Kornuc and Mr. Christopher Bull. I learned the most through teaching the both of you, and in return you gave me many laughs and great memories! I appreciate all the long hours you both accompanied me in the lab, and just talking about chemistry. Thank you to Jim Engle for solving the crystal structures for my molecules. Thanks to all the other wonderful people that I have had the honor to work beside, learn from, and teach. Graduate school has truly been and awesome experience!

I would also like to give a special thank you to the Chemistry Department and my dissertation committee members: Dr. Christopher Ziegler, Dr. David Modarelli, Dr. Michael Taschner, Dr. Wiley Youngs, and Dr. Richard Londraville for giving me valuable input on this work and taking the time to attend my defense. Also, thanks to Jean Garcia and Nancy Homa in the chemistry office, for being such exceptional resources over the years. Lastly, I would like to give a special thank you to Dr. Friedrich Koknat and Dr. John A. Jackson for being such inspirational chemistry professors. Without the foundation they provided during my undergraduate career, I would have never been able to build such a strong love and understanding of the subject.

TABLE OF CONTENTS

Page

LIST OF TABLES xii

LIST OF FIGURES xiii

LIST OF SCHEMES xv

LIST OF ABBREVIATIONS xvii

CHAPTER

I. INTRODUCTION 1

1.1 The Influenza Virus 1

1.2 Current Therapeutics 2

1.3 Influenza A M2 Ion Channel 9

1.4 Amino Acid Mutations in the M2 Protein 15

1.5 Current M2 Inhibitor Candidates 17

1.6 Previous Studies Involving Trithiaadamantane 27

II. SYNTHESIS OF 2,4,9-TRITHIAADAMANTANE DERIVATIVES 32

2.1 Introduction 32

2.2 Experimental Section 37

2.2.1 Materials and Methods 37

2.2.2 Derivative Syntheses 38

2.2.2.1 Synthesis of 2,4,9-trithiaadamantan-7-amine (**18**) 39

2.2.2.1.1 Formation of the acyl hydrazide (**25**) 39

2.2.2.1.2 Formation of the acyl azide (**26**) 40

2.2.2.2 Attempted syntheses of 1-(2,4,9-trithiaadamantan-7-yl)ethan-1-amine (**19**) 42

2.2.2.2.1 Formation of N-diphenylphosphinoylimine (**31**) 44

2.2.2.2.2 Formation of N-sulfinylimine (**32**) 45

2.3 Results and Discussion 47

2.3.1 2,4,9-trithiaadamantan-7-amine (**18**) syntheses 49

2.3.1.1 Hydrazine dichloride method 50

2.3.1.2 Sodium azide method 52

2.3.2 1-(2,4,9-trithiaadamantan-7-yl)ethan-1-amine (**19**) syntheses 57

2.3.2.1 N-diphenylphosphinoylimine reaction 59

2.3.2.2 N-sulfinylimine reaction 61

2.4 Conclusions and Future Work 64

III. NEW SYNTHETIC ROUTES TO METHYL-2,4,9-TRITHIAADAMANTANE-7-CARBOXYLATE AND OTHER ALTERNATIVE SYNTHESES 66

3.1 Introduction 66

3.2 Experimental Section 77

3.2.1 Materials and Methods 77

3.2.2 Syntheses 78

3.2.2.1 Grubbs catalyst reaction to give $TpCO_2Me$ (**17**) 78

3.2.2.2 Formation of methyl-2,4,9-trithiaadamantane-7 carboxylate (**51**) 79

3.2.2.3 Acetal protection of triallyl methylacetate (**23**) 81

3.2.2.3.1 Methanol as a solvent during ozonolysis 81

3.2.2.3.2 Ethylene glycol protection reaction 82

3.2.2.4 Attempted triallyl carbinol (**45**) reaction 84

3.2.2.5 Ketone attempt using (trimethylsilyl)methyllithium 85

3.3 Results and Discussion 86

3.3.1 Synthesis of $TpCO_2Me$ via Grubbs intermediate reaction 86

3.3.2 Methyl-2,4,9-trioxaadamantane-7-carboxylate (**51**) 87

3.3.3 Acetal protected triallyl methylacetate (**23**) 93

3.3.3.1 Methoxy protection 94

3.3.3.2 Ethylene glycol protection 96

3.3.4 Triallyl carbinol (**45**) to tripod reaction 99

3.3.5 Attempt towards 2,4,9-trithiaadamantane-methylketone 100

3.4 Conclusions and Future Work 102

REFERENCES 105

APPENDICES 111

APPENDIX A: ^{1}H and ^{13}C NMR SPECTRA OF SELECTED COMPOUNDS 112

APPENDIX B: IR SPECTRA OF SELECTED COMPOUNDS 131

APPENDIX C: COPYRIGHT PERMISSIONS 140

LIST OF TABLES

Table Page

1.1 FDA-approved drugs for the treatment of the influenza A virus 3

1.2 Inhibitory results of various 1-adamantyl-pyrrolidines and piperidines 19

1.3 Drug activity of 1,2-annulated piperidines and pyrrolidines 26

1.4 Heteroatom substituted derivatives of spiro-piperidine **11** 30

2.1 Crystal data and structural refinement parameters for 2,4,9-trithiaadamantane-7-amine (**17**) 56

2.2 Selected bond lengths and angles of 2,4,9-trithiaadamantane-7-amine (**17**) 57

3.1 Crystal data and structural refinement parameters for methyl-2,4,9-trioxaadamantane-7-carboxylate (**51**) 92

3.2 Selected bond lengths and angles of methyl-2,4,9-trioxaadamantane-7-carboxylate (**51**) 93

LIST OF FIGURES

Figures Page

1.1 Features of influenza A virion structure 2

1.2 The M2 proton channel crystal structure 10

1.3 The omit map of Amantadine bound within the M2 lumen....12

1.4 Ribbon representation of the Rimantadine-bound M2 protein as determined by solution NMR....13

1.5 Positions of known amino acid mutations of the M2 protein that transmit resistance to the adamantane drugs....15

1.6 Structures of new M2 channel blocker candidates developed by Stamatious *et al*..18

1.7 Structures of the spiro-piperidines and spiran-amine M2 blocker candidates 21

1.8 Structures of 1,2-annulated adamantane piperidines **15** and **16**....25

1.9 The 2,4,9-trithiaadamantane molecule with a random substitution at the 7-position....27

2.1 Examples of 7-substituted trithiaadamantane derivatives....33

2.2 Competing mechanistic representations of the Curtius rearrangement 36

2.3 The FTIR spectra of the Curtius rearrangement of $TpCON_3$ (**28**) to TpNCO (**33**)..54

2.4 High resolution mass spectrometry of 2,4,9-trithiaadamantane-7-amine (**18**)....55

2.5 The X-ray crystal structure of 2,4,9-trithiaadamantane-7-amine (**18**) with 35% thermal ellipsoids....55

2.6 The ^{1}H NMR spectrum of the crude mixture of tripod with *P,P*-diphenylphosphinic amide and PTSA after 48 h 61

2.7 High resolution mass spectrometry of the sulfinylimine intermediate **32** 63

3.1 Formation of the trimer by-product, trithiane, from formaldehyde and hydrogen sulfide 67

3.2 Structures of thiaadamantanes with oxygen atom substitutions 69

3.3 A proposed mechanism of cyclization of the trialdehyde to form the oxygenated ring of **51** 89

3.4 The ^{1}H NMR spectra of **A**, methyl-2,4,9-trithiaadamantane-7-carboxylate (**17**) and **B**, methyl-2,4,9-trioxaadamantane-7-carboxylate (51) 90

3.5 High resolution mass spectrometry of methyl-2,4,9-trioxaadamantane-7-carboxylate 51) 91

3.6 The X-ray crystal structure of -2,4,9-trioxaadamantane-7-carboxylate (**51**) with 35% thermal ellipsoids 91

3.7 The ^{1}H NMR spectrum of the formation of acetal **52** 95

3.8 Proposed structure of the acetal achieved from **23** when performing ozonolysis in methanol 95

3.9 The FTIR spectrum of the reaction of triallyl methylacetate with ethylene glycol .. 98

3.10 The ^{1}H NMR spectrum of the reaction of triallyl methylacetate with ethylene glycol 98

3.11 The ^{1}H NMR spectrum of the reaction of **17** with (trimethylsilyl)methyllithium 102

LIST OF SCHEMES

Scheme Page

1.1 Enzymatic mechanism of influenza A sialidase 4

1.2 Original synthesis of amantadine (**3**) 6

1.3 Alternative synthesis of amantadine (**3**) 7

1.4 Original synthesis of rimantadine (**4**) 7

1.5 A lower temperature and pressure synthesis of rimantadine (**4**) 8

1.6 A versatile preparation of rimantadine developed by Liu 9

1.7 Synthesis of 2-(1-adamantyl0pyrrolidine (**5**) 20

1.8 Synthesis of the spiro-piperidines **10** and **11** 22

1.9 Synthetic routes to form spiro[5,5]undecan-3-amine (**12**) 24

1.10 Lindgren's synthesis of ethyl-2,4,9-trithiaadamantane-7-carboxylate 28

1.11 Synthesis of methyl-2,4,9-trithiaadamantane-7-carboxylate, $TpCO_2Me$ (**17**) 29

2.1 Various routes to 2,4,9-trithiaadamantane-7-amine (**18**) and 1-(2,4,9-trithiaadamantan-7-yl)ethan-1-amine (**19**) 35

2.2 Synthesis of methyl-2,4,9-trithiaadamantane-7-carboxylate 48

2.3 First attempt towards 2,4,9-trithiaadamantane-7-amine (**18**) 51

2.4 The synthesis of 2,4,9-trithiaadamantane-7-amine (**18**) 53

2.5 The synthesis of 2,4,9-trithiaadamantane-7-aldehyde (**30**) 58

2.6 First attempt at 1-(2,4,9-trithiaadamantan-7-yl)ethan-1-amine (**19**) via an N-diphenylphosphinoylimine 60

2.7 Second attempt at 1-(2,4,9-trithiaadamantan-7-yl)ethan-1-amine (**19**) via an N-sulfinylimine 62

3.1 Original synthesis of tripod (**17**) 67

3.2 Ring closing metathesis of triallyl methylacetate using a Grubbs 1st generation catalyst 68

3.3 Synthesis of a protected intermediate (**37** or **38**) followed by thionation to afford tripod (**17**) 70

3.4 The acetalization of cyclohexene as proposed by Claus and Schrieber 71

3.5 Reaction of the dealkylation of ethers using trichloro(methyl)silane and sodium iodide 72

3.6 Addition of hydrogen sulfide gas and chlorotrimethylsilane to an aldehyde 73

3.7 The synthesis of 7-hydroxy-2,4,9-trithiaadamantane (**46**) by way of triallyl carbinol (**45**) 74

3.8 Various routes to synthesize 18 and 19 from the hydroxyl-tripod (**46**) starting material 75

3.9 Direct transformation of an ester to a methyl ketone using $TMSCH_2Li$, as proposed by Evans and Morken 76

3.10 Reaction of a Grubbs catalyst (**50**) with **23** to give the dimer **36** and ultimately the tripod (**17**) 87

3.11 The synthesis of methyl-2,4,9-trioxaadamantan-7-carboxylate (**51**) 88

3.12 Generic reaction scheme showing acetal formation followed by thionation and cyclization 94

3.13 First attempt at reaction of an acetal with hydrogen sulfide gas and a silane to give **17** 95

3.14 Second reaction using an acetal intermediate (**38**) to form tripod (**17**) 97

3.15 Attempted synthesis of 7-hydroxy-2,4,9-trithiaadamantane (**46**) 99

3.16 Attempted synthesis of tripod methyl ketone (**49**) 101

LIST OF ABBREVIATIONS

AcOH	Acetic acid
ATR	Attenuated reflectance
^{13}C NMR	Carbon nuclear magnetic resonance
DIBAL	Diisobutylaluminium hydride
DMF	Dimethylformamide
DMSO	Dimethyl sulfoxide
EC_{50}	Half maximal effective concentration
EtOAc	Ethyl acetate
EtOH	Ethanol
FDA	U.S. Food and Drug Administration
FTIR	Fourier transform infrared spectroscopy
HMPA	Hexamethylphosphoramide
^{1}H NMR	Proton nuclear magnetic resonance
IC_{50}	Half maximal inhibitory concentration
LAH	Lithium aluminum hydride
LDA	Lithium diisopropylamide
MeOH	Methanol
NIH	National Institutes of Health
ppm	Parts per million
PPTS	Pyridinium *p*-toulenesulfonate
PTSA	*p*-Toluenesulfinic acid

r.t.	Room temperature
SI	Selectivity index
THF	Tetrahydrofuran
TLC	Thin-layer chromatography
TMSCN	Trimethylsilyl cyanide
Tripod	Methyl-2,4,9-trithiaadamantan-7-carboxylate
Tp	Tripod or methyl-2,4,9-trithiaadamantan-7-carboxylate
UV	Ultraviolet

CHAPTER I

INTRODUCTION

1.1 The Influenza Virus

It is estimated that over 40 million people perished during the 1918 Spanish influenza pandemic, and nearly 35% of the global population was infected with the disease.[1] From Europe to America and even reaching as far as the wilderness of Alaska and remote Pacific islands, this virus was exceptionally widespread during a time when global travel was not very prominent. This pandemic has been regarded as one of the single most devastating infectious disease events in recorded history.[1] It is currently believed that the influenza strain responsible for the 1918 Spanish flu is genetically linked to the N1H1 influenza that emerged in 2009 and threatened another pandemic.[1,2] With the advent of modern vaccinations, the death toll from the flu virus has been substantially lowered, but there still remains the possibility for a recurrent epidemic. Should the virus mutate in such a way that a new variant circulates, there would be little defense against the spread of the disease and a global outbreak would be almost inevitable.

Since its identification in the 1930's, the influenza virus has been extensively studied and characterized, yet many aspects of its mechanism of infection still remain unclear. To date, only four antiviral drugs have been approved by the Food and Drug Administration (FDA) to treat influenza illness (Table 1.1). Of those four drugs, two have developed resistance among the most common influenza A strains in circulation and are rarely used today. Although every year new developments in prophylactic vaccinations are made, few options for post-infection treatment are available. For this reason, there is a vast opportunity in this area for continued drug development.

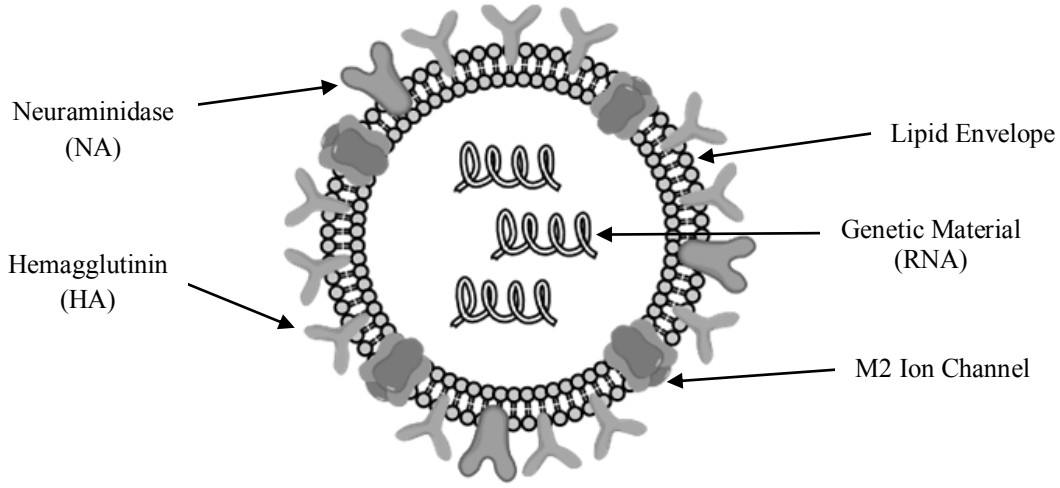

Figure 1.1: Features of influenza A virion structure. The RNA is contained in a helical capsid, which is enveloped and has two types of glycoprotein peplomers (HA and NA) on the surface in a 4:1(HA:NA) ratio.

1.2 Current Therapeutics

The development of new antiviral drugs is hindered because of the relatively simple structure of the influenza virus (Fig. 1.1) and the fact that few known areas in the

viral life cycle can be targeted for inhibition. The two current drug inhibition targets in the influenza virus are the M2 proton channel, which aids in releasing virus particles from an infected host cell, and the neuraminidase (NA) enzyme, which is required for viral recognition and entry into a host cell (Fig 1.1). The neuraminidase

Table 1.1: FDA-approved drugs for the treatment of the influenza A virus.

Neuraminidase Inhibitors		M2 Ion Channel Blockers	
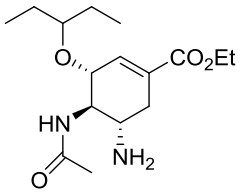	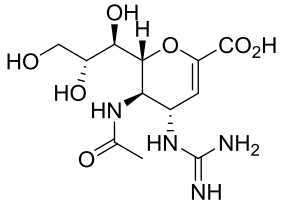	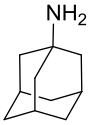	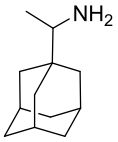
Oseltamivir (**1**)	Zanamivir (**2**)	Amantadine (**3**)	Rimantadine (**4**)

inhibitors (Table 1.1) are currently the only useful FDA-approved treatments for the influenza virus, in that they have not yet acquired resistance within the virus. These drugs, oseltamivir (**1**, Tamiflu®, Genentech) and zanamivir (**2**, Relenza ®, GalaxoSmithKline), Table 1.1, function by inhibiting the neuraminidase (NA) protein of the virus. The neuraminidase enzyme is responsible for cleaving host cell sialic acid residues from viral hemagglutinin, thus releasing the new viruses to carry on and infect other healthy cells. The viral NA catalytic site is highly conserved among all influenza A and B viruses. Both oseltamivir and zanamivir function by acting as stable transition state analogs of the sialosyl cation, which is a highly unstable transition state complex in the enzymatic mechanism of viral sialidase (Scheme 1.1).[3-5] The NA

inhibitor drugs **1** and **2** are similar enough in structure to the sialosyl cation transition state complex, allowing them the ability to bind tightly to the sialic acid active site and prevent viral budding.

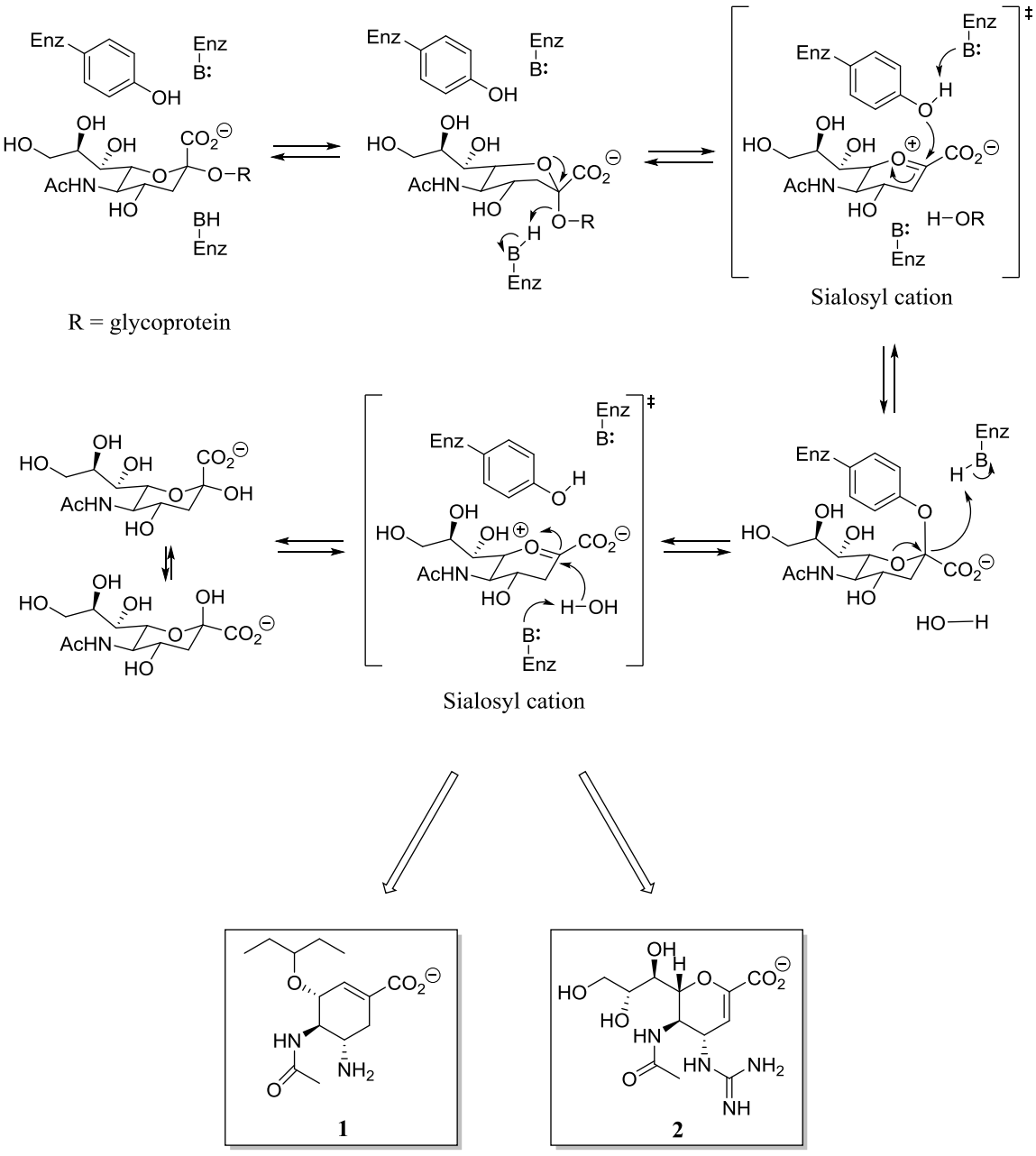

Scheme 1.1: Enzymatic mechanism of influenza A sialidase.[3-5]

Of particular interest to this work is the structure and function of the M2 ion channel. This channel is the target for the adamantane family of antiviral drugs and has recently become a popular topic for research in this area.[6-8] The two current FDA-approved M2 ion channel blocker drugs are the adamantanes: amantadine (**3**, Symmetrel, Endo Health solutions) and rimantadine (**4**, Flumadine, Impax Laboratories) (Table 1.1). These drugs specifically target and inhibit the ion channel function of the M2 protein, which aids in the viral uncoating process after the virions undergo endocytosis and gain entry into a host cell. However, due to a single amino acid substitution occurring in the transmembrane portion of the M2 protein, these drugs no longer have therapeutic effects.[1] Speculation surrounding the exact resistance mechanism acquired by the virus continues, however.[9] The resistance could be due to the ion channel not binding the blocker at all, or the blocker is bound but with no or minimal inhibition, still allowing the flux of protons. Also, particularly for amantadine, there have been documented cases of CNS side effects from the use of these drugs.[10] Regardless, this group of compounds still has potential as future antiviral chemotherapeutics, and this topic will be further examined in the next section of this work.

Both antiviral drugs rimantadine and amantadine have similar adamantane-based structures, but differ only by the amine head-group present on the adamantyl moiety. Because this dissertation outlines similar syntheses as those developed for these molecules, the different routes and their development will be examined in the following section.

Amantadine was first shown to have antiviral activity in 1964 and was initially used as a preventative medicine for the influenza A virus when the H2N2 subtype first surfaced around 1966.[1] The original preparation was published by Stetter *et al.* in 1960 and eventually patented in 1967 by Paulshock and Watts.[11,12] The synthesis is based on the reaction of adamantane with bromine to give 1-bromoadamantane. A subsequent Ritter-type reaction with acetonitrile and sulfuric acid give the 1-acetylaminoadamantane

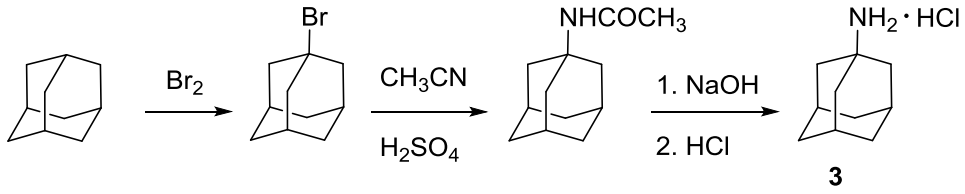

Scheme 1.2: Original synthesis of amantadine (**3**).[11,12]

intermediate, which can be treated with sodium hydroxide to give the final amine product in the hydrochloride salt form (**3**) (Scheme 1.2).[11,12] To avoid using bromine and the harsh conditions that Stetter reported, a modified synthesis of amantadine was later developed by Moiseev and co-workers where the nitrate of adamantanol is the key intermediate instead of the bromo- analog (Scheme 1.3).[13] In this reaction, adamantane is treated with nitric acid (94%) at room temperature to yield the nitrate intermediate. From this point, the reaction proceeds similarly to the previous method with the formation of a carboxamide species followed by treatment with an aqueous base to give the primary amine. The benefit of this reaction was the ability to have other sensitive functional groups present on the adamantane moiety that may otherwise be destroyed by employing Stetter's method.

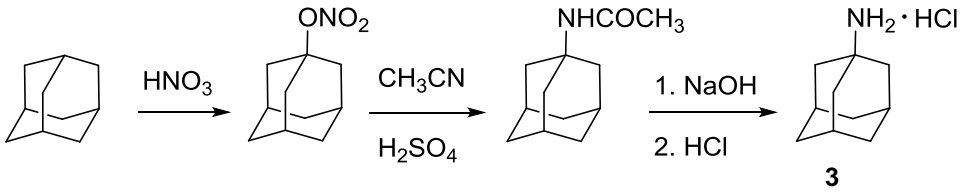

Scheme 1.3: Alternative synthesis of amantadine (**3**).[13]

Although rimantadine was discovered around the same time as its closely related predecessor, amantadine, it wasn't until the 1990s that it was approved by the FDA for influenza infections, although it had previously been used as an antiviral for many years in the Soviet Union.[1] Originally patented in 1967 by Prichard for the DuPont Company, the synthesis of rimantadine consisted of the reduction of the corresponding ketoxime using lithium aluminum hydride (LAH).[14] In this preparation, the ketone from which the ketoxime is derived can be made via reaction of dimethylcadmium with 1-adamantanecarbonyl chloride. The alkyl ketoxime can then be reduced to the amine using LAH.[14,15] Naturally, the use of dimethylcadmium is problematic due to its toxicity and sensitivity to air, moisture and light. So, to address this issue, an alternative

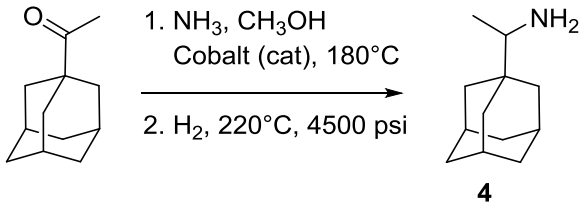

Scheme 1.4: Original synthesis of rimantadine (**4**).[16]

preparation was developed in 1970 by Brake.[16] This synthesis does not require organocadmium compounds, but instead consists of the reductive amination of 1-acetyladamantane to give rimantadine (**4**). In this preparation, the acetyl compound, hydrogen, ammonia, and metal catalyst (Co, Ru, Ni) are reacted at high temperatures (~250°C) and pressures up to 15,000 psi (Scheme 1.4).[16] Although more appealing than the previous synthesis, this process is still highly unfavorable for a commercial scale operation, requiring specialized equipment to handle such high pressures and temperatures.

In 1985, a new synthetic approach to rimantadine was patented by Liu, again out of the DuPont Company.[17] This new preparation addressed the high temperature, high pressure requirements, and utilized 1-adamantyl methyl ketoxime as the starting compound. The reduction of the ketoxime with hydrogen gas and a metal catalyst (Pt on carbon) could be carried out using lower temperatures (10-60°C) and lower pressures (25-215 psi) as described in Scheme 1.5.[17] This procedure proved to be more commercially accessible than previous routes. Several other reports of rimantadine preparation can be found, with one of the more interesting pathways being a synthesis by

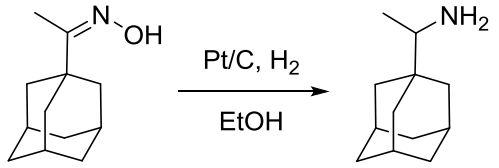

4

Scheme 1.5: A lower pressure and temperature synthesis of rimantadine (**4**).[17]

Liu starting from 1- adamantanecarbonitrile.[18] In this process, the nitrile moiety is alkylated using either methyllithium (CH_3Li) or a methyl Grignard reagent (CH_3MgX, X=Cl, Br), followed by reduction with LAH or catalytic hydrogenation of the imino intermediate (Scheme 1.6).[18] This versatile procedure easily allows for the introduction of various alkyl groups, which could be useful in creating a set of analogs for testing antiviral activity.

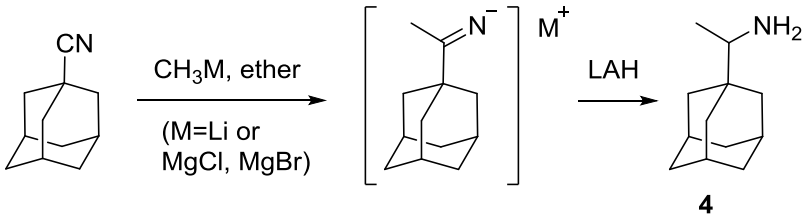

Scheme 1.6: A versatile preparation of rimantadine developed by Liu.[18]

With the renewed interest in discovering novel M2 ion channel blockers, alternative syntheses can be examined to provide the synthetic utility needed to yield various derivatives. The work outlined in this dissertation examines unique routes to prepare 2,4,9-trithiaadamantane derivatives, some of these routes are related to the previous work just discussed.

1.3 Influenza A M2 Ion Channel

The M2 protein of the influenza A virus functions as a pH-activated proton channel, which plays an important role in viral replication. Once the influenza virus

undergoes endocytosis and gains entry into a host cell, the endosome containing the virus has an acidic environment. The M2 proton channel is responsible for allowing an influx of protons across the viral envelope and into the interior of the virion. This acidification of the virus core aids in uncoating, protein dissociation, and the ultimate release of viral ribonucleoproteins (RNPs). Because this ion channel plays such an integral role in the replication of virus particles, it has become the target of antiviral drugs, namely amantadine and rimantadine. This proton channel is also a prime target for antivirals because all influenza A viruses encode the M2 protein. The most conserved portion of this protein is the transmembrane hydrophobic region, which is also thought to be the

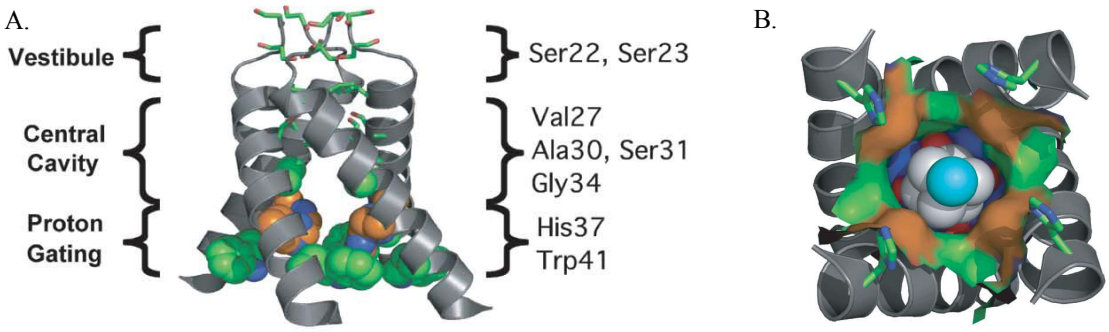

Figure 1.2: The M2 proton channel crystal structure. A, The entire transmembrane region with relevant residues shown. B, An amantadine molecule bound showing surface interactions with residues from the C-terminal side of the protein. Figures taken with permission from Stouffer, A.L. *et al*. *Nature* **2008,** *451*, 596.[19]

drug-binding site. Due to the threat of a global influenza pandemic, new research has uncovered more details regarding the structure and function of the M2 proton channel, as well as possible drug binding interactions. The actual M2 proton channel consists of four (tetrameric) M2 protein subunits, with each protein unit consisting of 97 amino acids, as

shown in Figure 1.2.[1,19] Each subunit is divided into three distinct sections: an N-terminal extracellular region (24 residues), a transmembrane domain (19 residues), and a cytoplasmic tail (54 residues). The transmembrane region is the most studied and most important with regards to drug binding, as it forms the actual aqueous filled lumen of the M2 protein. In the low pH environment of the endosome, the channel is activated through the protonation of His37, allowing the Trp41 "gate" of the pore to open and further conduct protons. In the closed position, the four helices of the protein yield a constricted pore, where intermolecular forces between the indole rings of the Trp41 residues prevents water or ions from entering the pore thus giving a "locked" conformation. Lowering the pH destabilizes the helical packing and opens the gate allowing water to conduct proton ions, while still keeping the carboxy-terminal base intact to prevent dissociation of the protein tetramer.

In 2008, Stouffer *et al.* were able to elucidate the X-ray structure (3.5 Å resolution) of the transmembrane region of the protein channel while both empty and with an amantadine molecule bound inside.[6] This work provided one of the earliest high-resolution structures of the M2 protein and gave the first glimpse of the drug binding interaction. Shown in Fig. 1.3, the omit map illustrates the electron density attributed to only one amantadine molecule bound within the lumen of the pore near residues 27, 30, 31 and 34. Because of the low resolution of the drug-binding site, two orientations of the amantadine molecule were probable: the amine head pointing towards the C-terminal end (amine- down) or pointing towards the N-terminal end (amine-up). However, it was determined by examining the electron densities that the polar amine moiety most likely

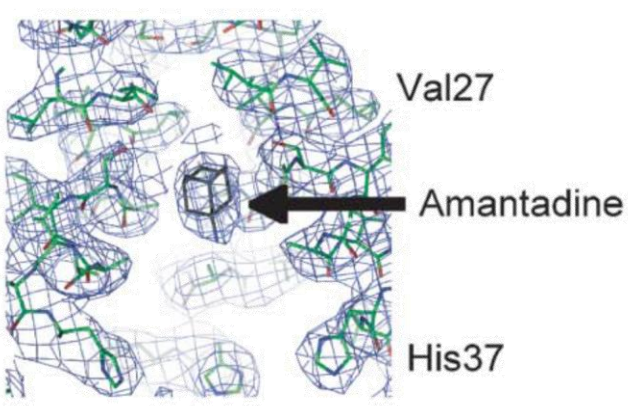

Figure 1.3: The omit map of amantadine bound within the M2 lumen. Figure taken with permission from Stouffer, A.L. *et al. Nature* **2008,** *451*, 596.[6]

faces down towards the His37 residue, which is consistent with the fact that when amantadine derivatives have a larger alkylamine present (i.e. rimantadine), they still show similar inhibitory effects. The drug activity is most likely due to the binding interactions in the lumen of the channel with the adamantane portion near the hydrophobic Val residues (of the N-terminus) and the amine moiety near the His residues (near the C-terminus). This position physically occludes the pore when the drug is bound, yet leaves sufficient room for other larger alkylamine substituents to also bind. Again, these conclusions were early findings by one group and have become quite an area of debate for this topic.[6-8]

In another study by Schnell and Chou, the structure of the M2 channel was determined using solution NMR.[7] Here, the channel was examined while in complex with rimantadine and interestingly the results of this study were quite different than those obtained by Stouffer *et al.* In this study, it was found that rimantadine binds in a 4:1

(drug:protein) molar ratio, with one molecule per each helix bound on the lipid-facing side of the channel near the Trp41 residue (Fig. 1.4). Instead of a physical occlusion inhibition, as previously reported, these findings suggest an allosteric mechanism of inhibition. Rather than physically blocking the channel by fitting tightly inside the pore, the bound rimantadine molecules bind to the periphery of the protein stabilizing the closed conformation. These conclusions were unexpected because it was generally accepted that the mutated amino acids responsible for the resistance to the adamantane-based drugs were pore-lining residues.[7]

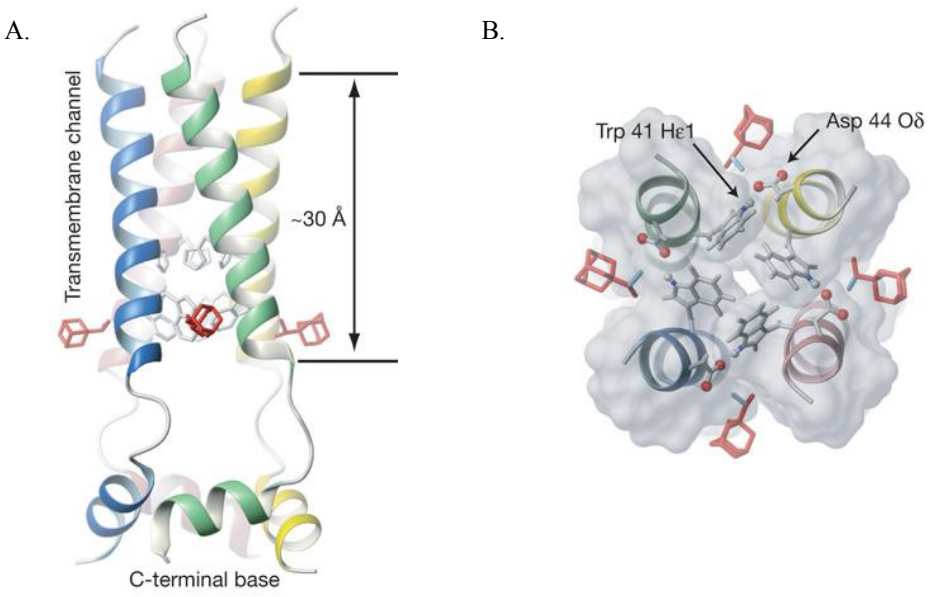

Figure 1.4: Ribbon representation of the rimantadine-bound M2 protein as determined by solution NMR. A, the entire tetrameric protein channel. B, a closer view from the C-terminal side showing the close interactions of the Trp gating residue and the Asp 44. Figure taken with permission from Schnell, J.R.; Chou, J.J. *Nature* **2008**, *451*, 591.[7]

With these findings, it became necessary to determine the exact positional binding of the M2 blockers in order to further develop a new line of antivirals. In a recent publication, Cady *et al*. set out to further examine the protein-drug binding interactions using solid-state nuclear magnetic resonance (SS-NMR) to prove the presence of two distinct binding sites. Both of these sites were found to be located in the phospholipid bilayer.[8] A "high-affinity" site, located in the lumen of the channel near Ser31, has been identified and can accommodate a single amantadine molecule. This binding site was shown to have several residues nearby that are mutated in the viruses that are resistant to the drug (Fig 1.5-A).[8] A second "low-affinity" site was found to be on the surface of the protein near the C-terminal end. This site is bound only when the concentrations of the drug reach a high enough concentration (> 7 mol%) in the lipid bilayer. This study not only used SS-NMR to give a high-resolution structure of a small molecule complexed with a membrane protein, but it also gave insight into the orientation and dynamics of each individual binding site which can aid the development of new antivirals. It was also found that amantadine is able to undergo a substantial amount of motion while bound in the lumen, meaning new drug candidates may evade resistance by having a more optimal fit within the pore. With this new knowledge, the mutations within the binding pocket can be evaluated to design drugs that will better block the "high-affinity" site. Another interesting finding by Cady *et al*. suggests that four molecules of the antiviral drugs bind to each M2 protein, one to each tetramer in a "barrel-loop" type closure of the ion channel through conformational changes.[8] This finding reveals a functioning of two separate pharmacophore groups present in the antiviral drugs, the adamantane ring and

the substituted amine on the 7-position. Here, the adamantyl motif interacts with one side of one tetramer, while the amine group hydrogen-bonds to residues on an adjacent tetramer. With this insight, novel drug design may involve the addition of a larger amine moiety to better span the width between mutated tetramers in the M2 protein.

1.4 Amino Acid Mutations in the M2 Protein

When developing new drug candidates as M2 channel blockers, many aspects must be considered. Several amino acid mutations have been proposed, which may be responsible for the acquired resistance of both rimantadine and amantadine. These mutations have rendered this class of drugs useless against most influenza strains by either directly preventing the adamantane drugs from binding within the pore, or

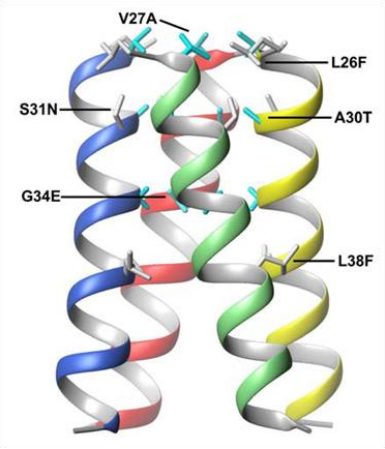

Fig. 1.5: Positions of known amino acid mutations of the M2 protein that transmit drug resistance to the adamantane drugs. Both pore-lining residues (dark gray) and residues that are in the helix-helix packing interface (light gray) are shown. Figure taken with permission from Schnell, J.R.; Chou, J.J. *Nature* **2008**, *451*, 591.[7]

through the weakening of the helix-helix packing of the protein. It is estimated that during the 2005-2006 flu season resistance had reached nearly 90% of the circulating influenza viruses.[6] The effects of these mutations on the binding site must be carefully evaluated to design drugs that will not encounter the same fate. Through genetic analysis of the amantadine-resistant strains four amino acid residues in the TM domain of the M2 protein were determined to convey resistance: Val27, Ala30, Ser31, and Gly34.[7,19,20] These mutations are illustrated in Fig. 1.5, and are noticeably close in proximity to the drug-binding pocket of the channel. Using SPR techniques to measure the binding of amantadine in the M2 channel, it was found that the mutations Ala30 and Ser31 caused the pore to lose its drug-binding ability, while the Val27 mutation still allowed for drug binding.[20] This difference can be explained by the amino acid that is substituted in the mutated pore. The Ala30 is replaced by a Thr residue (A30T) and Ser31 by an Asn residue (S31N). Both of these replacement residues are larger and more polar, explaining the direct connection to resistance. The Val27 residue, on the other hand, is replaced with a smaller counterpart, Ala (V27A), which may be why it can still bind the drug properly and block the pore. These substitutions alter the conformation of the drug binding site and increase the size and polarity of the pore.

In a study just published in 2011, Leonov *et al*. set out to determine the mechanism by which the adamantane drugs block the channel, and also how and why the mutations prevent this blockage while still allowing the conductance of protons.[21] To avoid inhibition, it was shown that the mutated protein could utilize two approaches. First, the mutation involves replacement with a larger amino acid, as in the S31N

mutation, which causes the drug-binding site to be physically occluded. Second, replacement with a smaller residue, as in the V27A mutation, gives an increase in the volume of the lumen (205 Å), which is greater than the amantadine volume.[21] This increase in volume allows the drug to have free movement, while protons are still able to move through the channel. Also, through computational analysis (PMF analysis and MD simulations) it was determined that the adamantanes inhibit conductivity of the channel through electrostatic hindrance from the positively charged amine moiety, which causes a repulsion of the protons.[21] In this analysis, the adamantane pharmacophore plays little to no role in the drug activity. However, through both strategies of inhibition, the drug cannot properly exert the positive potential to prevent the flow of protons, which prevents its inhibitory function.

With these findings, new chemotherapeutics need to be slightly more hydrophilic on the usually apolar adamantane pharmacophore, as well as increased size to optimally fit the mutated channel while still maintaining the presence of a charged amine moiety to repel protons electrostatically. The analogs synthesized and described in this dissertation address these structural requirements, and will be examined in the next chapter.

1.5 Current M2 Inhibitor Candidates

In response to all the new discoveries regarding the drug binding interactions and mutations present in the M2 proton channel, several novel inhibitor candidates have been reported and are being investigated for their clinical relevance. Because two binding sites for the adamantane drugs have been recognized, most studies aim at identifying where

these derivatives bind so as to better tailor new drug candidates to fit the mutated pore. A few representative molecules and their syntheses will be described in this section. Most of the new candidates are based on the structures of rimantadine and amantadine, with altered sized hydrocarbon portions and amine groups to enhance potency and better block the mutated pore. Reduction in CNS toxicity is also an objective when designing new antivirals.[38]

Some examples of promising rimantadine derivatives, developed by Stamatiou *et al*. are 2-(1-adamantyl)pyrrolidine **5** and 2-(1-adamantyl)piperidine **6**, with both structures shown in Figure 1.6.[22] The structure of rimantadine is depicted again to demonstrate the similarities of the derivatives.

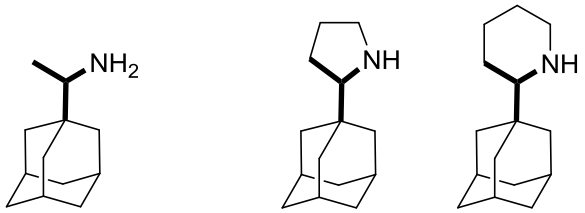

Rimantadine **5** **6**

Figure 1.6: Structures of new M2 channel blocker candidates developed by Stamatiou *et al*. 2-(1-adamantyl)pyrrolidine **5** and 2-(1-adamantyl)-piperidine **6**.[22]

When looked at *in vitro*, both compounds showed much higher potency (lower EC_{50}) than rimantadine, with compound **5** (Table 1.2, entry i) having an 18-fold increase in inhibition and compound **6** (Table 1.2, entry ii) having a 14-fold increase.[22] Attempts at N-alkylation led to a significant decrease in inhibition potency (Table 1.2, entries iii and

iv) and altering the size of the N-alkyl group also showed no increase in drug activity (Table 1.2, entries v and vi).[22] It seems the 1-aminoethyl pharmacophore group present in rimantadine has an important role in binding the pocket of the protein. These conclusions are in agreement with the many other studies looking at similar compounds to rimantadine. Because rimantadine is thought to prefer the "secondary binding site" around the periphery of the pore, which is outside of the central lumen, this aminoethyl group may be necessary to bind properly between helices of the M2 monomers.

Table 1.2: Inhibitory results of various 1-adamantyl-pyrrolidines and 1-adamantyl-piperidines. The potency of selected derivatives on inhibition of the influenza A virus as compared to amantadine and rimantadine. Table modified from Stamatiou, G. *et al. Bioorg. Med. Chem.* **2003**, *11*, 5485–5492.[22]

Entry	Compound	EC_{50} (μM)	Entry	Compound	EC_{50} (μM)
i	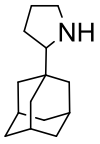 **5**	2.5	v	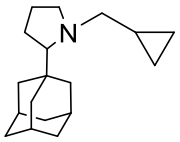	244
ii	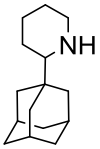 **6**	3.3	vi	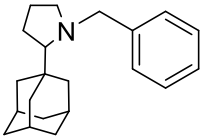	522
iii	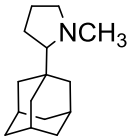	>196	Amantadine	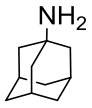	45
iv	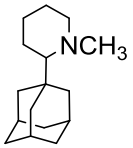	>978	Rimantadine	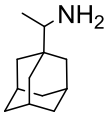	13.9

The synthesis of compound **5**, outlined in Scheme 1.7, begins with the addition reaction of commercially available compounds 1-(trimethylsilyl)-2-pyrrolidinone (**7**) and 1-adamantanecarbonyl chloride to give the intermediate adamantyl-pyrrolidinone (**8**). A dry distillation of **8** with CaO yields **9**, followed by a reduction with sodium borohydride to give the final pyrrolidine **5** in decent yields.

Some of the earliest examples of amantadine derivatives as new drug candidates are the spiro piperidines and spiran-amine derivatives. As early as 1995, a compound known as 2-[3-azaspiro(5,5)undecanol]-2-imidazoline, or BL-1743 (**10**), shown in Figure 1.7, was found to inhibit ion channel activity similarly to amantadine.[23,24] This

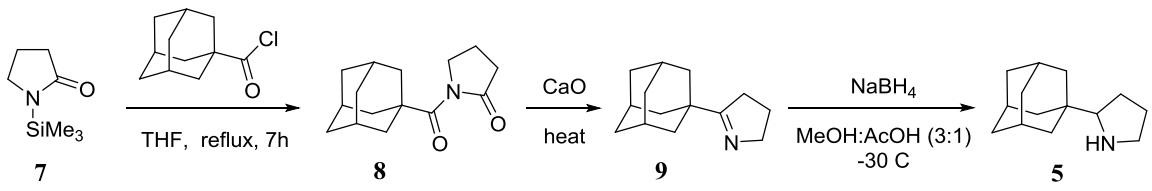

Scheme 1.7: Synthesis of 2-(1-adamantyl)pyrrolidine (5). The scheme is modified from reference 22.

compound was one of the first analogs investigated as an M2 inhibitor. Looking at **10** as a blocker of M2 protein expressed in oocytes of *Xenopus laevis*, Tu *et al*. were able to determine that the pore was indeed blocked by this molecule. The binding was found to be reversible, whereas similar studies of amantadine binding proved to be irreversible or only slowly reversible.[24] The binding affinity is important when understanding the acquisition of mutations of the protein since reversible binding may prevent the drug

molecules from remaining in the pore long enough for mutations to occur. On the other hand, it could translate into non-antiviral activity by not blocking the channel for a long enough period of time to prevent the flux of protons. Another setback to the antiviral activity of **10** is most influenza strains that are resistant to amantadine were also found to be resistant to this molecule. Regardless, many new structure-function insights were gained by examining the binding of **10** in the M2 protein.

Based on the findings of **10**, several other novel sets of derivatives have been designed and synthesized bearing in mind the necessary presence of both the amine and hydrocarbon portions of the molecule. The compounds with the most promising

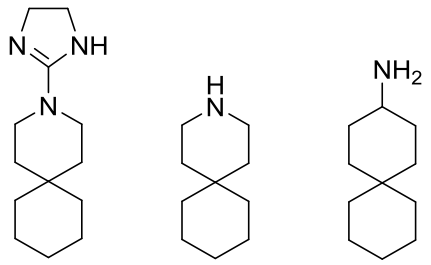

10 **11** **12**

Figure 1.7: Structures of the spiro piperidines and spiran-amine M2 blocker candidates. They were developed by Kurtz *et al*. (**10**), Wang *et al*. (**11**) and Balanik *et al.* (**12**).[23,25,26]

antiviral activity are shown in Fig. 1.7.[25,26] The results using these compounds would appear to indicate that the adamantane structure may not be required for binding after all, but rather any similarly sized, multi-ring, hydrophobic system may be sufficient for the hydrophobic pharmacophore. The amine functionality appears to still be necessary to

convey drug activity. One such alternative derivative to come from the study of **10** is 3-azaspiro[5,5]undecane (**11**), also depicted in Figure 1.7.[25,27] Developed by Wang *et al*., this molecule is an intermediate in the synthesis of **10** and this reaction is described in Scheme 1.8. Starting with 3,3-pentamethylene glutarimide, a reduction using LAH in THF followed by addition of HCl gives compound **11** in the hydrochloride form.

To achieve **10**, or any other N-substituted derivative of **11**, a subsequent nucleophilic substitution reaction is performed. To yield **10**, compound **11** is reacted with 2-methylthio-2-imidazoline in refluxing methanol (Path **I**, Scheme 1.8). Following Path **II** in Scheme 1.8, a reductive amination of **11** using various aldehydes with

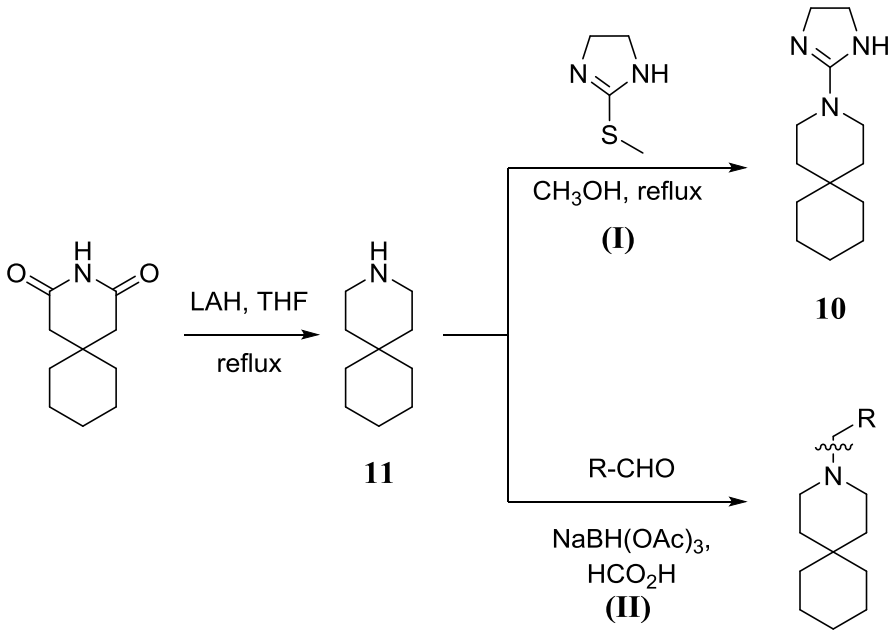

Scheme 1.8: Synthesis of the spiro-piperidines **10** and **11**. The scheme is modified from reference 25.

$NaBH(OAc)_3$/AcOH, gives the corresponding N-substituted spiro-piperidines. A complete set of derivatives made this way were analyzed for antiviral activity, although **11** showed the most potential when compared to amantadine.

Experiments evaluating **11** for drug activity indicated this molecule was superior to amantadine at inhibiting the M2 channel. Molecule **11** had an IC_{50} of 0.92 μM and amantadine had an IC_{50} of 16 μM, showing **11** was nearly an order of magnitude more potent. Investigations of the binding effects of **11** on the TM protein region using NMR in comparison to amantadine indicated a more uniform conformation for the M2 protein. The 34-35 residue structure in proximity to the aqueous cavity of the pore was not altered, and there also was no alteration of the magnetic environment and dynamics of surrounding amino acids within the M2 protein. Through optimized docking studies, the amine group was found to be hydrated in either an upward or downward position. All together, these findings suggest that **11** may bind to the pore residues more effectively leading to enhanced potency.

Also depicted in Figure 1.7, spiro[5.5]undecan-3-amine (**12**), has been shown to have improved antiviral activity when compared to the drug amantadine.[26] This compound was also the first to show inhibition of not just the wild-type pore, but also the mutated (L26F and V27A) pore. This drug was also reported to bind in the N-terminal lumen of the pore, which was identified as the "primary binding site." With the discovery of this drug and its ability to bind both wild type and amantadine-resistant M2 pores, hope is renewed for overcoming the influenza resistance to these inhibitors. Compound **12** was synthesized by a reaction scheme starting with commercially available

cyclohexanecarbaldehyde and pyrrolidine (scheme 1.9). Two paths were investigated to form the enone intermediate **13**: (**I**) a Diels- Alder reaction with subsequent acid hydrolysis and ring formation, and (**II**) a one-pot Robinson annulation with an acid catalyst. Although both reactions led to the desired intermediate, path (**I**) was preferred because it had significantly higher yields and reportedly avoided forming a polymer from the methyl vinyl ketone. Regardless of the path taken, the next step converted the spiro-α,β-unsaturated ketone (**13**) into the corresponding spiro-ketone (**14**) through catalytic hydrogenation. The final amine **12** was formed by reaction of **14** with hydroxylamine and subsequent reduction using LAH.

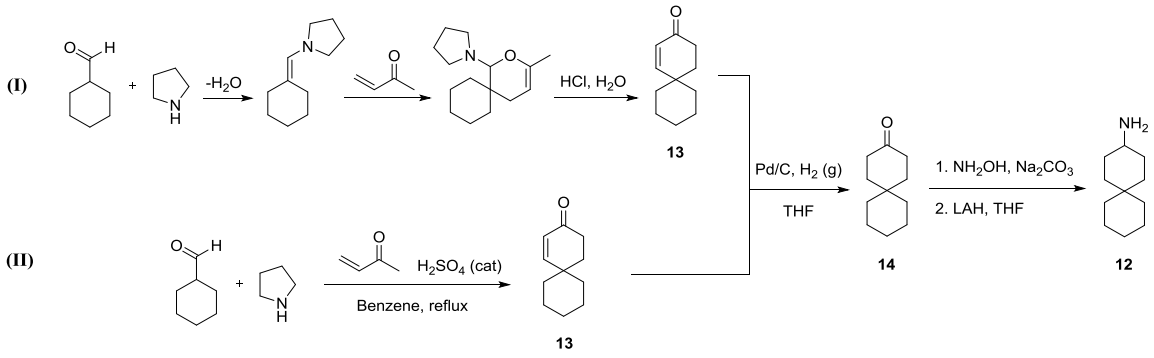

Scheme 1.9: Synthetic routes to form spiro[5,5]undecan-3-amine (**12**). The scheme is modified from reference 26.

Some other interesting derivatives of rimantadine are the 1,2-annulated adamantane -piperidines (**15**) and -pyrrolidines (**16**), illustrated in Fig. 1.8.[28] These compounds were investigated for their drug activity in context of the stereoelectronic requirements for providing optimal inhibition of the M2 channel. When the drug activity

of several unique derivatives of the adamantane family of antivirals was examined, many key features affecting new drug design were recognized, and are outlined in Table 1.3.[28] The first finding was that extending the amine ring from a pyrrolidine to a piperidine made no difference in the potency of the compound. Comparison of the piperidine **15** (entry viii, EC_{50} = 0.6) and the pyrrolidine **16** (entry xiii, EC_{50} = 0.5) from Table 1.3 exemplifies this lack of difference. It seems as though the presence of a large lipophilic group around the adamantane moiety still allows for drug binding, suggesting there may be a complementary binding site in the pore lumen. It was found that the nitrogen of the amine moiety gains enhanced activity when moved from the 2- adamantyl position.

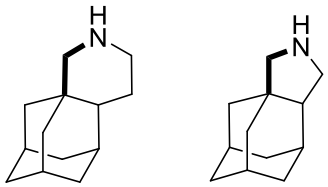

15 **16**

Figure 1.8: Structures of 1,2-annulated adamantane piperidine 15 and pyrrolidine 16. These potential M2 blockers were developed by Zoidis *et al*.[28]

Looking at entries vii versus viii, and x versus xiii of Table 1.3, an almost 7-fold increase in activity is seen when moving the nitrogen from the 1- to the 4- position in the piperidine ring and almost 5-fold increase when moving it from the 1- to the 2- position on the pyrrolidine ring. Conformational studies determined that when the nitrogen atom is moved to the 3-position of the annulated piperidine ring, the charged amine pharmacophore portion of the molecule is unable to hydrogen-bond properly with surrounding amino acids and all activity is lost. The final conclusions of this study

suggest that N-alkylation on the amine leads to a marked decrease in drug potency and drug selectivity. This conclusion becomes especially clear when examining entries viii versus ix, x versus xi, xiii versus xiv. Interestingly and quite contrary to these findings, it has been previously reported that N-alkylation of amantadine and rimantadine actually enhances activity.[29]

Table 1.3: Drug activity of 1,2-annulated piperidines and pyrrolidines. The table is modified from reference 28.

Entry	Compound	EC_{50}	SI	Entry	Compound	EC_{50}	SI
vii	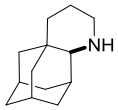	4.1	106	xii	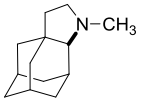	7.7	11
viii	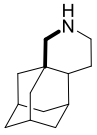 **15**	0.6	732	xiii	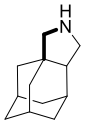 **16**	0.5	200
ix	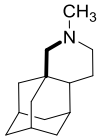	N/A	—	xiv	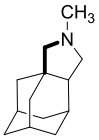	2.4	35
x	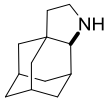	2.2	217	Amantadine	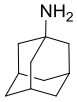	2.0	>250
xi	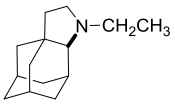	3.4	128	Rimantadine	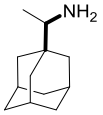	0.36	1389

All of the studies and syntheses just described need to be taken into account when designing and synthesizing new M2 ion channel blockers for the influenza A virus. Although some results contradict each other, the overall understanding of the structure-function relationships between drug binding in both the wild type and mutated M2

proteins is becoming clearer. Because this dissertation outlines new drug candidates, a comprehensive look at other additional studies in this area was necessary to rationalize the drug design of these new compounds.

1.6 Previous Studies Involving Trithiaadamantanes

As described in 2002, a unique tridentate sulfur ligand (Fig. 1.9) was designed and synthesized by Kittredge *et al.*, as a surface linker for peptide growth on gold nanoparticles.[30] First reported by Lindgren in 1976, this molecule has an very unique adamantane-like cage modified with three sulfur atoms and a head group that can be manipulated into desirable functional groups.[31]

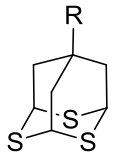

Figure 1.9: The 2,4,9-trithiaadamantane molecule with a random I substitution at the 7-position.

Lindgren's approach (Scheme 1.10) involves the reduction of the ozonide intermediate by triphenylphosphine and thionation of the resulting trialdehyde by means of H_2S in an acidic alcohol environment. The yields of this reaction were modest, at best, and the procedures proved to be irreproducible. Kittredge's method was a slightly modified version of Lindgren's with little improvement on the yields (<15%) and

requiring semi-preparative HPLC for purification. Because the only known syntheses for 2,4,9-trithiaadamantane and its derivatives had meager yields, used unfavorable reagents and were nearly impossible to reproduce, the advancement in this class of molecules was hindered and further investigation into other applications was never fully explored.

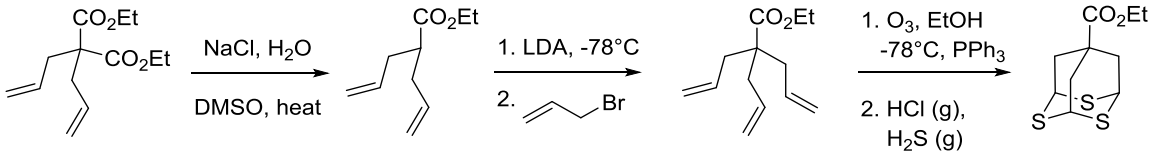

Scheme 1.10: Lindgren's synthesis of ethyl 2,4,9-trithiaadamantane-7-carboxylate.[31]

In 2004, the trithiaadamantane molecule was re-examined by Hu and Khemtong regarding its use as a photoreactive surface anchor on gold thin films.[32] A new procedure for the synthesis of trithiaadamantane derivatives was established.[32,33] The first major advancement of this work was the use of Lawesson's reagent with a Lewis acid (BF_3) or P_4S_{10} on alumina for thionation, no longer requiring the use of hydrogen sulfide gas. This new synthesis utilized dimethyl malonate as the starting material and slightly improved upon the yield (>30%). The product of this reaction is the methylester derivative **17**, methyl-2,4,9-trithiaadamantane-carboxylate, or tripod (Tp) for short. The yields of this reaction were reported as 25-30%, when synthesized according to Scheme 1.11, which are significantly better than previously obtained, however still not optimal.

Another enhancement in this procedure was the ability to use flash column chromatography and recrystallization for purification, making HPLC no longer necessary.

Since the trithiaadamantane molecule could now be produced in greater quantities with easier purification, several new derivatives were synthesized and their physical properties were characterized. One such investigation looked at the formation of inclusion complexes in β- cyclodextrin.[34] Interestingly, the use of cyclic sugars, such as β-cyclodextrin, are able to serve as mimics of biological ion channels, although Khemtong and Hu never explored this area of interest.[35]

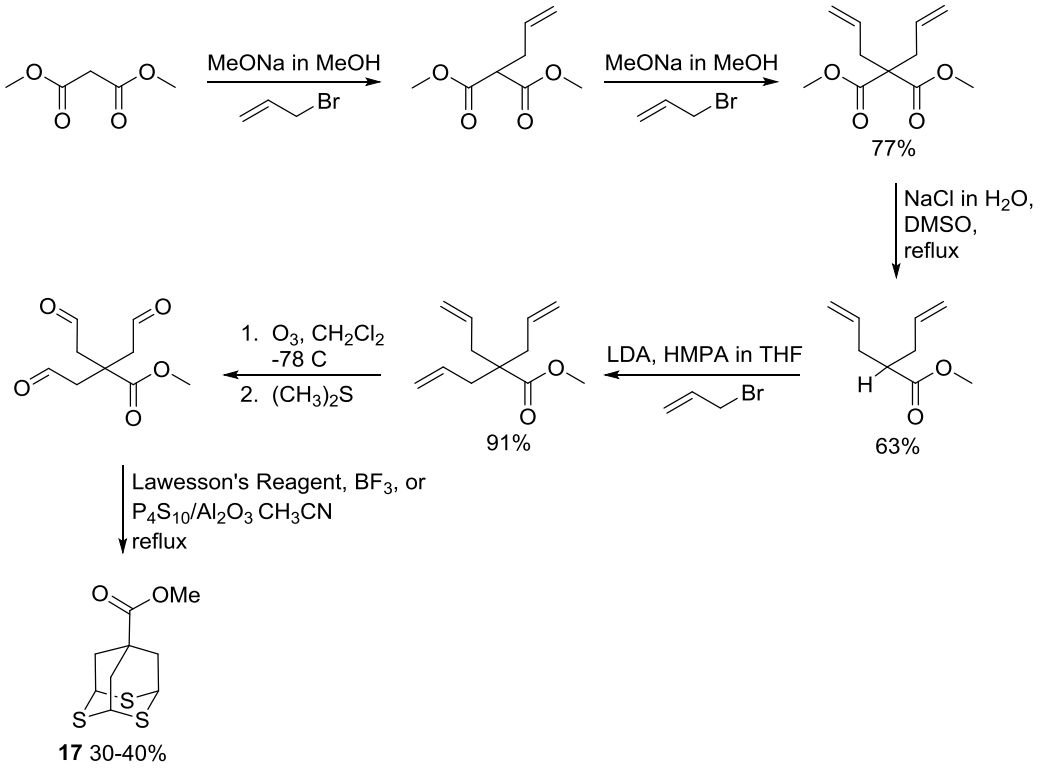

Scheme 1.11: Synthesis of methyl-2,4,9-trithiaadamantane-7-carboxylate, $TpCO_2Me$ (**17**).[33]

One current drug analog, which is still under investigation, has sulfur atoms in the hydrocarbon framework, and also the presence of the amine pharmacophore, similar to the tripod molecule (Entry xv, Table 1.4).[25] Also reported, is an analog containing oxygen atoms in the hydrocarbon ring (Entry xvi, Table 1.4), although this molecule has not shown improved inhibition of the M2 channel when compared to the parent compounds rimantadine and amantadine. Interestingly, a trioxaadamantane-methylester derivative was synthesized and will be discussed later. Although the results for these drug analogs are not as conclusive as previous examples, mainly because they were not studied as in depth, there was retention of binding affinity for the dithiene molecule (Entry xv, Table 1.4).[25] The ketal version (Entry xvi, Table 1.4) showed no binding affinity; however, the molecule was only tested on the wild type pore.

Table 1.4: Heteroatom substituted derivatives of the spiro-piperidine **11**. The table is modified from reference 25.

Entry	Compound	Activity remaining (after 100 μM)	IC_{50} (μM)
xv	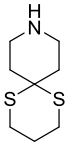	12%	38
xvi	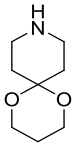	100%	>100

Both the ketal and dithiene derivatives retain the 6-member, spiro-piperidine moiety, but due to the heteroatoms they have an increased hydrophilicity when compared

to compound **11**, which was the molecule with the most potential in this study. The ketal was found to have a clog $P = -0.30$ and the dithiene clog $P = 1.28$, while compound **11**, with no heteroatoms in the ring, had a clog $P = 3.38$. Here, clog P is the calculated log of the distribution coefficient, which gives an idea as to the hydrophilicity of the molecule.[25] Considering the mutated pore is speculated to have a slightly larger, more polar binding pocket, these types of drugs have the potential to be the next generation of antivirals. Therefore, it is the main focus of this dissertation to design, synthesize and characterize new derivatives of the tripod molecule as potential M2 ion channel blockers based on the tripod molecule, bearing in mind the recent findings regarding the M2 protein and drug activity.

CHAPTER II

SYNTHESIS OF 2,4,9-TRITHIAADAMANTANE DERIVATIVES

2.1 Introduction

When considering novel pharmaceuticals as M2 ion channel blockers, new functionalized adamantane-type compounds must be evaluated for their possible use as antivirals. Because the known M2 inhibitor drugs both share similar adamantane cage structures with varying amino-functionalized head groups, it is possible that additional compounds with similar structures will also function as ion channel blockers, as discussed in Chapter 1. With the recent elucidations of the M2 ion channel protein and binding pocket, and the proposed amino acid mutations, new designs for anti-virals must be more hydrophilic, larger in diameter, maintain the charged amine pharmacophore within hydrogen bonding distance of lumen residues, and be more easily degraded so resistance is not acquired by the virus.

The trithiaadamantane sub-structure may address all of these considerations for the design of new anti-influenza drugs that would inhibit a mutated ion channel. The structures of the trithiaadamantane analogs of amantadine and rimantadine are shown in Figure 2.1. In light of the dithiene drugs previously discussed, showing retention of binding affinity for the pore lumen, there is a good possibility for these sulfur-containing

molecules to block the M2 channel as well.[25] Relative to C-C bonds, C-S bonds tend to be both longer and weaker.[36] The incorporation of the three sulfur atoms in the adamantane portion of the molecule slightly increases the polarity of the carbon framework allowing for enhanced solubility in water and better interaction with the more polar mutated amino acid residues. The presence of the sulfur atoms also improves the biodegradability by oxidation of the base thioether moiety to a sulfoxide and again to a sulfone.[37]

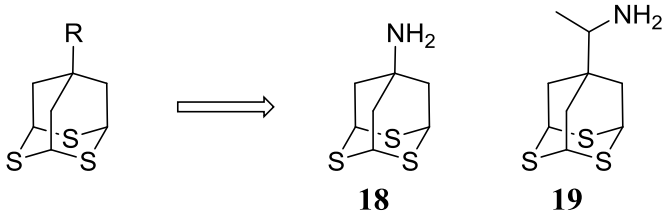

18 **19**

Figure 2.1: Examples of 7-substituted trithiaadamantane derivatives. Structures of random substituted 2,4,9-trithiaadamantane and antiviral analogs 2,4,9-trithiaadamantan-7-amine (**18**) and 1-(2,4,9-trithiaadamantan-7-yl)ethan-1-amine (**19**).

Amantadine and rimantadine have carbon cage structures that are more difficult to break down by biological enzymes leading to enhanced biodistribution and exposure times, which may cause the development of drug resistance. There have also been several studies indicating that both of the adamantane-based drugs may lead to varying levels of CNS toxicity.[38] Remarkably, amantadine is significantly (~18%) more toxic to the CNS than rimantadine. It is also known that amantadine is excreted from the body essentially unchanged, whereas rimantadine is metabolized both renally and hepatically.[39] Another attribute of the trithiaadamantane molecules that may better block the mutated

M2 channel is the larger diameter of the bottom of the trithiaadamantane unit. Near the Val 27 residue of the wild type pore, the diameter is ~2.5 Å, which widens to ~5 Å when the valine is replaced with a suspected mutation residue, such as alanine.[40] Considering the average bond length of a C-C single bond is 1.54 Å and a C-S single bond length is 1.82 Å, the incorporation of sulfur atoms adds girth, making it possible to fit a larger diameter mutated pore.[41] The only issue in pursuing these compounds as a new pharmaceutical are the meager reported yields (~30%) obtained by both Kittredge and Khemtong.[30,34] Chapter 3 of this dissertation will present new synthetic schemes to increase the yields of the trithiaadamantane molecule.

This chapter will focus on describing the syntheses and attempted syntheses of 7-substituted-2,4,9-trithiaadamantane derivatives as possible M2 channel blockers. From the tripod molecule, several different routes were taken to transform the methyl ester moiety into the desired functionalities of potential drug candidates. Scheme 2.1 outlines a variety of the reactions that were employed to lead to novel 7-substituted-2,4,9-trithiaadamantanes that will be discussed in this chapter.

The synthesis of 2,4,9-trithiaadamantane-7-amine relies on the Curtius rearrangement of the acyl azide **28**, derived from either the acyl hydrazide intermediate, **25** (Path I, Scheme 2.1)[39] or directly from the methyl ester **17**, by way of hydrolysis to give **26**, conversion to the acid chloride **27** and treatment with sodium azide (Path II, Scheme 2.1).[42,43] The exact mechanism of this rearrangement, specifically the formation of the isocyanate intermediate, has been debated since Stieglitz first proposed a nitrene intermediate in1896.[44] Some authors agree with Stieglitz and believe a transient nitrene

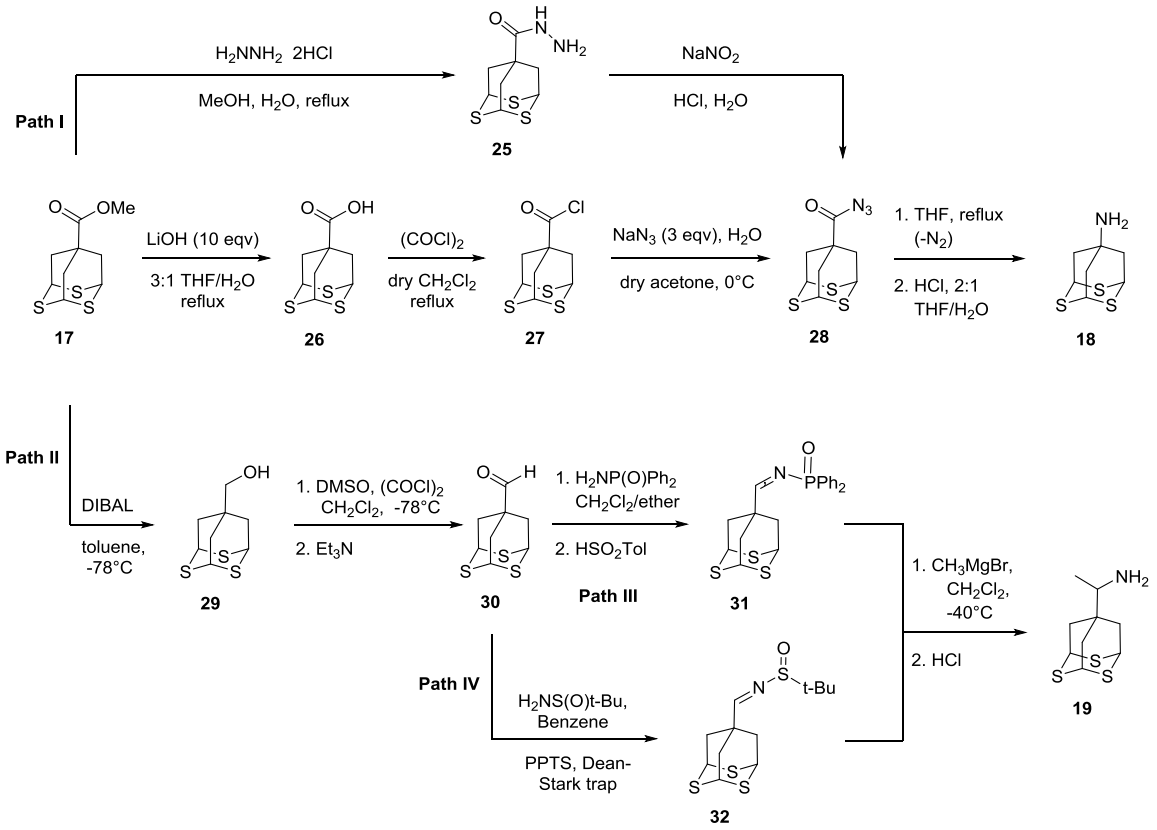

Scheme 2.1: Various routes to 2,4,9-trithiaadamantan-7-amine (**18**) and 1-(2,4,9-trithiaadamantan-7-yl)ethan-1-amine (**19**).

intermediate exists, which is formed when N_2 gas is expelled prior to the rearrangement in a step-wise mechanism (Fig. 2.1, Path II).[44] On the other hand, some prefer a concerted mechanism where the N_2 molecule is expelled during the rearrangement in the formation of the isocyanate (Fig. 2.1, Path I).[45,46] The two competing mechanisms depicting this unique rearrangement are shown in Figure 2.1. Both mechanistic versions behave similarly once the isocyanate is formed. Addition of an aqueous solution forms an unstable carbamic acid, which decomposes to give an amine and carbon dioxide. Ideally, a methyl ketone moiety on the starting compound would allow for reductive

amination to give the free amine, however that is beyond the scope of this work although some ideas regarding new starting molecules will be further discussed in Chapter 3.

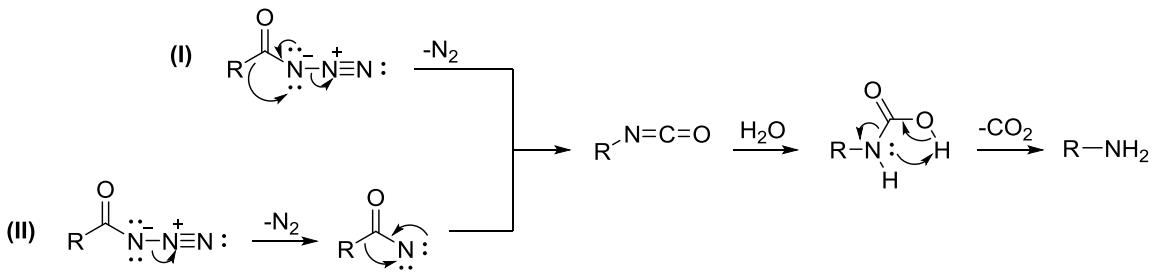

Figure 2.2: Competing mechanistic representations of the Curtius rearrangement. Also showing the hydrolysis of the resulting isocyanate.[44-50]

The syntheses of 1-(2,4,9-trithiaadamantan-7-yl)ethan-1-amine were attempted keeping three basic steps in mind: the formation of an imine, nucleophilic addition to the imine, and cleavage of the activating group. Owing to the fact that oxygen is more electronegative than nitrogen, the imine counterpart to a carbonyl is far less electrophilic. For this reason, a highly reactive nucleophile, such as a Grignard reagent or organolithium reagent, must be used to alkylate the imine. Also, electron-withdrawing groups present on the imine can increase the electrophilicity of the carbon atom, thus allowing for a smooth addition of the alkyl moiety. Several groups have been demonstrated to activate imines, namely phosphinoyl and sulfonyl adducts. Keeping this in mind, several attempts at the synthesis of **19** were performed. The syntheses begin with the tripod aldehyde, which can be achieved via reduction of the ester **17** to the alcohol **29** utilizing DIBALH, then re-oxidized to the aldehyde **30** using a Swern

oxidation (Scheme 2.1, Path II). The formation of the imine adduct **31** or **32**, followed by methylation using either a Grignard reagent or an alkyllithium reagent are the routes of choice for this transformation (Scheme 2.1, Path III and IV).

2.2 Experimental Section

The experimental details of all attempted and successful syntheses of 7-substituted-2,4,9-trithiaadamantane derivatives are described in this section.

2.2.1 Methods and Materials

Methyl-2,4,9-trithiaadamantane-carboxylate (**17**), was synthesized according to a previous procedure as outlined in Scheme 2.1.[33] Unless otherwise indicated, all materials were obtained from commercial suppliers (Aldrich, Fisher, or Acros) and used without further purification. All organic solvents used were of reagent grade. Tetrahydrofuran (THF) was distilled from sodium benzophenone ketyl, under argon gas. Methylene chloride, toluene, and acetonitrile were all distilled from calcium hydride before use and stored briefly over molecular sieves. Reactions ran under anhydrous conditions were carried out in glassware that was both oven-dried and flame-dried under vacuum. Any moisture- or oxygen-sensitive reactions were performed under an N_2 gas environment. Synthetic products were purified using flash column chromatography and recrystallization. Thin layer chromatography (TLC) was performed using Whatman 250 μm thickness, pre-coated silica gel glass plates and visualized using ultraviolet light

and/or iodine stain. EM silica gel 60 Å (particle size 35-75 μm) was used for purifications done via column chromatography.

All ^{1}H NMR and ^{13}C NMR spectra were obtained using a Varian Mercury-300 spectrometer operating at 300 MHz for ^{1}H and 75 MHz for ^{13}C. The chemical shifts of NMR spectra are reported in parts per million (ppm) relative to the chosen deuterated solvent's reference peak. ^{1}H NMR multiplicity was noted as follows: s, singlet; d, doublet; t, triplet; q, quartet; m, multiplet. Melting points were taken using a MelTemp apparatus. IR spectra were recorded on a Nicolet Nexus 870 FTIR spectrometer equipped with a Thunderdome Attenuated Reflectane (ATR) accessory and peaks recorded in wavenumbers (cm^{-1}). Single crystal X-ray diffraction data were collected at 100K (Bruker KRYOFLEX) on a Bruker SMART APEX CCD-based X-ray diffractometer system equipped with a Mo-target X-ray tube ($\lambda = 0.71073$Å). The detector was placed at a distance of 5.009 cm from the crystal. Crystals were placed in paratone oil upon removal from the mother liquor and mounted on a plastic loop in the oil. Integration and refinement of crystal data were done using Bruker SAINT software package and Bruker SHELXTL (version 6.1) software package, respectively. Absorption correction was completed by using the SADABS program.

2.2.2 Derivative Syntheses

In this section the synthesis of 2,4,9-trithiaadamantan-7-amine (**18**) is described using two different approaches. Also, the attempted syntheses of 1-(2,4,9-trithiaadamantan-7-yl)ethan-1-amine (**19**) as the rimantadine analog are described in

detail. Finally, other attempts at the synthesis of 2,4,9-trithiaadamantane derivatives are reported.

2.2.2.1 Synthesis of 2,4,9-trithiaadamantan-7-amine, $TpNH_2$ (**18**)

Two different methods were used to form the acyl azide intermediate (**27**). The first utilizes hydrazine dihydrochloride to first form the acyl hydrazide directly from $TpCO_2Me$ (**17**). The second method involves conversion of **17** to the acid chloride and then upon treatment with sodium azide yields the acyl azide intermediate.

2.2.2.1.1 Hydrazine dihydrochloride method

Synthesis of the acyl hydrazide (25)

To a 25 mL round bottom flask equipped with a magnetic stir bar was added hydrazine dihydrochloride (0.131 g, 1.25 mmol) and LiOH (0.06 g, 2.51 mmol). The solids were dissolved with H_2O (1 mL) and put on an ice water bath with stirring for 5 min. To a separate 25 mL round bottom flask was added methyl-2,4,9-trithiaadamantane-carboxylate ($TpCO_2Me$, **17**) (0.150 g, 0.604 mmol) and THF (4 mL). This mixture was added dropwise to the flask containing the hydrazine mixture. Additional water (1 mL) was added with stirring. A condenser was added to the reaction flask and the mixture was refluxed for 6 h, during which time solvent evaporated so additional THF (~1 mL) was added to the flask. The reaction was monitored via TLC. Once the reaction had completed, as determined by TLC, the reaction flask was allowed to cool to r.t. and the

solvent was removed under reduced pressure. Residual H_2O remained in the flask with crystals, which were filtered using a Büchner funnel and rinsed with cold H_2O (2 × 5 mL). TLC results were inconclusive due to the large spot of starting material (1:4 EtOAc/hexane, R_f = 0.45) present and two faint spots (1:4 EtOAc/Hexane, R_f = 0.18, 0.74). The tiny amount of crystals on the filter paper was analyzed using FTIR: large C=O peak at 1740 cm^{-1} representative of starting material. A slight peak at 1660 cm^{-1} may indicate some formation of the C=O of the desired amide.

2.2.2.1.2 Sodium azide method

Synthesis of $TpCO_2H$ (26)

Hydrolysis of methyl-2,4,9-trithiaadamantane-carboxylate ($TpCO_2Me$, **17**) (0.252 g, 1.01 mmol) was carried out in THF/H_2O (4 mL, 4:1) in a 25 mL round bottom flask equipped with a magnetic stir bar. To the flask, LiOH (0.252 g, 10.5 mmol) was slowly added and allowed to dissolve completely. The mixture was allowed to stir at r.t. for 1 h. A condenser was attached to the flask, and the reaction was allowed to reflux while stirring for 2 h. The reaction was monitored via TLC. Upon completion, the reaction was cooled to r.t., diluted with H_2O (2.5 mL) and then put on an ice bath. The reaction was acidified using HCl (6 M) to pH ≈ 2 and the solvent was removed using rotary evaporation. The solids were then filtered and the filtrate was extracted using CH_2Cl_2 (3 × 5 mL) and dried over Na_2SO_4. The organic portion was then combined with the solids and dissolved using NaOH (1 M, 5 mL) and washed with CCl_4 (2 × 5 mL). The water layer was then purified using C18 reverse-phase chromatography (20% MeOH in H_2O). The product

was acidified and crystallized upon standing at r.t. giving a pale yellow solid of $TpCO_2H$ (0.220 g, 92%). Melting point: 232-235 °C. R_f = 0.1 (25% EtOAc in hexane). ^1H NMR ($CDCl_3$) δ: 2.96 (d, *J* = 3 Hz, 6H), 4.36 (t, *J* = 3 Hz, 3H). FTIR (ATR): 1702, 2852, 2918, 2700-3200 cm^{-1}.

Synthesis of $TpCON_3$ (27)

To a 25 mL round bottom flask, cooled with an ice bath and equipped with an N_2 inlet, was added a solution of $TpCO_2H$ (**26**) (0.157 g, 0.58 mmol) in CH_2Cl_2 (3 mL). To this solution, while stirring, was added oxalyl chloride (0.5 mL, 0.87 mmol, 2.0 M in CH_2Cl_2) dropwise while under an inert atmosphere. The resulting mixture was allowed to warm to r.t. and then refluxed for 2 h. After evaporation of the solvent and excess reagents under vacuum, an off-white crystalline solid of TpCOCl (0.162 g, 0.641 mmol, 95%) was produced. The crystals were dissolved in dry acetone (3 mL) and a solution of sodium azide (0.125 g, 0.641 mmol) in H_2O (1 mL) was added dropwise via an addition funnel over 1 h while stirred and cooled in an ice bath. The reaction was monitored via FTIR. After stirring at 0°C for 2 h, the reaction warmed to r.t. and H_2O (7 mL) was added. The reaction mixture was extracted using CH_2Cl_2 (3 × 4 mL). The organic layer was collected and dried over $NaSO_4$. After removal of the solvent by rotary evaporation, the $TpCON_3$ was collected as a white crystalline solid (0.108 g, 65%) and used in the next step without further purification. ^1H NMR ($CDCl_3$) δ: 2.87 (d, *J* = 3 Hz, 6H), 4.34 (t, *J* = 3 Hz, 3H) ppm. FTIR (ATR): 1700, 2147, 2916 cm^{-1}.

Synthesis of $TpNH_2$ (18) via a Curtius Rearrangement

The crude $TpCON_3$ (**27**) (0.108 g, 0.42 mmol) was dissolved in THF (12 mL) in a 50 mL round bottom flask with a magnetic stir bar. The reaction flask was equipped with a condenser and refluxed at 60°C for 6 h. The progression of the Curtius rearrangement was monitored via FTIR, which showed a shift from 2136 cm^{-1} to 2239 cm^{-1}. Once the reaction was complete, and the isocyanate intermediate was formed, the flask was cooled to r.t. and HCl (4 mL, 2 M) was added with vigorous stirring for 24 h. Upon complete degradation of the isocyanate group to the amine, as monitored by FTIR, the reaction was considered complete. To the flask, H_2O (5 mL) was added and NaOH (2 M) was used to adjust from a pH of 2 to a pH of 10 with stirring. The solution was washed with CH_2Cl_2 (3 × 15 mL) and the aqueous layer was then purified using C18 reverse-phase chromatography (15% isopropanol in H_2O). The evaporation of solvent gave the product as a waxy, pale yellow crystalline solid (0.077 g, 77%). Crystals suitable for X-ray diffraction were obtained from slow evaporation of the solvent. Melting point: 229-233 °C. ^{1}H NMR ($CDCl_3$) δ: 2.54 (d, J = 3 Hz, 6H), 2.56 (s, 2H), 4.44 (t, J = 3 Hz, 3H) ppm; ^{13}C NMR ($CDCl_3$) δ: 43, 45, 49 ppm; FTIR (ATR): 1421, 1588, 2850, 2918, 3158, 3270, 3328 cm^{-1}. MS (ES) calculated for $C_7H_{11}ClNaNS_3$ [M + H]: 207.0210, found 207.0217.

2.2.2.2 Attempted syntheses of 1-(2,4,9-trithiaadamantan-7-yl)ethan-1-amine

All syntheses in this section rely on conversion of $TpCO_2Me$ to TpCHO before attempts at further transformations. To achieve the aldehyde, the ester is first subjected

to a DIBAL reduction followed by subsequent oxidation, via Swern conditions, to give the aldehyde. The experimental details for these reactions will be covered first, followed by the attempted syntheses of 1-(2,4,9-trithiaadamantan-7-yl)ethan-1-amine.

Reduction of $TpCO_2Me$ (17) to $TpCH_2OH$ (29)

To a flame-dried, 25 mL round bottom flask was added $TpCO_2Me$ (**17**) (0.280 g, 1.10 mmol) and a magnetic stir bar. The reaction flask was equipped with a 3-way stopcock sealed with a rubber septum, and flushed with N_2. The solids were dissolved in freshly distilled toluene (8 mL) and put in an ice/acetone bath at -78°C with stirring. To this mixture, diisobutylaluminum hydride (DIBAL-H) (2.0 mL, 2.42 mmol, 1.2 M in toluene) was added dropwise via syringe at -78°C. The dry ice/acetone ice bath was removed and replaced with an ice bath and the reaction stirred for 2 h at 0°C. The reaction progression was monitored via TLC. Upon completion, MeOH (3 mL) was added and the flask was allowed to warm to r.t. To the reaction H_2O (3 mL) and a saturated NH_4Cl aqueous solution (0.5 mL) was added, during which time a yellow precipitate formed. The mixture was filtered using a Büchner funnel and a pad of Celite. The solvent was then removed under reduced pressure and the product was purified via flash column chromatography (25% EtOAc in hexane) and recrystallization using MeOH to give pale brown crystals of $TpCH_2OH$ (0.233 g, 45%). ^{1}H NMR ($CDCl_3$) δ: 2.56 (d, J = 6 Hz, 6H), 3.36 (d, J = 6 Hz, 2H), 4.30 (t, J = 3 Hz, 6 H).

Oxidation of $TpCH_2OH$ (29) to TpCHO (30)

To a flame-dried 25 mL round bottom flask equipped with a magnetic stir bar and N_2 inlet was added oxalyl chloride (0.07 mL, 0.72 mmol) and CH_2Cl_2 (4 mL). The flask was

put in a dry ice/acetone bath and kept at -78°C with stirring for 5 min. To the reaction vessel, DMSO (0.1 mL, 1.43 mmol) was added dropwise and allowed to stir for 15 min. To this mixture was added $TpCH_2OH$ (**29**) (0.105 g, 0.48 mmol) in CH_2Cl_2 (5 mL) dropwise and allowed to stir at -78°C for 1 h. The reaction was monitored via TLC and upon completion triethylamine (5 mL) was added and the flask was allowed to warm to r.t. The reaction was quenched by addition of H_2O (12 mL) and extracted using CH_2Cl_2 (3 × 5 mL). The solvent was removed using rotary evaporation and yielded a pale tan, crystalline crude product of TpCHO (0.098 g, 94%). ^{1}H NMR ($CDCl_3$) δ: 2.76 (d, J = 3 Hz, 6 H), 4.34 (t, J = 3 Hz, 3H), 9.35 (s, 1H). This material was used in the next reaction (synthesis of the sulfinyl-phosphinamide adduct) without further purification due to its instability.

2.2.2.2.1 Synthesis of N-diphenylphosphinoylimine

Synthesis of *p*-toluenesulfinic acid (PTSA)

To a 500 mL Erlenmeyer flask equipped with a stir bar, was added *p*-toluenesulfinic acid sodium salt (15.5 g, 80 mmol) and H_2O (80 mL). The mixture was allowed to stir vigorously until a clear solution was obtained (70 min). To this solution, *tert*-butyl methyl ether (TBME) (72 mL) was added followed by the dropwise addition of aqueous HCl (12 M, 6.5 mL) and the resulting mixture was allowed to stir at r.t. for 25 min. The mixture was transferred to a separatory funnel and the aqueous layer was drained and toluene (70 mL) was added to the existing organic layer and the solvent was removed using rotary evaporation to give fluffy, white crystals. Heptane (24 mL) was added and

the crystals were collected using a fritted filter and rinsed with heptane. The resulting crystals of *p*-toluenesulfinic acid (10.5 g, 76%) were dried under vacuum.

Synthesis of Tp-sulfinyl-phosphinamide adduct (31)

To a 25 round bottom flask equipped with a magnetic stir bar, was added diphenylphosphinamide (0.10 g, 0.45 mmol), CH_2Cl_2 (1 mL) and diethyl ether (5 mL). This solution was allowed to stir for 5 min. To the stirring solution was slowly added TpCHO (**30**) (0.098 g, 0.45 mmol) in CH_2Cl_2 (2 mL) and diethyl ether (3 mL). This mixture was stirred for 5 min. and then *p*-toluenesulfinic acid (0.071 g, 0.45 mmol) was added and the reaction flask was capped with a rubber septum and allowed to stir at r.t. for 48 h. No product formed during the 48 h reaction. IR and NMR analysis showed that starting material remained. BF_3 was added in an attempt to make the carbonyl carbon more electrophilic without success. Reaction did not take place on the starting material possibly due to steric issues.

2.2.2.2.2 Synthesis of the N-sulfinylimine

Synthesis of pyridinium *p*-toulenesulfonate (PPTS)[61]

To a 25 mL round bottom flask equipped with a stir bar, was added *p*-toluenesulfonic acid (PTSA) (1.42 g, 7.46 mmol) and pyridine (3.0 mL, 37.3 mmol). The mixture was allowed to stir at r.t. for 30 min. The solvent and excess reagent was removed by rotary evaporation and the product was recrystallized using acetone. PPTS was produced as a clear solid (1.72 g, 92%).

Synthesis of Tp-*tert*-butylsulfinimine (32)

A solution of *tert*-butyl sulfonamide (0.29 g, 2.40 mmol) and PPTS (0.24 g, 0.96 mmol) in benzene (15 mL) was added to a 100 mL round bottom flask. The flask was then equipped with a Dean-Stark trap and the side arm was filled with benzene (6 mL) and a small amount of CaH_2. A condenser was attached to the trap and the solution was then heated with stirring. To the warm mixture was added TpCHO (**30**) (0.105 g, 0.48 mmol) dissolved in benzene (10 mL) slowly. A Dean-Stark trap was attached to the flask, and the reaction was allowed to reflux for 2 h, until accumulation of H_2O in the trap subsided and FTIR showed the reaction was complete. The reaction was allowed to cool to r.t. and filtered through a fritted filter with a silica pad and Na_2CO_3 and rinsed with cold CH_2Cl_2. The crude mixture was purified via micro-flash column chromatography (30% EtOAc in hexane). When solvents were removed via reduced pressure, **32** (0.102 g, 66%) was isolated as a fine, white crystalline material. Melting point: 221-226 °C (decomposed). ^{1}H NMR ($CDCl_3$) δ: 1.51 (s, 9H), 2.78 (d, J = 3 Hz, 6H), 4.34 (t, J = 3 Hz, 3H), 7.81 (s, 1H). ^{13}C NMR ($CDCl_3$) δ: 14, 32, 35, 40, 42, 109. FTIR (ATR): 1074, 1620, 2926, 2955 cm^{-1}. MS (ES) calculated for $C_{12}H_{19}NaNOS_4$ [M + Na]: 344.0247, found 344.0247.

Methylation of Tp-*tert*-butylsulfinimine (32) to TpCH(CH_3)NH_2 (19)

To a flame dried 25 mL round bottom flask equipped with an N_2 inlet and a magnetic stir bar was added **32** (0.061 g, 0.190 mmol) dissolved in THF (8 mL). The reaction was cooled to -78°C using a dry ice/acetone bath. Methylmagnesium chloride (0.86 mL, 0.209 mmol, 3.0 M in THF) was added dropwise to the solution and the resulting mixture was allowed to stir for 10 min. The dry ice bath was replaced with an ice/H_2O/NaCl bath

and the flask was allowed to stir for 30 min at -10°C. To quench the reaction, a saturated NH_4Cl solution (5 mL) was added slowly, followed by addition of EtOAc (5 mL). The mixture was separated and the organic layer was washed with a brine solution (5 mL) and dried over $MgSO_4$, filtered and the solvent was removed using rotary evaporation. TLC analysis showed presence of starting material ($R_f = 0.40$), two spots that were UV-visible ($R_f = 0.50$ and 0.81), and a baseline spot. Upon purification using micro-flash column chromatography, four fractions were collected. TLC analysis showed starting material (Tp-CHO) was present, but also a new spot that may be a small amount of the methylated imine. ^{1}H NMR analysis showed the presence starting material and possibly a methylated product.

2.3 Results and Discussion

All syntheses in this chapter begin using **17**, the methyl-2,4,9-trithiaadamantane-carboxylate molecule or tripod (Tp), which was synthesized according to the procedure developed by Khemtong *et al*. (Scheme 2.1) with minor variations. The product was then purified via flash column chromatography and recrystallization until reasonably pure as determined by NMR and TLC analysis. From this tripod molecule several transformations of the methyl ester moiety were performed or attempted to yield the desired functional groups and are described herein. The designed derivatives all have a common starting synthesis, which is described in Scheme 2.2.[33]

Beginning with commercially available dimethyl malonate, the methyl ester tripod ($TpCO_2Me$) was obtained in decent yields (18-34%), through a six-step procedure. the dimethyl malonate (**20**) was converted to the diallyl dimethyl malonate (**21**) by two

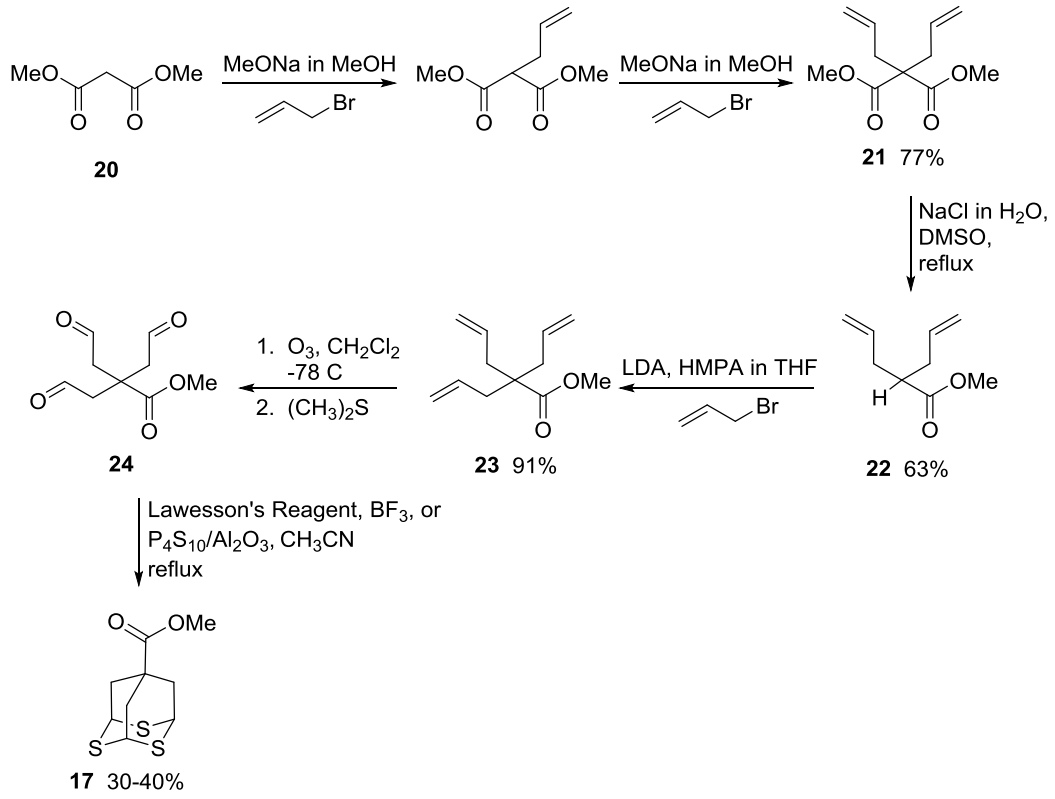

Scheme 2.2: Synthesis of methyl-2,4,9-trithiaadamantane7-carboxylate (**17**). This material serves as the starting material for the syntheses of 2,4,9-trithiaadamantan-7-amine and 1-(2,4,9-trithiaadamantan-7-yl)ethan-1-amine.[33]

successive S_N2 reactions. The next step employs a Krapcho-type decarboxylation using NaCl in DMSO to obtain diallyl methyl acetate (**22**) as an intermediate. To add a third allyl group to afford the triallyl methyl ester (**23**), stronger conditions were required and lithium diisopropylamide (LDA) was used for the deprotonation with hexamethylphosphoramide (HMPA) and again allyl bromide as the allyl source. It

should be noted that this intermediate (**23**) is commercially available from specialty chemical companies; although in this work it was always synthesized directly from dimethyl malonate in the manner just described. The triallyl methyl acetate was purified by vacuum distillation, providing satisfactory yields (84-93%). The triallyl compound could be stored at room temperature for long periods of time with no degradation.

To convert the triallyl methyl acetate to the trialdehyde intermediate, ozonolysis of the allyl group was performed in methylene chloride, followed by reduction of the ozonide intermediate with dimethyl sulfide, successfully converting the triallyl compound to the trialdehyde (**24**). Upon treatment with a thionating agent (P_4S_{10}/Al_2O_3 or Lawesson's reagent/BF_3) and heating, $TpCO_2Me$ (**17**) was achieved in modest yields (10-30%). The final product was typically purified via two or more flash columns, eluting off the column at 25% EtOAc in hexane. In this synthesis, either dimethyl malonate or diethyl malonate could be utilized as starting compounds, but it was found that when the diethyl malonate was used, the decarboxylation step was significantly slower than when using the dimethyl equivalent.[33] Also, transesterification was observed when using the diethyl malonate in methanol during formation of the alkoxide reactants. To avoid transesterification from occurring, the corresponding alkyl groups must be used as both the starting malonate and the solvent during the alkoxide formation.

2.3.1 2,4,9-Trithiaadamantan-7-amine (**18**) syntheses

Existing syntheses for amantadine and compounds similar to **18**, although not very common, can be found in the literature and several were discussed in Chapter 1.[11-15]

A major problem in the manipulation of the methyl ester functionality on the trithiaadamantane is the harsh reaction conditions required when performing transformations on similar adamantane-based starting materials. The degradation of the tripod base has been observed when attempting to use similar reactions reported in the literature for syntheses of amantadine and similar molecules. It has been observed that the tripod molecule does not tolerate strong acids or bases, and it decomposes upon treatment with *n*-butyllithium.[33] The strategy employed here was to first convert the tripod-methyl ester to the azide, followed by thorough heating and acid work-up, via a Curtius rearrangement, the primary amine derivative could be achieved.[42-48] There were two routes taken to form the azide intermediate. The first route starts directly with $TpCO_2Me$ and via the addition of hydrazine to the carbonyl, gives an acyl hydrazide intermediate, which is subsequently oxidized using nitrous acid to the azide, and then thermally decomposed via the Curtius rearrangement. This route is depicted in Path I of Scheme 2.2. A second, longer route, involves the conversion of the $TpCO_2Me$ to the carboxylic acid, and further to the acid chloride. The amine is then formed by treatment of the acid chloride with sodium azide and again a thermal decomposition of the azide to the isocyanate intermediate, which is subsequently hydrolyzed to the free amine.

2.3.1.1 Hydrazine dichloride reaction

The first attempt to generate **18** was through the synthesis of an acyl hydrazine intermediate (**25**) from the treatment of **17** with hydrazine as described by Koza, and is shown in Scheme 2.3.[39] Once the hydrazine intermediate could be obtained, treatment

with HCl would lead to the azide product (**26**). The azide could then be subjected to the Curtius rearrangement to liberate the primary amine. To first form the acyl hydrazine, following similar reaction conditions to those used by Koza, the $TpCO_2Me$ and hydrazine dihydrochloride were dissolved in methanol (wet) and the reaction stirred while refluxing for 18 h. This reaction provided trace amounts, at best, of the desired hydrazine product. FTIR and TLC analysis of the reaction mixture showed mainly just the starting material ($TpCO_2Me$). This result was possibly due to solubility issues of the tripod in methanol, or even an equilibrium issue with using methanol. The second attempt at this reaction included re-evaluation of the solvents used. Since there were only trace amounts of the desired product obtained, it was thought that maybe the methanol solvent was causing a shift in the equilibrium favoring the addition of methanol to the amide giving the ester as the product. The reaction was ran a second time using a mixed solvent system of

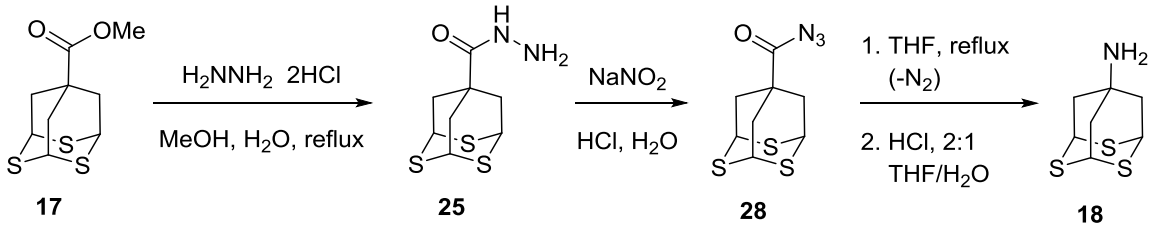

Scheme 2.3: First attempt towards 2,4,9-trithiaadamantan-7-amine (**18**).[39]

THF:H_2O (2:1). Also, lithium hydroxide (1 equiv) was added to further help shift the equilibrium. FTIR and TLC analysis of the reaction showed the acyl hydrazine product was present in very small amounts, but again a majority of the mixture was still the starting ester. The tripod ester carbonyl peak was present around 1730 cm^{-1} and the

hydrazine amide peak was present (albeit very faint) at around 1660 cm^{-1}. The TLC analysis showed mostly starting material (R_f = 0.45) with two additional spots above (R_f = 0.74) and below (R_f = 0.18) that both stained with iodine, but were not UV visible. It was assumed the two non-UV visible spots were side products present from impurities in the reaction because the tripod is both UV visible and stains with iodine. Attempts at separating this mixture, if even to recover the starting ester, proved to be unsuccessful in the solvent systems that were evaluated.

2.3.1.2 Sodium azide reaction

Considering the poor results of the previous experiment, a more traditional synthetic approach was used to make **18** as described in Scheme 2.4.[42,43] Starting with **17**, the methyl ester moiety was easily hydrolyzed to the corresponding carboxylic acid (**26**) using lithium hydroxide in excellent yields (92%). After neutralization of the reaction using dilute hydrochloric acid, the $TpCO_2H$ was then converted to the corresponding acid chloride (**27**) using oxalyl chloride with yields over 95%. Subsequent treatment of crude TpCOCl (**27**) with sodium azide in cold, freshly distilled acetone yielded $Tp\text{-}CON_3$ (**28**). This product was used without purification due to its instability. Upon re-dissolving in freshly distilled THF, **28** was refluxed for 24 h under an inert atmosphere to induce the Curtius rearrangment.[47-50] The reaction was monitored while refluxing via FTIR and spectra were collected at 0 h, 1 h, 3 h, 6 h, and 24 h increments until the azide peak at 2136 cm^{-1} was almost completely gone and the isocyanate (**33**) peak at 2239 cm^{-1} appeared. The compilation of FTIR spectra showing the degradation of the azide to the

isocyanate are shown in Figure 2.3. After formation of **33** was confirmed, HCl (2M) was added to hydrolyze the isocyanate giving amine **18** in the hydrochloride salt form. The free amine was obtained in a 77% yield, through deprotonation of the ammonium salt using 2M sodium hydroxide.

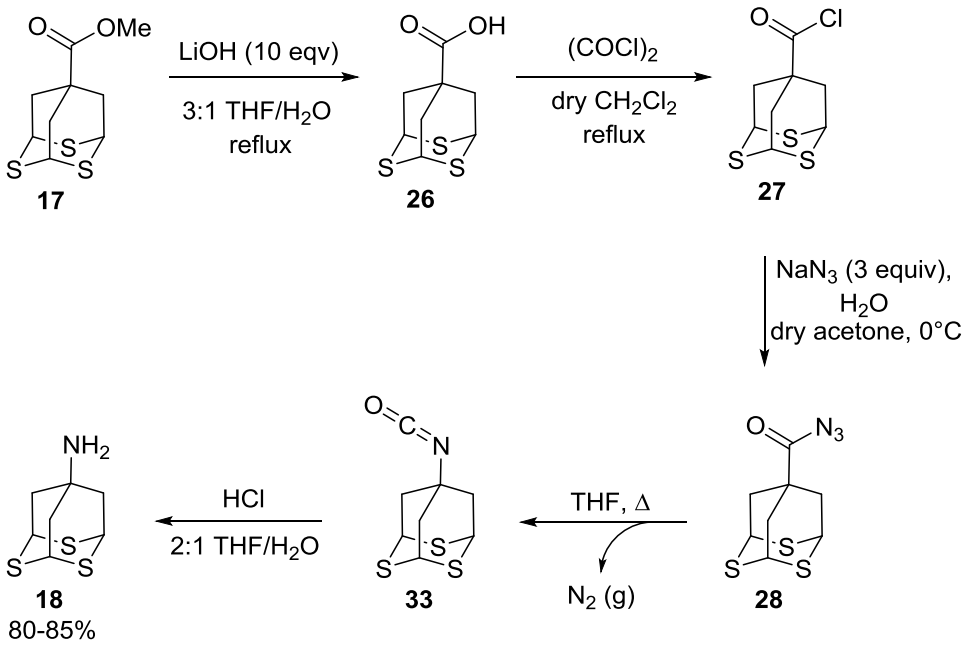

Scheme 2.4: The synthesis of 2,4,9-trithiaadamantan-7-amine (**18**).[42,43,47-50]

^{1}H NMR analysis confirmed the presence of **18**, showing slightly shifted peaks of the trithiaadamantane structure at 2.55 (C*H*$_2$) and 4.44 (SC*H*S) ppm, mass spectrometry was performed on **18**, and a crystal structure was obtained. The bond angles of the carbon atoms are close to tetrahedral, ranging from 97-113°. The bond angles of the carbon atoms at the shoulder of the molecule have the upper limit of the tetrahedral angle (113°), most likely due to the large, sulfur containing ring at the base of the molecule

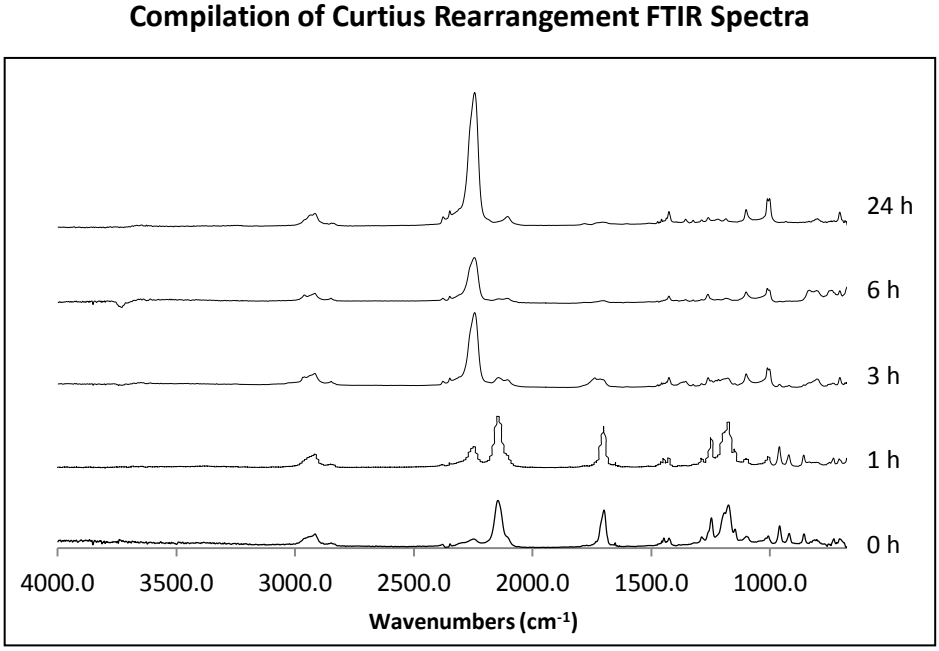

Figure 2.3: The FTIR spectra of the Curtius rearrangement of $TpCON_3$ (**28**) to TpNCO (**33**). Normalized to the CH peak at 2913 cm^{-1}.

exerting a pull on that angle. The bond angles surrounding the carbon atoms at the top of the molecule are all at 110° because there is no direct strain from the sulfur-containing ring on these bonds. The bond angles surrounding the carbon and sulfur atoms adapt a distorted tetrahedral shape, with bond angles ranging from 97-112°. The amine H-N-H bond angle was found to be 113°, which is close to the trigonal pyramid geometry typical in primary aliphatic amines. The bond lengths were close to what was expected, with the C-S bond lengths close to 1.82 Å, and C-C bond lengths ranging from 1.52-1.54 Å.[36] The mass spectrometry and crystal structure results are shown in Figures 2.4 and 2.5 respectively. The single crystal X-ray diffraction parameters are summarized in Table 2.1 and selected bond lengths and angles are presented in Table 2.2.

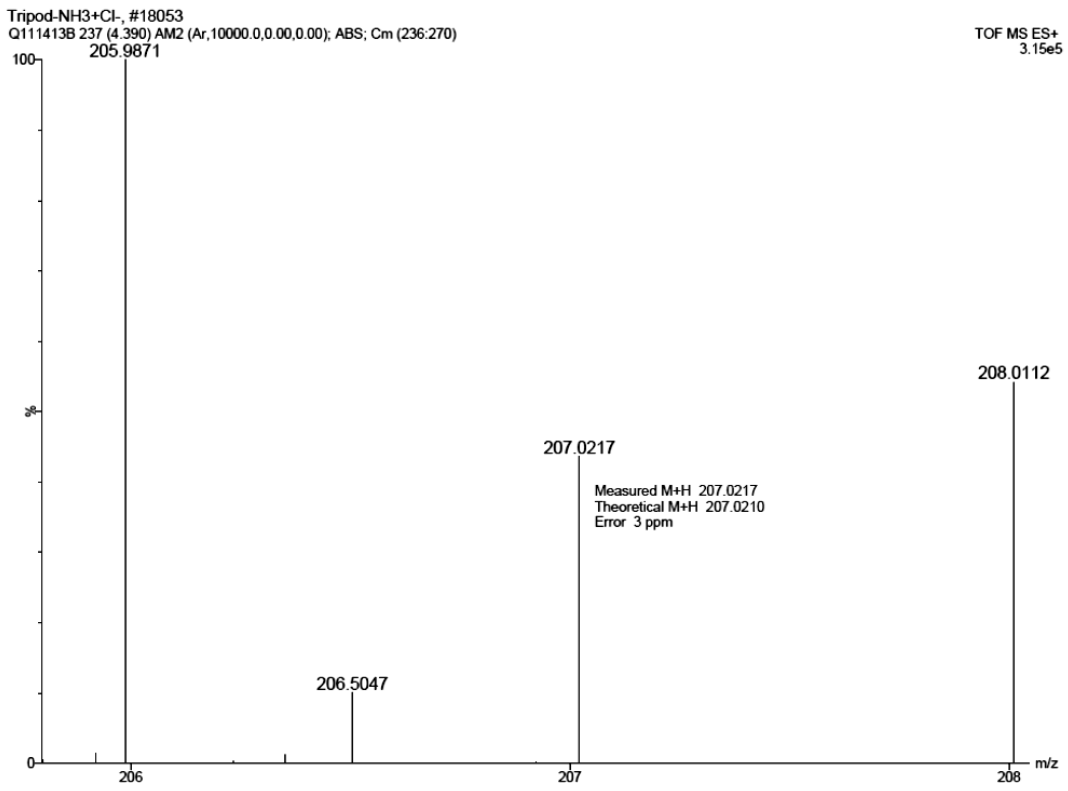

Figure 2.4: High resolution mass spectrometry of 2,4,9-trithiaadamantan-7-amine (**18**).

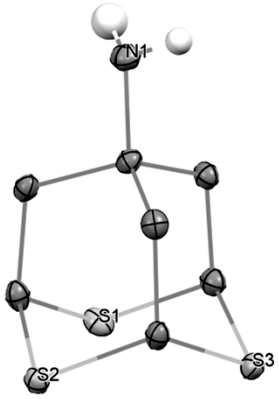

Figure 2.5: The X-ray crystal structure of 2,4,9-trithiaadamantan-7-amine (**18**) with 35% thermal ellipsoids. Hydrogen atoms on the carbon positions were omitted for clarity.

Table 2.1: Crystal data and structure refinement parameters for **18**.

Empirical formula	$C_7H_{11}NS_3$	
Formula weight	205.35	
Temperature	100(2) K	
Wavelength	0.71073 Å	
Crystal system	Orthorhombic	
Space group	P2(1)2(1)2(1)	
Unit cell dimensions	a = 6.732 (3) Å b = 11.308 (5) Å c = 11.602 (5) Å	α = 90° β = 90° γ = 90°
Volume	883.2(6) $Å^3$	
Z	4	
Density (calculated)	1.544 Mg/m^3	
Absorption coefficient	0.771 mm^{-1}	
F(000)	432	
Crystal size	0.18 × 0.14 × 0.10 mm^3	
Theta range for data collection	2.52° to 25.18°	
Index ranges	$-8 \leq h \leq 8$, $-13 \leq k \leq 13$, $-13 \leq l \leq 13$	
Reflections collected	6286	
Independent reflections	1575 [R(int) = 0.0504]	
Completeness to theta = 25.14°	100%	
Absorption correction	SADABS	
Max. and min. transmission	0.9269 and 0.8737	
Refinement method	Full-matrix least-squares on F^2	
Data / restraints / parameters	1575 / 0 / 108	
Goodness-of-fit on F^2	1.054	
Final R indicies [$I > 2\sigma(I)$]	R1 = 0.0260, wR2 = 0.0664	
R indicies (all data)	R1 = 0.0268, wR2 = 0.0671	
Absolute structure parameter	0.05(9)	
Largest diff. peak and hole	0.277 and -0.260 e $Å^{-3}$	

Table 2.2: Selected bond lengths and bond angles of **18**.

Bond Lengths, (Å)	
C-C	1.540(3), 1.535(3), 1.540(3), 1.527(3), 1.534(3), 1.526(3)
C-S	1.820(2), 1.827(2), 1.821(2), 1.823(2), 1.828(2), 1.823(2)
C-N	1.472(3)
N-H	0.95(2), 0.83(2)
Bond Angles, (°)	
C-C-C	110.6(2), 110.4(2), 110.4(2), 113.2(2), 113.0(2), 113.0(2)
C-C-S	111.6(1), 111.6(1), 111.0(1), 111.7(1), 111.4(1), 111.4(1)
S-C-S	112.0(1), 112.7(1), 112.6(1)
H-N-H	113(2)
C-S-C	97.5(1), 97.38(9), 97.45(9)
C-C-N	110.6(2), 107.6(2), 107.1(2)

2.3.2 1-(2,4,9-Trithiaadamantane-7-yl)ethan-1-amine syntheses

The synthesis of the rimantadine analog proved to be much more difficult than the amantadine analog. The first step in transformation of the ester to an imine, and ultimately to a α-branched amine, is the formation of an aldehyde. The transformation was easily achieved by first performing a reduction of $TpCO_2Me$ using diisobutylaluminum hydride (DIBAL) to give the alcohol $Tp\text{-}CH_2OH$, followed by a Swern oxidation of the alcohol to give the desired aldehyde (**16**) in excellent yields (94%). This reaction sequence is outlined in Scheme 2.5.[51,52] Here, 2 equivalents of

DIBAL were used to reduce the ester completely to the primary alcohol (**29**). In an attempt to stop the reduction at the aldehyde in only one step, the reaction was run using only 1.0 equivalent of DIBAL with strict temperature control, but a mixture of alcohol and aldehyde products resulted. So it was preferred to reduce the ester all the way to the alcohol and then re-oxidize to the aldehyde. The reduction was carried out in toluene and kept at -78°C during addition of the reagents. The reaction was allowed to warm to 0°C until TLC analysis showed the reaction was complete. Upon completion, methanol was added to quench the reaction. The yields of this reaction ranged from 40-57%, mainly due to solubility issues during extraction.

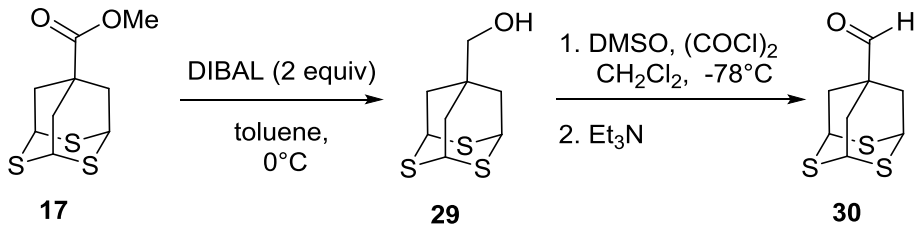

Scheme 2.5: The synthesis of 2,4,9-trithiaadamantane-7-aldehyde (**30**).[51,52]

The alcohol (**29**) was then re-oxidized to **16** using Swern oxidation conditions. This reaction was carried out at -78°C in dry CH_2Cl_2 using Et_3N as the base. The aldehyde product **30** achieved was usually pure enough, as determined by ^1H NMR and FTIR, to use in subsequent reactions without further purification.

From **30**, an imine adduct could be added, by use of either *P,P*-diphenylphosphinic amide or *tert*-butylsulfinamide.[53-58] Both pathways are outlined in

Scheme 2.1 (Path III and IV, respectively). From this imine intermediate, the introduction of a methyl group can be achieved by way of a Grignard reagent or an organolithium reagent, and the attempts at these reactions are discussed in the following sections.[59,60]

2.3.2.1 N-Diphenylphosphinoylimine reaction

The first attempt at **19** was through an adaptation of a procedure by Desrosiers and co-workers (Scheme 2.6) by creating an *N*-phosphinoylimine via a stable sulfinyl adduct and subsequent conversion to an imine followed by hydrolysis and release of the free amine.[53] In this procedure, **30** served as the starting material for which the imine adduct was formed. The aldehyde was dissolved in a solvent mixture of 5:1 diethyl ether/CH_2Cl_2 and added to a solution of *P,P*-diphenylphosphinic amide in methylene chloride and ether followed by addition of *p*-toluenesulfinic acid (PTSA). The *p*-toluene sulfinic acid is commercially available, but it was synthesized from the treatment of *p*-toluene sulfinic acid sodium salt with HCl (conc)/H_2O, in TBME according to the procedure by Sisko and co-workers.[55] It was anticipated that this reaction would yield the α-tosyl amine intermediate **33**, however according to TLC and ^{1}H NMR analysis the reaction did not take place. The most likely reason this reaction did not go forward is the steric issues of the reactants. The presence of a tertiary carbon adjacent to the carbonyl and the large aromatic substituents present on the nucleophilic diphenylphosphinic amide

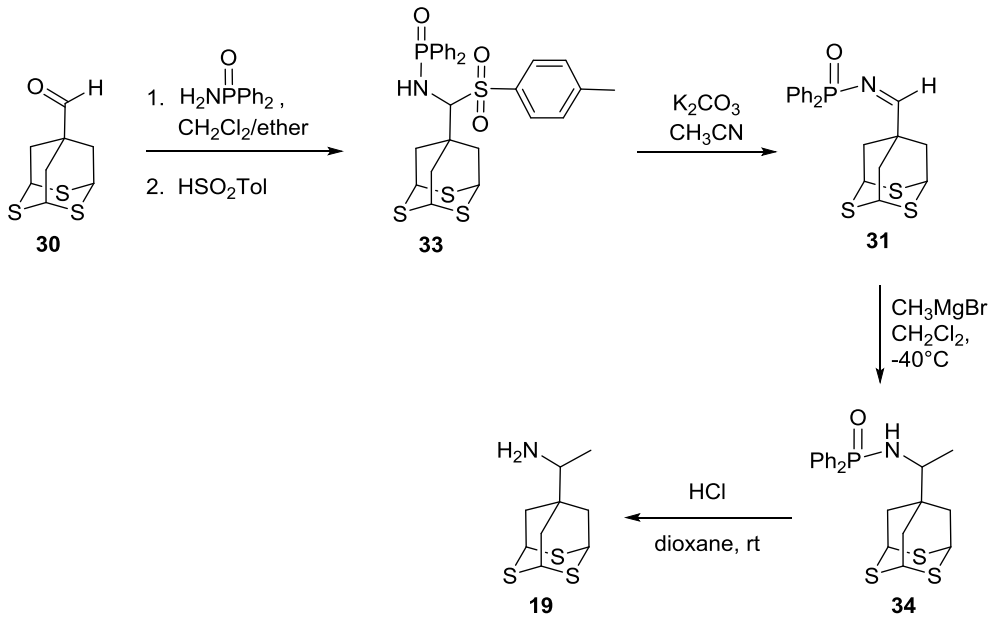

Scheme 2.6: First attempt at 1-(2,4,9-trithiaadamantan-7-yl)ethan-1-amine (**19**) via an N-diphenylphosphinoylimine.[53-55]

and PTSA may not allow for room to add the amide to the aldehyde. Further adding to the congestion of the electrophilic site is the bulky tripod ring-system itself. The TLC and NMR analysis showed no reaction had occurred, and not even trace amounts of product had formed. After 48 h, an aldehyde peak at 9.35 ppm in the ^{1}H NMR, characteristic of the TpCHO, still remained. Also, the FTIR analysis showed the presence of the carbonyl still present at 1715 cm^{-1}. A Lewis acid (BF_3) was added to the reaction to try and enhance the electrophilicity of the carbonyl, but this had no effect on the reaction. If there was a solubility or reactivity issue, at least trace amounts of product should have been detected. The ^{1}H NMR spectrum of the resulting mixture is shown in Figure 2.6. After two attempts at this reaction and no production of the desired

phosphinoyl adduct or the imine, a different reaction scheme was investigated, which involves a less bulky sulfinylimine intermediate.

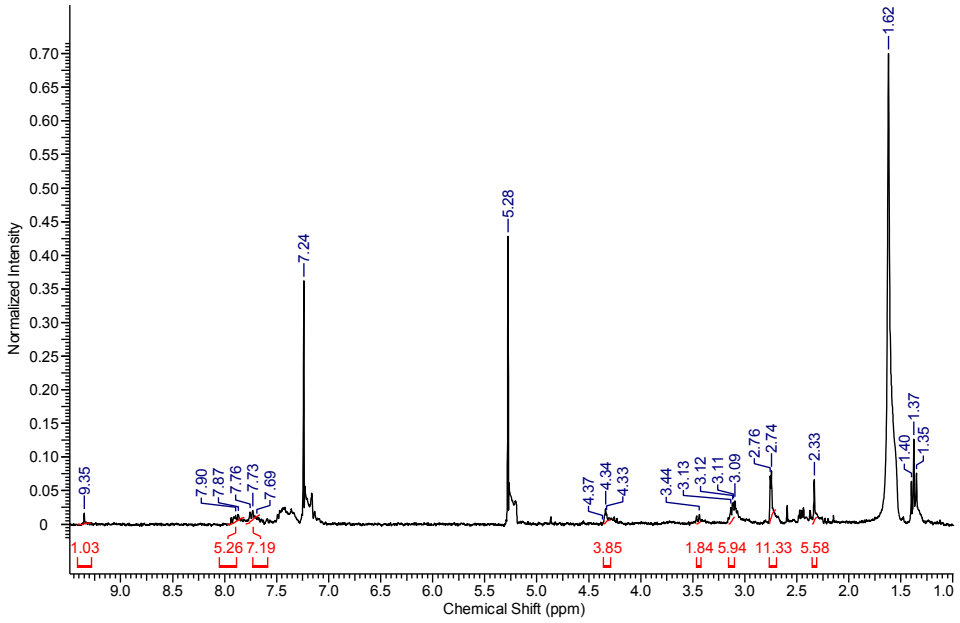

Figure 2.6: The ^{1}H NMR spectrum of the crude mixture of **16** with *P,P*-diphenylphosphinic amide and *p*-toluenesulfinic acid after 48 h. The peaks at 7.24, 5.28, 3.12-3.09, 1.62, 1.39-1.35 ppm correspond to solvents $CDCl_3$, CH_2Cl_2, diethyl ether, H_2O, and diethyl ether, respectively.

2.3.2.2 N-Sulfinylimine reaction

The next synthesis aimed at producing the rimantadine analog **19** involved the formation of a less bulky, N-*tert*-butanesulfinyl imine intermediate. From this intermediate, the methyl group could be added using similar rationale as the previous attempt, using methylmagnesium chloride (or methyllithium), and a subsequent hydrolysis of the protecting group to give the desired ethyl amine moiety. This procedure was adapted from Modhu[56] and Han[58], and the reaction sequence is outlined in Scheme

2.7. In this reaction sequence, the aldehyde **30** again serves as the starting material to which the *t*-butylsulfinyl imine could be added, using pyridium *p*-toluenesulfonate

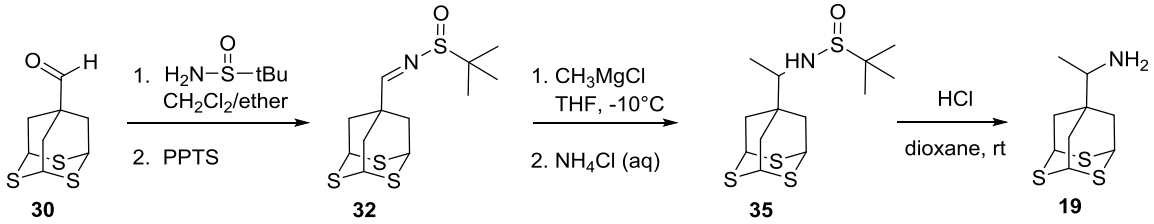

Scheme 2.7: Second attempt at 1-(2,4,9-trithiaadamantan-7-yl)ethan-1-amine (**19**) via an N-sulfinylimine.[56-58]

(PPTS) as the acid catalyst.[56] The PPTS was synthesized prior to the reaction in a procedure similar to that by Miyashita and co-workers.[61] This high-yielding reaction converted *p*-toluenesulfonic acid to PPTS by addition of pyridine with stirring at room temperature for 25 min. Recrystallization of the product in acetone gave pure PPTS in 92%.

The first attempts at this reaction used CH_2Cl_2 or THF as the solvent, due to the high solubility of **30** in these solvents. During the reactions, magnesium sulfate and sodium sulfate were added to the reaction flask to remove any water produced; however, both reactions yielded the starting compound, and no desired product was indicated by TLC and NMR analysis. A Dean-Stark trap was then employed to better remove any H_2O produced and prevent hydrolysis of the imine adduct prior to methylation. In this method, benzene was used as the solvent. The *t*-butyl sulfinamide, benzene and PPTS were added to a flask, which was equipped with the Dean-Stark trap and condenser. The mixture was warmed and compound **30** was slowly added. After stirring for 2 h, H_2O

accumulation in the trap subsided and ^{1}H NMR analysis showed the aldehyde peak at 9.35 ppm was no longer present. The reaction was filtered and rinsed with cold CH_2Cl_2

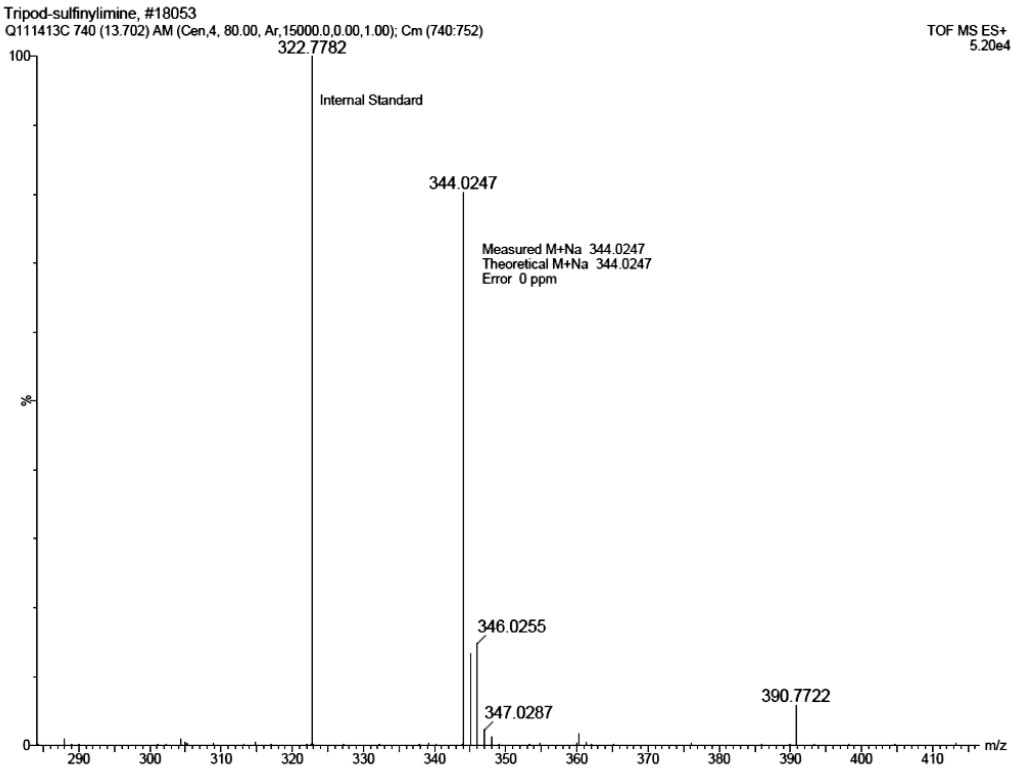

Figure 2.7: High resolution mass spectrometry of the sulfinylimine intermediate **32**.

and purified using a micro-flash column. The product eluted off the column as the second component using 30% EtOAc in hexane. This isolated intermediate was characterized through FTIR, ^{1}H NMR, ^{13}C NMR, and mass spectrometry. The mass spectrometry results are shown in Figure 2.7.

To introduce the methyl substituent onto the imine, a Grignard reagent was used. The imine was added to methylmagnesium chloride in THF at -78°C, to reduce the

competing radical reaction, and then warmed to -10°C using a salt water/ice bath for the remaining 30 minutes of the reaction. Once a saturated solution of ammonium chloride was added to quench the reaction, extraction was done using ethyl acetate to remove all product from the aqueous phase. After a micro flash column separation was carried out, TLC analysis, using 25% EtOAc in hexane, on the four fractions collected showed the presence of starting material, which is UV-visible, stains with iodine and has an R_f = 0.45. There was also two faint spots present that were UV-visible and stained using iodine with R_f values of 0.50 and 0.81. There was a baseline spot present that was both UV-visible and stained with iodine. The spot at R_f = 0.50 may be indicative of a small amount of methylated product present. ^{1}H NMR analysis on the crude mixture confirmed the presence starting material. The reaction may not have been allowed to stir for a long enough period of time, or the temperature may have been too low for the reaction to have taken place.

2.4 Conclusions and Future Work

As described in this chapter, the synthesis of 2,4,9-trithiaadamantan-7-amine was successful, and full characterization of the molecule was carried out, including the crystal structure. The synthetic pathway to creating this molecule has low yielding reactions, and will need to be re-evaluated to be of any commercial use. An agreement with NIH for testing on this molecule for antiviral activity was achieved. Once this molecule is evaluated for its efficacy against the influenza A virus, other derivatives can be designed and synthesized to accommodate the results.

The 1-(2,4,9-trithiaadamantan-7-yl)ethan-1-amine compound was much more difficult to obtain, and reactions attempted thus far have been unsuccessful at synthesizing this molecule. The 2,4,9-trithiaadamantane-7-*tert*-butylsulfinimine intermediate was isolated and characterized. From this intermediate, the addition of the methyl group can be carried out with methyllithium, instead of a Grignard reagent. Because the Grignard reagents require a low temperature during addition, this may have been the reason for the reaction not occurring. However, use of an organolithium reagent may allow for the reaction to be run at higher temperatures. Furthermore, alternative reaction schemes leading to the direct transformation of the $TpCO_2Me$ into the methyl-amine derivative need to be explored. The conversion of the methyl ester to a methyl ketone would be ideal for this reaction. A Weinreb-type reaction on the acyl chloride intermediate could lead to a methyl ketone, which may then be converted to the amine by reductive amination.[62] The reaction conditions for such a transformation would need to be evaluated to make certain the carbon/sulfur ring of the tripod is not opened during the reaction, a problem that is all too common when working with this molecule. Also, an idea for improving the overall reaction would rely on beginning with the desired amine on the triallyl starting material, and then reacting further to cyclize the tripod C-S-C ring. The next chapter will discuss some advances in the synthesis of starting materials.

CHAPTER III

NEW SYNTHESES TO METHYL-2,4,9-TRITHIAADAMANTAN-7-CARBOXYLATE AND OTHER POSSIBLE ROUTES TO NEW DERIVATIVES

3.1 Introduction

The starting material used to prepare 7-substituted-2,4,9-trithiaadamantane derivatives varies depending on the desired product. All previous synthetic schemes for the preparation of this material, designed by Khemtong *et al*., began with the ozonolysis of triallyl methyl acetate, followed by sulfonation of the trialdehyde to give the methyl ester version of the tripod molecule.[32-34] This reaction sequence is shown in Scheme 3.1. Transformation of the methyl ester moiety in **17** to the desired functional group takes several additional steps in an already lengthy, low-yielding synthesis. The highest reported yield of trithiaadamantane itself is 38%.[32] Even this unsatisfactory yield was not always possible by this synthetic route and much lower yields ranging from 8-20% were often obtained. The aim of this chapter is to evaluate new approaches for the preparation of methyl-2,4,9-trithiaadamantane carboxylate ($TpCO_2Me$) in a more efficient manner, as well as to examine new materials that may better serve as starting points for future 2,4,9-trithiaadamantane derivatives as antiviral candidates.

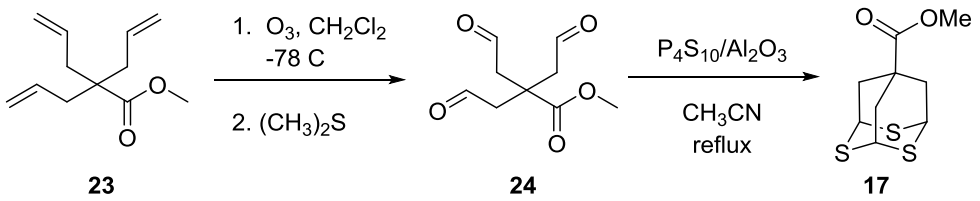

Scheme 3.1: Original synthesis of **17**.[32-34]

One of the issues with the original synthesis of $TpCO_2Me$ is the formation of formaldehyde during the reduction of the ozonide intermediate. Formaldehyde is not a desirable molecule to have in the reaction mixture, not only because it's a suspected carcinogen, but because it can lead to the production of side products, such as trithiane, when present during the thionation reaction (Figure 3.1).[63] Trithiane has been observed in the analysis of crude tripod product mixtures, and separating it from the tripod has required exhaustive measures. Although some of the formaldehyde gets further oxidized to carbon dioxide during the reaction, there may still be some present, especially when using H_2S as the thionating agent.[63] If this side reaction could be avoided, the yields would increase and purification efforts would be simpler. To prevent the formation of formaldehyde, a Grubbs catalyst was employed to induce a ring closing metathesis of the triallyl methyl acetate (Scheme3.2).[64] Prior to the ozonolysis of triallyl methylacetate,

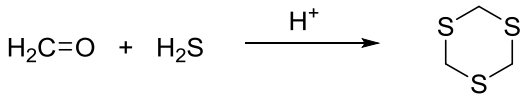

Figure 3.1: Formation of the trimer by-product, trithiane, from formaldehyde and hydrogen sulfide.[63]

the Grubbs catalyst can be added to form a dimer intermediate (**36**). Upon ozonolysis and reduction, intermediate **36** then forms the same product as the original synthesis (**24**) without creating formaldehyde.

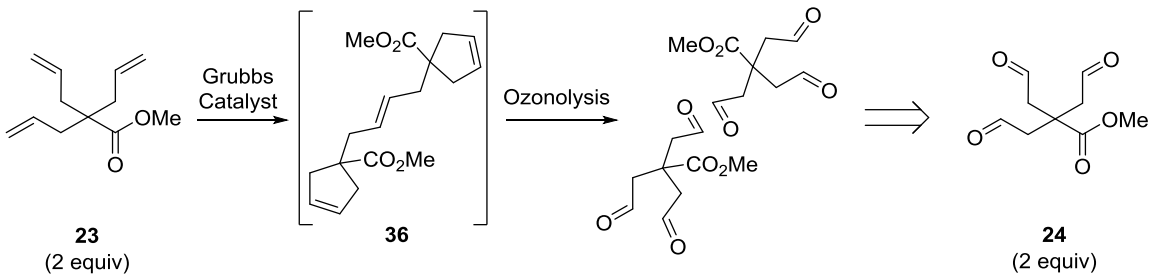

Scheme 3.2: Ring closing metathesis of triallyl methylacetate using a Grubbs first generation catalyst. Reaction with **23** gives a proposed dimer (**36**), and subsequent ozonolysis and reduction to afford **24**.[64,65]

Furthermore, once the thionating agent is added, the formation of a thiocarbonyl intermediate is thermodynamically unfavorable. Comparison of a thiocarbonyl (~128 kcal/mol) to a carbonyl (~192 kcal/mol) bond energy indicates the C-S double bond is much weaker in strength due to the poor overlap of carbon 2p orbital and the sulfur 3p orbital.[41] Adding a reagent such as a silane to bond to the oxygen atoms of the intermediate may be beneficial to ensure proper incorporation of sulfur into the ring system and reduce the amount of mixed products.

The original synthesis of $TpCO_2Me$ commonly led to an inseparable mixture of compounds with oxygen, instead of sulfur, incorporated into one or more positions on the base on the tripod (Fig. 3.2). NMR analysis can confirm the presence of oxygen atoms in

the base of the tripod ring and the trioxaadamantane product has been successfully isolated and characterized. However, the formation of these oxygenated products becomes an issue if the trithia-tripod is the sole desired product. To address this problem, the use of an "oxygen scavenger" reagent, such as a silane, can be used to decrease the likelihood of incorporation of oxygen into the trithiaadamantane ring (Scheme 3.3).[66-69] With the formation of a Si-O bond as the driving force, the addition of sulfur atoms to the carbonyl is more likely.[66,68]

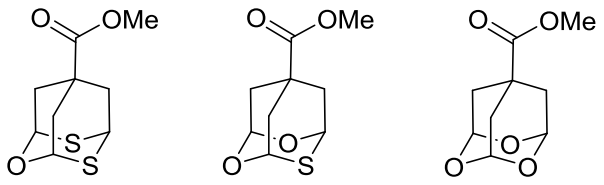

Figure 3.2: Structures of oxygen-substituted trithiaadamantanes.

Formation of a thiocarbonyl at the ester moiety of the molecule is also possible when a silane is used to promote the formation of the thiaaldehyde intermediate, making characterization of the compound difficult. To prevent this side-reaction from occurring, the methyl ester could be easily substituted with a more bulky alkyl group, such as a *tert*-butyl group, via a transesterification reaction.[70] This substitution would sterically hinder the carbonyl enough to reduce the likelihood of sulfur addition during thionation.

A reactive trialdehyde species (**24**) is also formed upon ozonolysis and reduction in the original synthesis. Because **24** is prone to oligomerization at low temperatures, the formation of a "sludge-like" polymeric by-product has been observed and hinders the

progression of the reaction, as well as purification of the desired product.[71] The incorporation of a mechanical stirrer slightly helped by breaking up the polymer sludge enough to prevent the reaction from burning, but a chemical resolution to the problem is needed. One such resolution to this issue was the protection (acetalization) of the trialdehyde via addition of either ethylene glycol or the use of methanol as a solvent during ozonolysis to form a triacetal intermediate (**37** or **38**) (Scheme 3.3).[72-75] This protection of the aldehyde moieties may help with reducing intramolecular polymerization and by-product formation.

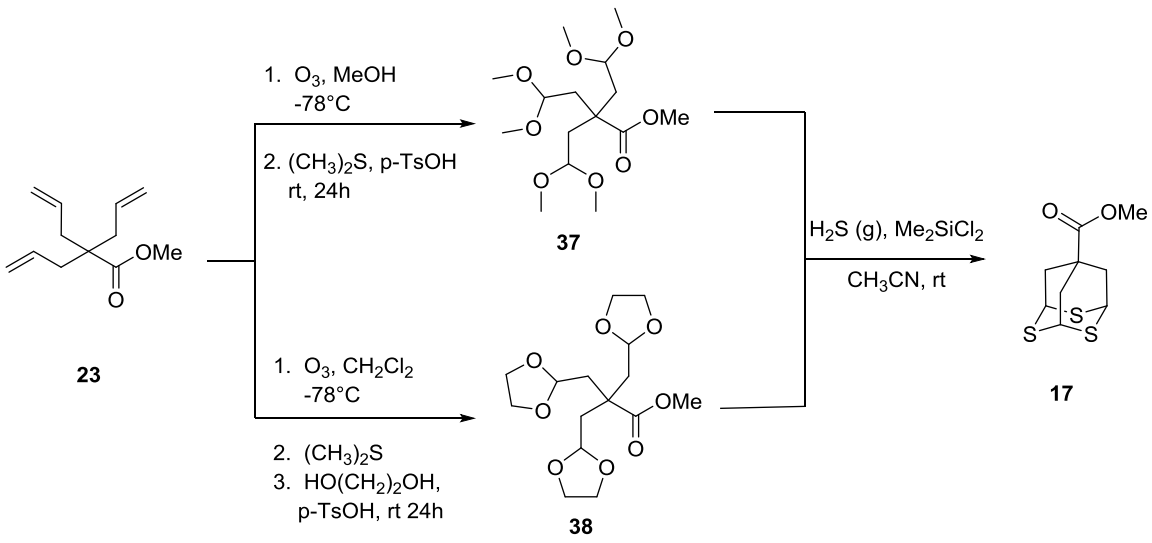

Scheme 3.3: Synthesis of a protected intermediate (**37** or **38**) followed by thionation to afford tripod (**17**).[66-69,72-75]

After the acetal is formed, subsequent treatment with H_2S and a silane (trimethylsilyl chloride or dichlorodimethyl silane) could induce cyclization of the trithiane ring without incorporation of oxygen atoms, leading to the tripod product

(Scheme 3.3).[66-69,72-75] In a procedure proposed by Claus and Schrieber, the ozonolytic cleavage of cyclohexene was performed in methanol, leading to the formation of the protected diacetal (**41**), as illustrated in Scheme 3.4.[72] This acetal is very similar in structure to **37**, and is formed under mild conditions. First, ozonolysis of the alkene gives a hydroperoxy hemiacetal (**39**), which undergoes dehydration to form the acetal **40**. Addition of *p*-toluenesulfonic acid catalyzes the acetal formation of the remaining aldehyde moiety to afford the diacetal **41**. If this intermediate could be obtained prior to thionation, then the incorporation of oxygen atoms into the ring and polymerization by-products would be avoided.

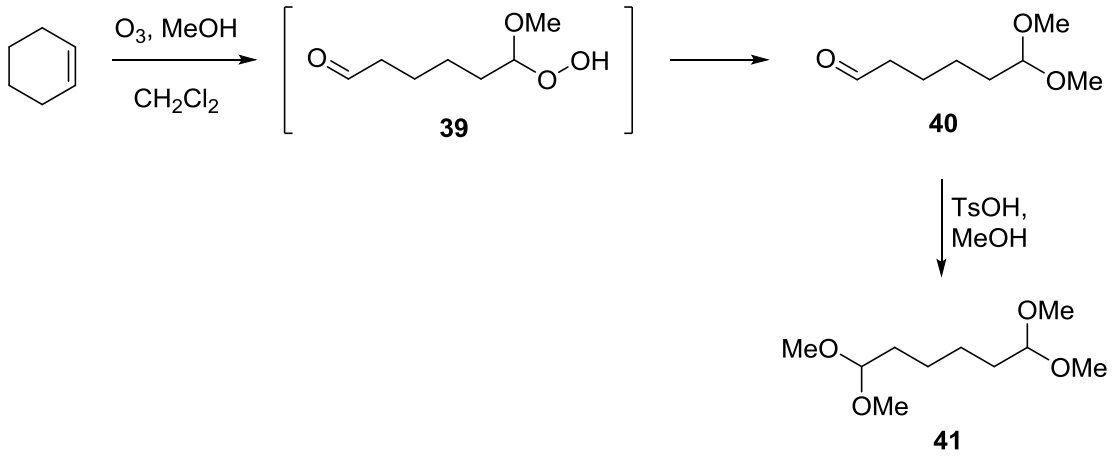

Scheme 3.4: Acetal formation of cyclohexene as proposed by Claus and Schrieber. The scheme is modified from reference 72.

To obtain the tripod molecule from an acetal, as proposed in Scheme 3.3, the cleavage of the ether groups and thionation must subsequently occur. A similar strategy was employed by Olah *et al.*, who were able to accomplish the cleavage (dealkylation) of

ethers using methyltrichlorosilane and sodium iodide to give alcohols and iodides.[66] The ethers used in this work had similar structures to **37** or **38** (Scheme 3.5).[66] This transformation was shown to occur via the addition of the silane to the oxygen atom of the ether, to form a suggested transition state structure **42**, followed by either an S_N1 or S_N2 reaction, depending on the ether. Primary and secondary alkyl ethers led to mainly alcohol products via an S_N2 pathway (Pathway I, Scheme 3.5) and ethers with tertiary alkyl groups led to the formation of iodides as the major product (Pathway II, Scheme 3.5).[66] This transition state structure is of particular interest when considering the reaction shown in Scheme 3.3. It is likely that this type of mechanism would be present in an attempt to remove the protective ether moiety with a silane, and also prevent the incorporation of oxygen atoms in the trithiane ring, in a reaction to prepare the tripod molecule.

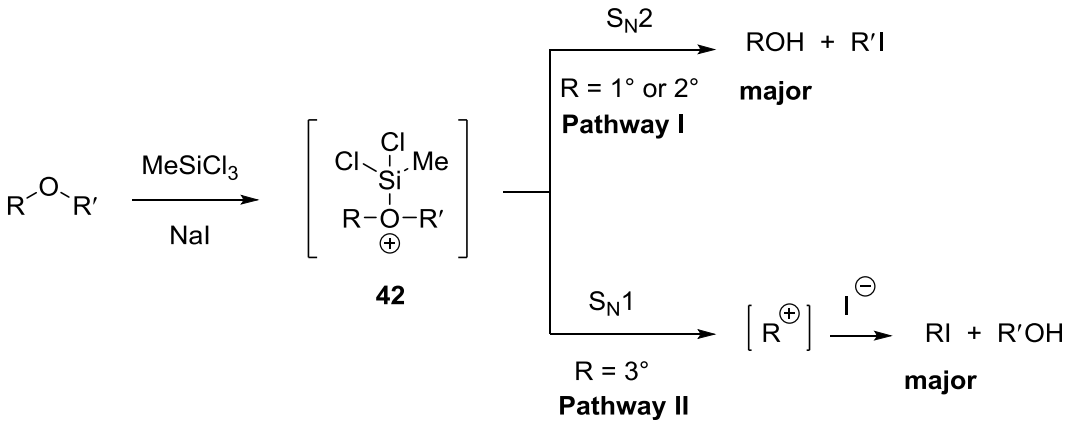

Scheme 3.5: Reaction of the dealkylation of ethers using trichloro(methyl)silane and sodium iodide. The scheme is modified from reference 66.

In another study by Aida *et al*., the preparation of α-trimethylsiloxythiols was accomplished by treating an aldehyde with chlorotrimethylsilane and hydrogen sulfide in the presence of pyridine.[67] This reaction is analogous to the proposed synthesis in Scheme 3.3, except no acetal is formed prior to thionation. This approach would be acceptable if formaldehyde production was not a concern. In Aida's procedure, the aldehyde (**43**), chlorotrimethylsilane, and pyridine, are first mixed together in dichloromethane, and H_2S gas is then bubbled through the solution at <15°C to yield the siloxythiol **44** (Scheme 3.6).[67] In Aida's work, the silyl ether was never removed, but removal would need to occur prior to cyclization of the trithiane ring. Because the three acetal moieties are in close proximity, the cyclization and removal of trimethylsilanol may occur spontaneously at higher temperatures.

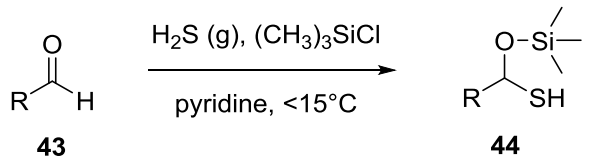

43 **44**

Scheme 3.6: Addition of hydrogen sulfide gas and chlorotrimethyl silane to an aldehyde. The scheme is modified from reference 67.

The next experiments probed new ways to allow for more direct substitutions of trithiaadamantane at the 7-position via alternative starting molecules. One such material examined was 4-allyl-1,6-heptadien-4-ol, or triallyl carbinol (**45**). Subjecting **45** to ozonolysis followed by reduction, and ultimately thionation and cyclization, could lead to the tripod analog where the 7-position has a hydroxyl group rather than an ester, in a

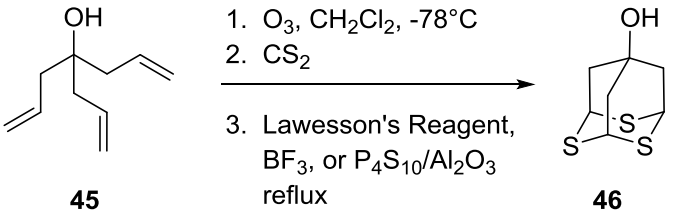

Scheme 3.7: The synthesis of 7-hydroxy-2,4,9-trithiaadamantane (**46**) by way of triallyl carbinol (**45**).[33]

synthetic scheme similar to that originally proposed by Khemtong *et al.* (Scheme 3.7).[33] From **46**, the amantadine analog (**18**), or any other novel derivative where the amine moiety is directly attached to the adamantane ring, can be achieved by first converting the alcohol (**46**) to a halide (**47**) via several different reactions, such as treatment with HBr or HCl, or thionyl chloride, or PCl_5, etc. (Scheme 3.8).[76-78] From intermediate **47**, further substitution of the tertiary halide with an amine can be achieved directly, although in low yields, through treatment with excess ammonia (Scheme 3.8, Pathway I).[76,78] In Scheme 3.8, the formation of the methyl ketone substituted tripod (**49**) is of particular interest. If the methyl ketone could be synthesized, a preparation of **19**, similar to the original synthesis of rimantadine (Scheme 1.4) could be implemented resulting in the product with fewer steps.[16] Also, the halide **47** could be treated with trimethylsilyl cyanide (TMSCN) in the presence of a metal-chloride catalyst to give the alkyl nitrile **48** in good yields.[79,80] This transformation could be achieved using a synthesis performed by Reetz and Chatziiosifidis (Scheme 3.8, Pathway II).[79,80] In this reaction, tertiary alkyl halides were successfully converted to the corresponding tertiary nitrile upon treatment with TMSCN and tin(IV) chloride as a catalyst.[79] In a similar reaction, by Zieger and Wo, the

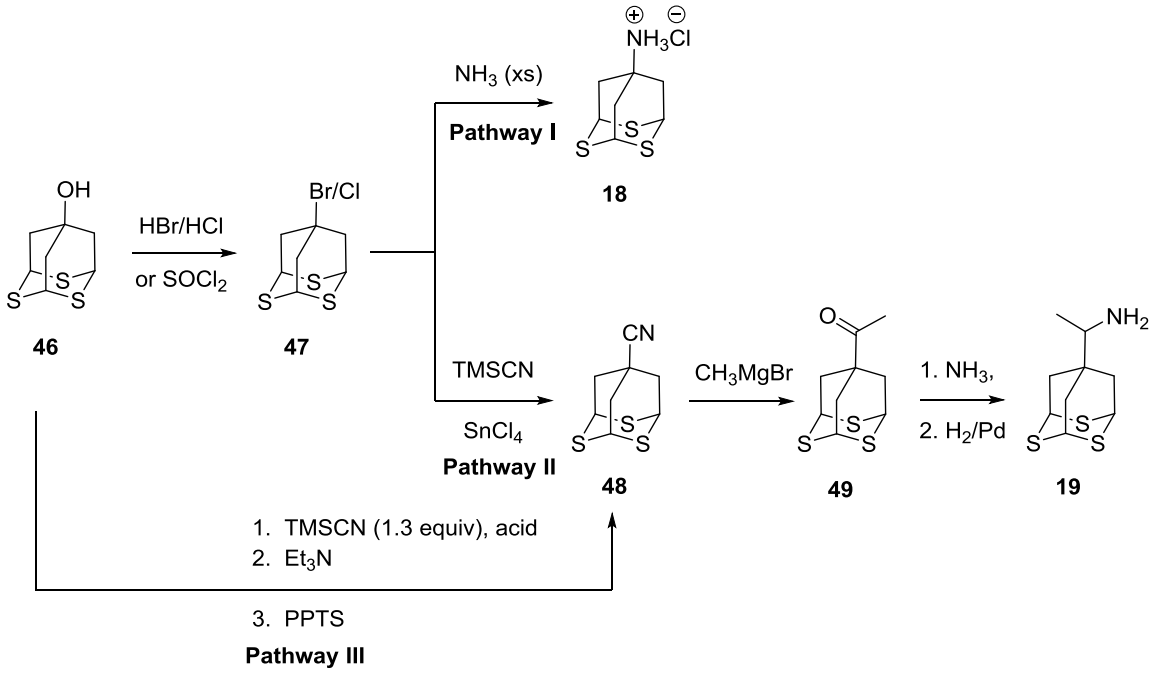

Scheme 3.8: Various routes to synthesize **18** and **19** from the hydroxy-tripod starting material (**46**).[77-84]

same transformation was accomplished by using TMSCN with titanium(IV) chloride as the catalyst instead of tin(IV) chloride.[80]

Alternatively, the hydroxy-tripod (**46**) can be directly converted to the nitrile by way of Pathway III, shown in Scheme 3.8.[81] In this method, by Okada and Kitano, treatment of the alcohol with a Brønsted acid (such as methanesulfonic acid) and trimethylsilyl cyanide, followed by neutralization with triethylamine and dehydration using pyridine/tosyl chloride, would yield nitrile **48**.[81] From **48**, the rimantadine analog (**19**) can be produced by treatment with a methyl Grignard reagent and subsequent reductive amination of the methyl ketone (**49**).[82-85] As another option, the nitrile group

could be directly reduced using a metal hydride, such as diisobutylaluminum hydride, yielding the aldehyde that was originally synthesized from the methyl ester.[86,87] Utilizing these reactions could both reduce the number of steps in the overall reaction and also allow for easier transformations to desired derivatives. The synthesis by Khemtong *et al*. requires six steps from dimethyl malonate to the tripod.[33] From the methyl ketone form, not only could analog **19** be synthesized in one step, but other derivatives could easily be obtained by using various substituted amines during the reductive amination step. It is for this reason the synthesis of the tripod-methylacetate was examined.

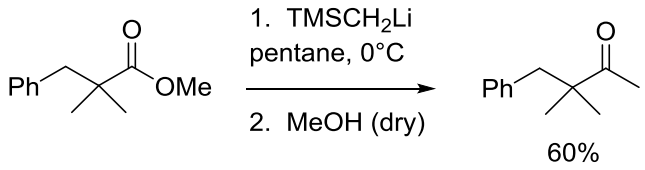

Scheme 3.9: Direct transformation of an ester to a methyl ketone using $TMSCH_2Li$, as proposed by Evans and Morken.[88] The scheme is modified from reference 88.

In principle, methyl ketone **49** can be used to produce the amantadine analog **18** in one step, and so a direct synthesis from the tripod methyl ester was attempted. In a study by Evans and Morken, the conversion of a methyl ester to a methyl ketone was achieved via addition of (trimethylsilyl)methyllithium ($TMSCH_2Li$), followed by addition of dry methanol, in decent yields (Scheme 3.9).[88] Also, in a study by Mulzer *et al*., a methyl ester was successfully transformed to the methyl ketone in 97% yield, using similar conditions to those in Scheme 3.9.[89]

The reactions just described were all attempted in this dissertation work, with varying degrees of success. The procedures and results are discussed in the following sections.

3.2 Experimental

The experimental details of all attempted and successful syntheses of methyl-2,4,9-trithiaadamantan-7-carboxylate and the synthesis of novel starting materials are described in this section.

3.2.1 Materials and Methods

BF_3 used was as the etherate form (48%) from Acros Organics. Unless otherwise indicated, all materials were obtained from commercial suppliers (Aldrich, Fisher, or Acros) and used without further purification. All organic solvents used were of reagent grade. Tetrahydrofuran (THF) was distilled from sodium benzophenone ketyl under argon. Methylene chloride, toluene, and acetonitrile were all distilled from calcium hydride before use and stored briefly over molecular sieves. Reactions run under anhydrous conditions used glassware that was both oven-dried and flame-dried under vacuum. Any moisture- or oxygen-sensitive reactions were performed under a N_2 gas environment. Synthetic products were purified using flash column chromatography or recrystallization. Thin layer chromatography (TLC) was performed using Whatman 250 µm thickness, pre-coated silica gel glass plates and visualized using ultraviolet light

and/or iodine stain. EM silica gel 60 Å (particle size 35-75 μm) was used for purifications done via column chromatography.

All ^{1}H NMR and ^{13}C NMR spectra were obtained using a Varian Mercury-300 spectrometer operating at 300 MHz for ^{1}H and 75 MHz for ^{13}C. The chemical shifts of NMR spectra are reported in parts per million (ppm) relative to the chosen deuterated solvent reference peak. ^{1}H NMR multiplicity was noted as follows: s, singlet; d, doublet; t, triplet; q, quartet; m, multiplet. Melting points were determined using a MelTemp apparatus. IR spectra were recorded on a Nicolet Nexus 870 FTIR spectrometer equipped with a Thunderdome Attenuated Reflectane (ATR) accessory and peaks recorded in wavenumbers (cm^{-1}). Single crystal X-ray diffraction data were collected at 100K (Bruker KRYOFLEX) on a Bruker SMART APEX CCD-based X-ray diffractometer system equipped with a Mo-target X-ray tube ($\lambda = 0.71073$Å). The detector was placed at a distance of 5.009 cm from the crystal. Crystals were placed in paratone oil upon removal from the mother liquor and mounted on a plastic loop in the oil. Integration and refinement of crystal data were done using Bruker SAINT software package and Bruker SHELXTL (version 6.1) software package, respectively. Absorption correction was completed by using the SADABS program.

3.2.2 Syntheses

The syntheses aimed at increasing the yields and purity of methyl-2,4,9-trithiaadamantan-7-carboxylate are described in this section.

3.2.2.1 Grubbs catalyst reaction for the synthesis of $TpCO_2Me$ (**17**)

To a 2-neck, 250 mL round bottom flask equipped with a magnetic stir bar, triallyl methylester (2.5 g, 12.87 mmol) dissolved in CH_2Cl_2 (125 mL) was added. This mixture was allowed to stir for 10 min before an N_2 inlet was attached and Grubbs catalyst bis(tricyclohexylphosphine) benzylidine ruthenium(IV)dichloride) (0.011 g, 0.013 mmol) was added to the solution. The resulting mixture was stirred for 24 h at r.t. The reaction flask was then put in a dry ice/acetone bath at -78°C and ozone was bubbled through the solution until a blue color persisted (1.5 h). NOTE: This reaction was performed in a fume hood with the sash closed. Ozone is toxic and ozonide intermediates can be explosive. This reaction should be performed using extreme caution. Pure O_2 was allowed to flush the system for 10 min to remove excess ozone. While still at -78°C, dimethyl sulfide (0.40 mL, 6.44 mmol) was added dropwise to the reaction with stirring. The resulting mixture was allowed to warm to r.t., was filtered through a funnel filled with Na_2SO_4, and then the solvent was removed via rotary evaporation. The resulting purple viscous liquid was re-dissolved in acetonitrile (125 mL), the flask was equipped with a N_2 inlet, and Lawesson's reagent (18.22 g, 45.05 mmol) was added. The reaction was allowed to stir at r.t. for 24 h. The reaction was monitored via TLC and FTIR. BF_3 (2 mL, 48.36 mmol) was added to the reaction due to incomplete thionation, and the solution was then stirred at r.t. for an additional 24 h. The reaction mixture was then treated with K_2CO_3 (10 mL, 5.0 M) with cooling. The resulting organic layer was then washed with H_2O, dried over $MgSO_4$ and the solvent was removed using rotary evaporation. The product was purified using flash column chromatography (25% EtOAc

in hexane) to give methyl-2,4,9-trithiaadamantane carboxylate (**17**) (0.324 g, 10%). ^{1}H NMR ($CDCl_3$) δ: 2.88 (d, J = 3 Hz, 6H), 3.73 (s, 3H), 4.30 (t, J = 3 Hz, 3H).

3.2.2.2 Formation of methyl-2,4,9-trioxaadamantane-7-carboxylate (**51**)

To a 3-neck 500 mL round-bottom flask, equipped with a magnetic stir bar was added triallyl methyl acetate (3.12 g, 16.0 mmol) dissolved in CH_2Cl_2 (120 mL). The resulting solution was cooled to -78°C using a dry ice/acetone bath. Ozone was bubbled through the solution for 2.5 h until a light blue color persisted. NOTE: This reaction was performed in a fume hood with the sash closed. Ozone is toxic and ozonide intermediates can be explosive. This reaction should be performed using extreme caution. Pure O_2 was allowed to flow through the solution for 10 min to remove excess ozone. Dimethyl sulfide (3.6 mL, 48.0 mmol) was added to the reaction while still in the dry ice bath and the mixture was allowed to stir for 10 min. The reaction was warmed to r.t. and then the reaction was refluxed in CH_2Cl_2 for approximately 5-6 h. The solvent was removed by rotary evaporation, and the resulting clear, viscous material was re-dissolved in CH_3CN (120 mL) and P_4S_{10} (8.6 g, 23.0 mmol) and Al_2O_3 (8.2 g, 80 mmol) were then added. The reaction was allowed to stir while refluxing over 15 h. TLC analysis showed a product spot slightly lower (R_f = 0.39) than the standard tripod spot (R_f = 0.45). The reaction was vacuum filtered using a fritted filter and rinsed with EtOAc (5 mL). The solution was put into a separatory funnel and washed with a saturated aqueous solution of $NaHCO_3$ (3 × 20 mL) and extracted with CH_2Cl_2 (3 × 15 mL). The combined organic layer were dried over $MgSO_4$ and filtered. The crude product was purified via flash column

chromatography (30% EtOAc in hexane). Large, clear crystals suitable for X-ray diffraction were obtained from slow evaporation of the solvent. Melting point: 135-138 °C. ^{1}H NMR ($CDCl_3$) δ: 2.27 (d, J = 3 Hz, 6H), 3.74 (s, 3H), 5.35 (t, J = 3 Hz, 3H) ppm. ^{13}C NMR ($CDCl_3$) δ: 35, 37, 93, 174 ppm. FTIR (ATR): 978, 1072, 1745, 2917, 2946 cm^{-1}. MS (ES) calculated for $C_7H_{11}ClNaNS_3$ $[M + Na]^+$: 223.0582, found 223.0586.

3.2.2.3 Acetal protection of triallyl methyl acetate

The following section describes the syntheses aimed at producing an acetal protected trialdehyde intermediate (**24**). Both syntheses begin with triallyl methylacetate (**23**).

3.2.2.3.1 Methanol as a solvent during ozonolysis

To a 500 mL 3-neck round bottom flask equipped with a magnetic stir bar, was added triallyl methyl acetate (4.23 g, 21.78 mmol) dissolved in MeOH (20 mL). The mixture was cooled to -78°C using a dry ice/acetone bath. Ozone was bubbled through the solution for 3 h, until a dark blue color persisted, showing ozone saturation. NOTE: This reaction was performed in a fume hood with the sash closed. Ozone is toxic and ozonide intermediates can be explosive. This reaction should be performed using extreme caution. The flask was then flushed with pure O_2 for 10 min. Dimethyl sulfide (0.66 mL, 10.89 mmol) was slowly added to the solution with stirring while still at -78°C. *p*-Toluenesulfonic acid (2.00 g, 10.89 mmol) was added to the resulting mixture and the

reaction stirred for 15 h at r.t. The MeOH was reduced to ~20 mL, and CH_2Cl_2 (75 mL) was added to the flask. The reaction was washed with H_2O (3 × 20 mL) and dried over $MgSO_4$. The solids were filtered off and the solvent was removed via rotary evaporation. The crude product was obtained as a clear/white oil. ^1H NMR shows multiple peaks, indicating the acetal may have polymerized or cyclized during formation. The product was purified via vacuum distillation (190 °C at 2 torr, 2.54 g, 35%) and used in the next reaction.

To a 3-neck 100 mL round bottom flask equipped with an addition funnel, a 3-way adapter, and a vacuum adapter connected to a Schlenk line, was added the methoxy protected trialdehyde **37** (1.20 g, 3.55 mmol) in CH_3CN (30 mL). The addition funnel was charged with a solution of Me_3SiCl (0.90 mL, 12.78 mmol) in CH_3CN (5 mL). A cylinder of H_2S gas was attached to the 3-way adapter via a Teflon hose and a balloon was also attached to the 3-way adapter. All air was evacuated from the closed system and the H_2S tank was opened until the balloon reached a well-inflated state. NOTE: This reaction was run inside a fume hood with the sash closed. H_2S gas is very toxic and should be used with extreme caution. The Me_3SiCl solution was added dropwise to the reaction flask over 15 min. The reaction was allowed to stir at r.t. for 40 h, adding additional H_2S gas when the pressure of the system decreased. $NaHCO_3$ (2.15 g, 25.56 mmol) was added to the reaction with stirring. The CH_3CN was removed via rotary evaporation and CH_2Cl_2 (25 mL) was added to the flask. The solution was washed with H_2O (3 × 7 mL) and extracted with CH_2Cl_2 (3 × 5 mL). The combined organic layers were dried over Na_2SO_4 and the solvent was removed using rotary evaporation. The

product was purified using micro flash column chromatography (25% EtOAc in hexane) to give methyl-2,4,9-trithiaadamantane-carboxylate (0.056 g, 6%). ^{1}H NMR ($CDCl_3$) δ: 2.88 (d, J = 3 Hz, 6H), 3.73 (s, 3H), 4.30 (t, J = 3 Hz, 3H).

3.2.2.3.3 Ethylene glycol protection reaction

To a 250 mL 2-neck round bottom flask equipped with a magnetic stir bar was added triallyl methyl acetate (8.09 g, 41.6 mmol) dissolved in CH_2Cl_2 (100 mL). The resulting solution was cooled to -78°C with a dry ice/acetone bath. Ozone was bubbled through the solution for 3.5 h, until a light blue color persisted. NOTE: This reaction was performed in a fume hood with the sash closed. Ozone is toxic and ozonide intermediates can be explosive. This reaction should be performed using extreme caution. Pure O_2 was allowed to flow through the solution for 10 min to remove excess ozone. Dimethyl sulfide (12.2 mL, 166.4 mmol) was added to the reaction while still in the dry ice bath and the mixture was allowed to stir for 10 min. Ethylene glycol (9.3 mL, 166.4 mmol) and *p*-toluenesulfonic acid (0.40 g, 2.08 mmol) was added to the resulting solution with stirring while at -78°C. The dry ice/acetone bath was then removed (due to freezing of the liquids) and the flask was allowed to warm to r.t. The reaction was monitored via FTIR. Once complete, $NaHCO_3$ was added to neutralize the reaction, and the solids were filtered off. The resulting solution of the tri-1,3-dioxolane product and CH_2Cl_2 was washed with H_2O (3 × 10 mL), dried over $MgSO_4$, and concentrated via rotary evaporation. The tri-acetal methylacetate product was purified via distillation to give a gold/yellow liquid (235°C at 2 torr, 11.95 g, 87%). ^{1}H NMR ($CDCl_3$) δ: 2.14 (d, J = 3

Hz, 6H), 3.71 (s, 3H), 4.75 (m, 12H), 5.34 (t, J = 3 Hz, 3H). FTIR (ATR): 1120, 1210, 1437, 1732, 2946, 3373 cm^{-1}.

To a 250 mL pressure vessel equipped with a magnetic stir bar and a 3-way stopcock was added tri-acetal methylacetate (3.18 g, 9.58 mmol) in freshly distilled CH_2Cl_2 (100 mL). The vessel was submerged in a dry ice/acetone bath and the liquids in the vessel were allowed to freeze completely and all gases were evacuated. A tank of H_2S gas was submerged in an ice water bath and connected to the 3-way stopcock of the pressure vessel, along with a balloon. NOTE: This reaction was run inside a fume hood with the sash closed. H_2S gas is very toxic and should be used with extreme caution. The reaction vessel was removed from the liquid N_2 and allowed to warm slightly before adding dichlorodimethyl silane (4.65 mL, 38.3 mmol). The vessel was then allowed to warm to r.t. During the warming process, pressure was released from the reaction by venting the balloon. The reaction was allowed to stir at r.t. for 24 h. Excess H_2S was removed from the vessel and $NaHCO_3$ was added to neutralize the reaction. The mixture was washed with H_2O (2 × 10 mL) and the aqueous portions extracted with CH_2Cl_2 (2 × 15 mL). The combined organic layers were dried over Na_2SO_4 and the solvent was removed via rotary evaporation. The product was purified via flash column chromatography (25 % EtOAc in hexane) and the solvent evaporated to give fine, white crystals of $TpCO_2Me$ (0.36 g, 15%). ^1H NMR ($CDCl_3$) δ: 2.88 (d, J = 3 Hz, 6H), 3.73 (s, 3H), 4.30 (t, J = 3 Hz, 3H).

3.2.2.4 Triallyl carbinol reaction trial

To a 2-neck, 250 mL round bottom flask equipped with a magnetic stir bar was added 4-allyl-1,6-heptadien-4-ol (triallyl carbinol) (2.5 g, 16.42 mmol) and CH_2Cl_2 (125 mL). Ozone was bubbled through the solution until a blue color persisted (6.5 h). NOTE: This reaction was performed in a fume hood with the sash closed. Ozone is toxic and ozonide intermediates can be explosive. This reaction should be performed using extreme caution. Pure O_2 was then run through the solution until clear. Dimethyl sulfide (2 mL, 32.84 mmol) was added to the reaction while still at -78°C. The mixture was stirred for 15 min before slowly adding Lawesson's reagent (6.64 g, 57.47 mmol) and BF_3 (4.3 mL, 16.42 mmol). The dry ice bath was removed and the reaction was allowed to warm to r.t. while stirring. A condenser was attached to the flask, and the reaction was refluxed for 24 h. The product had possibly polymerized, giving a dark blue/black viscous material. NMR and IR showed no desired product was formed, but rather a polymerization may have occurred.

3.2.2.5 Attempted synthesis of 2,4,9-trithiaadamantane-methylketone via (trimethylsilyl)methyllithium

To a flame-dried, 50 mL round bottom flask equipped with a magnetic stir bar was added $TpCO_2Me$ (0.204 g, 0.82 mmol) dissolved in freshly distilled THF (12 mL). The solution was put in an ice bath at 0°C, equipped with a N_2 inlet, and stirred for 10 min. To this mixture, (trimethylsilyl)methyllithium (0.90 mL, 0.90 mmol, 1.0 M in pentane) was added dropwise via a syringe. The reaction was allowed to stir at 0°C for 3 h. TLC

analysis of the reaction was inconclusive. MeOH was added to the stirring solution and the ice bath was removed. Once the solution reached r.t., the product was extracted using CH_2Cl_2 (3 × 5 mL) and dried over Na_2SO_4. The solvent was removed using rotary evaporation to give a pale yellow viscous material. A crude ^1H NMR analysis shows the presence of an oxygenated ring, and a mixture of products. ^1H NMR ($CDCl_3$) δ: 0.10 (s, 9H), 1.56 (d, J = 1.2 Hz, 6H), 2.28 (d, J = 1.2 Hz, 6H), 3.75 (d, J = 3 Hz, 3H), 3.84 (d, J = 3 Hz, 3H), 5.37 (s, 3H).

3.3 Results and Discussion

The reactions presented in this chapter were designed to increase the yields of the tripod methyl ester reaction, beginning the tripod synthesis with different starting materials that would easier allow for manipulations at the 7-position, or reducing problematic by-products.

3.3.1 Synthesis of TpCO2Me (**17**) via Grubbs intermediate reaction

First generation Grubbs catalysts, discovered in 1992, have been commonly used in synthesis for olefin metathesis reactions.[90] A first generation Grubbs catalyst, ruthenium carbene complex **50**, was used in a reaction to convert the starting material, triallyl methyl acetate (**23**), to the proposed dimer **36** (Scheme 3.10). This transformation was carried out to prevent the formation of formaldehyde upon ozonolysis, which is the next step in the tripod synthesis.

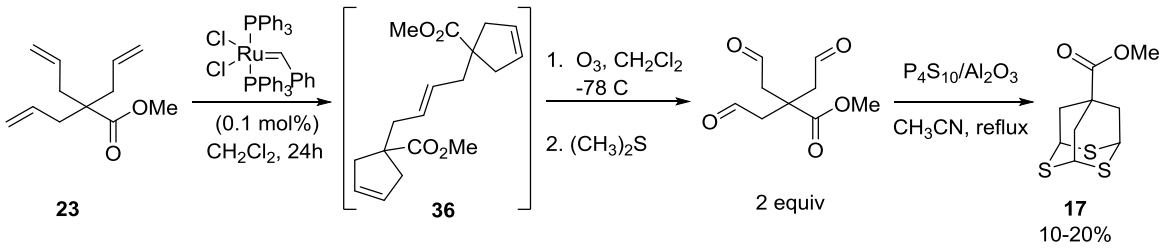

Scheme 3.10: Reaction of a Grubbs catalyst (**50**) with **23** to give the proposed dimer **36** and ultimately **17**.[90,33]

The reaction was done by adding 0.1 mol% of (bis(tricyclohexylphosphine) benzylidine ruthenium(IV)dichloride) to a solution of triallyl methyl acetate in CH_2Cl_2. The reaction was then subjected to ozonolysis and thionation/cyclization. The pure tripod was achieved in yields similar to those previously obtained (>10%). With this attempt at increasing the yield of the tripod reaction, it became clear that the issue was not so much the presence of formaldehyde, but rather the thionation and cyclization steps. Further efforts to increase yields of this reaction focused on preventing the polymerization of the trialdehyde intermediate via acetal proctection[72-75] and the prevention of oxygen incorporation into the base of the tripod via use of a silane.[66-69]

3.3.2 Methyl-2,4,9-trioxaadamantane-7-carboxylate

As previously discussed, when the tripod molecule is synthesized according to the reaction proposed by Khemtong *et al*., incorporation of oxygen into the trithiane ring is observed.[33] These products, shown in Figure 3.2, are nearly impossible to separate from

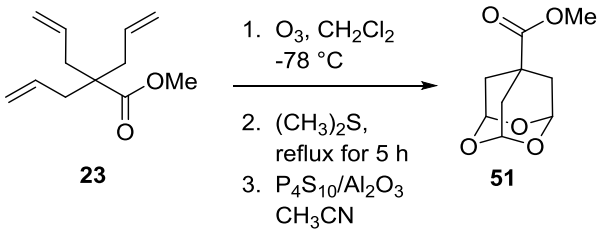

Scheme 3.11: The synthesis of methyl-2,4,9-trioxaadamantan-7-carboxylate (**51**).

the desired product using the standard techniques applied in this synthesis, such as flash column chromatography and TLC. However, the oxygenated tripod molecule (**51**) was accidently obtained as the major product, in appreciable amounts, during a routine tripod synthesis. During this reaction, after reduction of the ozonide intermediate with dimethyl sulfide, the P_4S_{10}/alumina was not added and the reaction was allowed to reflux for 5-6 h prior to the addition of the thionating agent. This reaction is shown in Scheme 3.11. Because the reaction appeared ruined since the aldehyde was refluxed without a thionating agent present, the reaction was allowed to reflux for a shorter amount of time (15 h) than is usually required (~36 h) after addition of the P_4S_{10}/alumina. In this reaction the trialdehyde intermediate could have enolized and cyclization occurred, similar to the polymerization of formaldehyde to form 1,3,5-dioxane.[91] A contamination of acid could have catalyzed this cyclization, enabling a reaction similar to that proposed in Figure 3.3 to occur. Reports of similar cyclizations can be found in the literature.[91,92] For example, Cullen and Guziec showed that using acetic acid as a catalyst with heating for several days induced cyclization of an aldehyde.[91] In another example by Whitesell and Minton, a tetraaldehyde was heated without a catalyst to yield a trioxane ring.[92] As

previously mentioned, there have been varying amounts of this compound in the synthesis of tripod. However, when the trialdehyde was heated in the absence of a thionating agent, a more significant amount of the trioxaadamantane was produced. In an attempt to synthesize the purely oxygenated tripod, **51**, the standard synthesis was followed, except no thionating reagent was added. Interestingly, instead of giving **51**, as anticipated, the trialdehyde apparently polymerized to yield an indistinguishable NMR spectrum consistent with a polymerized mixture.

The presence of the oxygen atoms in the base of the tripod was confirmed by ^{1}H NMR analysis. The three hydrogen atoms of the trithiane ring produce a signal at 4.3 ppm corresponding to the S-C*H*-S linkage (Fig. 3.4, A). However, when the sulfur is replaced by oxygen, this peak is shifted downfield to 5.35 ppm, corresponding to the O-

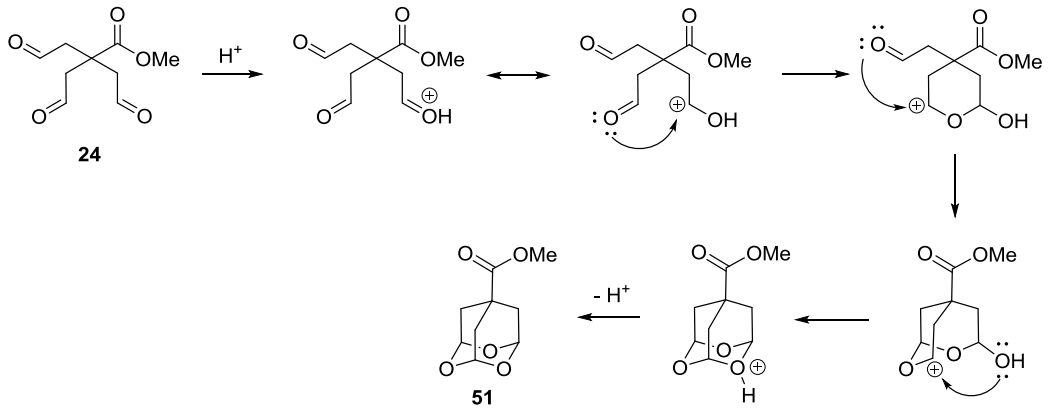

Figure 3.3: A proposed mechanism of cyclization of the trialdehyde to form the oxygenated ring of **51**.[91,92]

C*H*-O linkage (Fig. 3.4, B).[33] For a direct comparison, the ^{1}H NMR spectra of methyl-2,4,9-trithiaadamantane-7-carboxylate (**17**) and methyl-2,4,9-trioxaadamantane-7-carboxylate (**51**) are presented side by side in Figure 3.4. The pure methyl-2,4,9-trioxaadamantane-7-carboxylate (**51**) obtained from the reaction shown in Scheme 3.11, was recrystallized using methylene chloride and the slow evaporation of solvent gave large, clear crystals suitable for X-ray crystallography and mass spectrometry.

The bond angles of the carbon atoms are close to tetrahedral, ranging from 107.5-113.9°, similar to the amine-tripod (**18**) results. The C-O-C angles of the base of the tripod are almost exactly tetrahedral, with angles of 109.5-110.2°. When compared with the findings of the C-S-C angles of **18**, which were slightly wider ranging from 112.0-112.6°, it is possible to see the difference due to the presence of the oxygen atoms. The C-O bond lengths in the trioxane ring were all found to be almost exactly 1.43 Å. When compared to the lengths of the C-S bonds of **18**, which were all found to be ~1.82 Å, this is a significant difference. The shorter bond lengths of C-O are to be expected, considering the smaller radius of oxygen. The mass spectrometry and crystal structure results are shown in Figures 3.5 and 3.6, respectively. The single crystal X-ray diffraction parameters are summarized in Table 3.1 and selected bond lengths and angles are presented in Table 3.2.

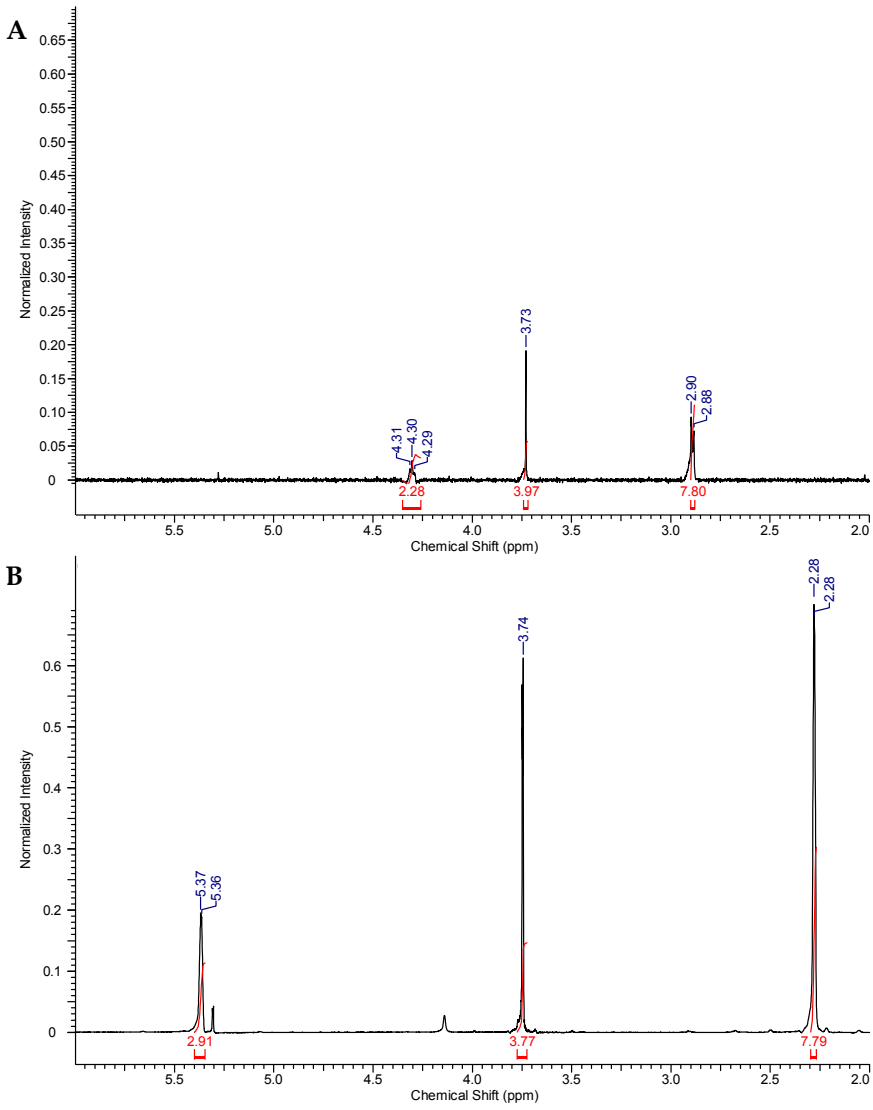

Figure 3.4: The ^{1}H NMR spectra of **A**, methyl-2,4,9-trithiaadamantan-7-carboxylate (**17**) and **B**, methyl-2,4,9-trioxaadamantan-7-carboxylate (**51**).

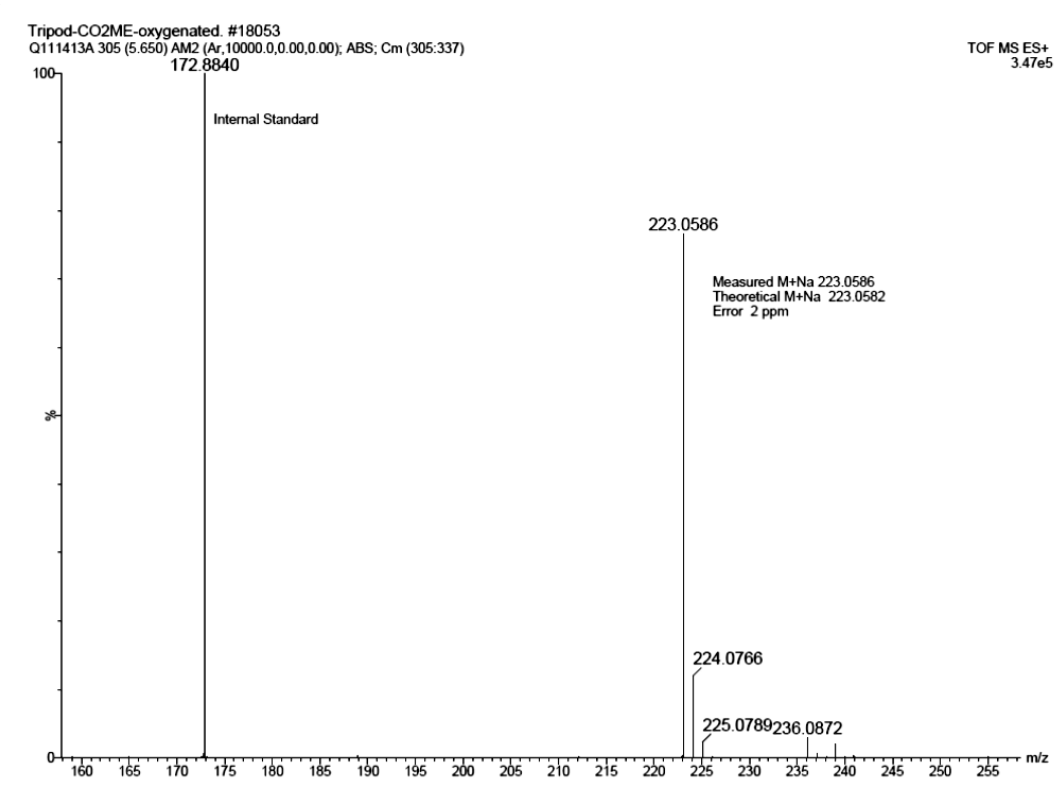

Figure 3.5: High resolution mass spectrometry of methyl-2,4,9-trioxaadamantan-7-carboxylate (**51**).

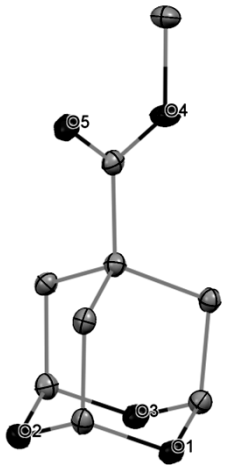

Figure 3.6: The X-ray crystal structure of methyl-2,4,9-trioxaadamantane-7-carboxylate (**51**) with 35% thermal ellipsoids. Hydrogen atoms on the carbon positions were omitted for clarity.

Table 3.1: Crystal data and structure refinement parameters for **51**.

Empirical formula	$C_9H_{12}O_5$	
Formula weight	200.19	
Temperature	100(2) K	
Wavelength	0.71073 Å	
Crystal system	Monoclinic	
Space group	P2(1)/n	
Unit Cell dimensions	a = 6.375 (3) Å b = 17.236 (7) Å c = 8.041 (3) Å	α = 90° β = 103.359(4)° γ = 90°
Volume	859.5(6) $Å^3$	
Z	4	
Density (calculated)	1.547 Mg/m^3	
Absorption coefficient	0.127 mm^{-1}	
F(000)	424	
Crystal size	0.38 × 0.32 × 0.18 mm^3	
Theta range for data collection	2.36° to 25.14°	
Index ranges	$-7 \leq h \leq 7$, $-20 \leq k \leq 20$, $-9 \leq l \leq 9$	
Reflections collected	5888	
Independent reflections	1535 [R(int) = 0.0520]	
Completeness to theta = 25.14°	99.7%	
Absorption correction	SADABS	
Max. and min. transmission	0.9775 and 0.9532	
Refinement method	Full-matrix least-squares on F^2	
Data / restraints / parameters	1535 / 0 / 128	
Goodness-of-fit on F^2	1.042	
Final R indicies [$I > 2\sigma(I)$]	R1 = 0.0417, wR2 = 0.1177	
R indicies (all data)	R1 = 0.0455, wR2 = 0.1252	
Absolute structure parameter	0.05(9)	
Largest diff. peak and hole	0.277 and -0.260 e $Å^{-3}$	

Table 3.2: Selected bond lengths and bond angles of **51**.

Bond Lengths, Å	
C-C	1.523(2), 1.521(2), 1.522(2), 1.536(2), 1.536(2), 1.542(2), 1.520(2)
C-O	1.428(2), 1.427(2), 1.429(2), 1.424(2), 1.428(2), 1.428(2), 1.449(2), 1.339(2)
C=O	1.205(2)
Bond Angles,°	
C-C-C	107.6(1), 108.0(1), 108.1(1), 108.1(1), 107.5(1), 111.3(1), 107.6(1)113.9(1), 108.1(1)
C-C-O	111.2(1), 110.6(1), 110.7(1), 111.0(1), 111.3(1), 111.3(1),
C-O-C	109.5(1), 109.6(1), 110.2(1), 116.2(1)
O-C-O	109.3(1), 109.2(1), 109.4(1), 124.2(1)
C-C-O	111.2(1), 124.5(1)

3.3.3 Acetal protected triallyl methylacetate

To prevent the incorporation of oxygen atoms in the ring during either ozonolysis or thionation, an acetal protection of the aldehyde moieties was used. The first attempt towards this reaction used methanol as a solvent during ozonolysis to add methoxy protection groups. However, this reaction led to the formation of an unexpected cyclized intermediate (Fig 3.8) and only trace amounts of tripod were obtained. In an alternative acetal formation reaction, ethylene glycol was used as the source of the acetal.

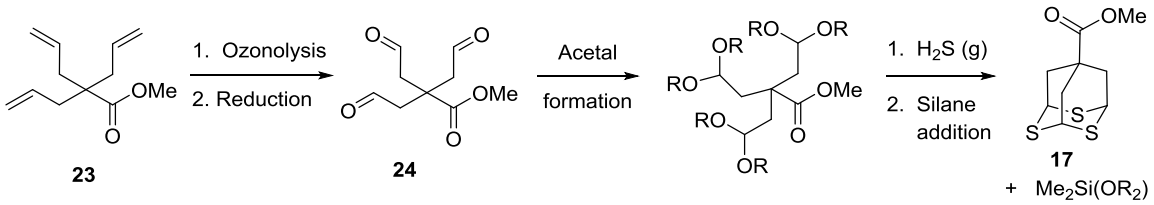

Scheme 3.12: Generic reaction scheme showing acetal formation followed by thionation and cyclization.

Also, to prevent the incorporation of oxygen into the ring, a silane was used to bond to the oxygen atoms of the aldehyde during thionation and cyclization. Both reactions follow a similar sequence, which is illustrated in Scheme 3.12. The results of these reactions are discussed in the next sections.

3.3.3.1 Methoxy protection

The first attempt at acetal protection was through an adaptation of a procedure by Claus and Schrieber (Scheme 3.13), where the ozonolysis of triallyl methylacetate was performed in methanol, rather than CH_2Cl_2. After reduction of the ozonide using dimethyl sulfide, *p*-toluenesulfonic acid was added.[72] The addition of acid at this step aids in acetal formation of the trialdehyde intermediate to give acetal **37**. However, when the crude acetal was analyzed using ^{1}H NMR spectroscopy, the spectrum showed a possible cyclization of the intermediate (Figure 3.7). Based on the NMR analysis, it was determined that rather than achieving the tri-acetal product **37**, a similar compound (**52**), shown in Figure 3.8, was obtained.

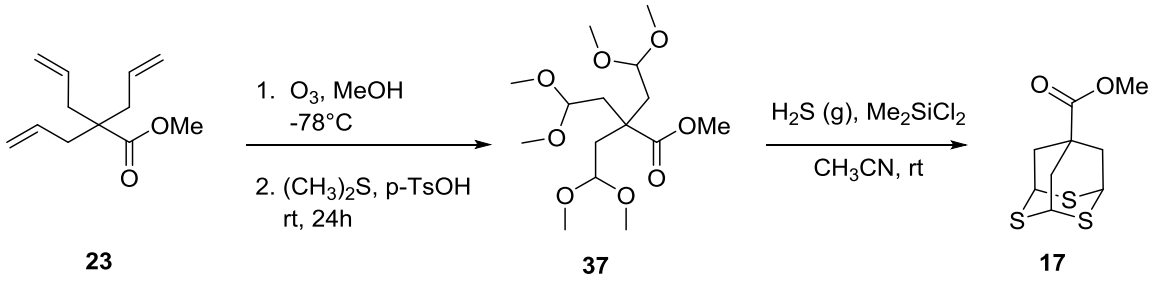

23 **37** **17**

Scheme 3.13: First attempt at reaction of an acetal with hydrogen sulfide gas and a silane to give **17**.[72]

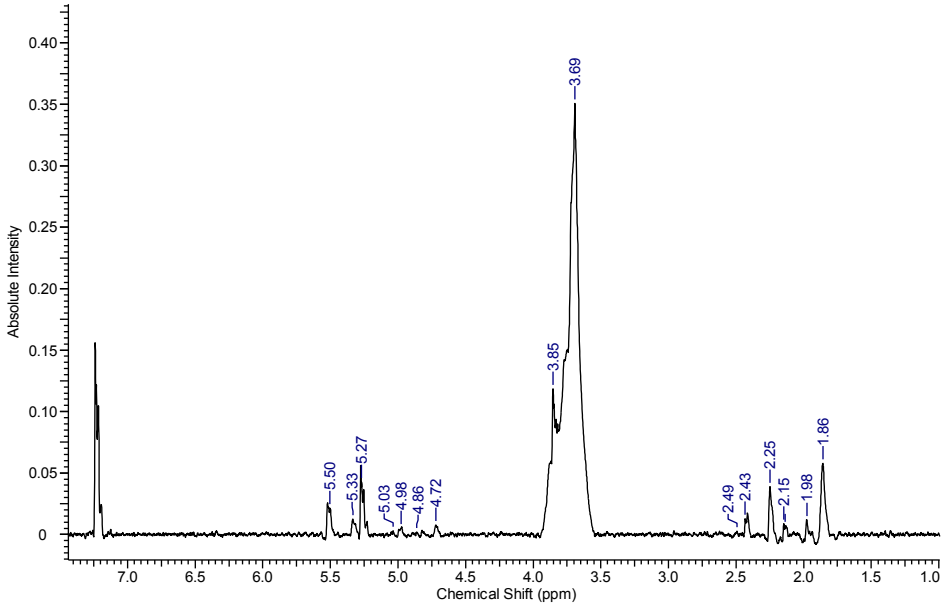

Figure 3.7: The ^{1}H NMR spectrum of the formation of acetal **52**.

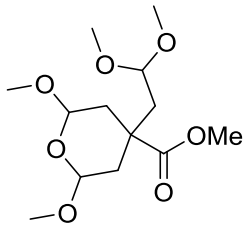

52

Figure 3.8: Proposed structure of the acetal achieved from 23 when performing ozonolysis in methanol.

The peaks at 1.86-1.98 ppm correspond to the methylene of the non-cyclized dimethoxy group, whereas the peaks at 2.15-2.25 and 2.43-2.49 ppm correspond to the methylene of the cyclic ether ring. The peak at 3.69 ppm correlates to the methyl of the methoxy groups and the peak present at 3.85 ppm is characteristic of the OC*H*$_3$ of the ester. At 4.72-4.98 ppm are peaks corresponding to the O-C*H*-O moiety present on the ether ring, and the peaks at 5.27-5.50 ppm correlate to the CH_2-C*H*-$(OCH_3)_2$ of the dimethoxy moiety. This acetal was further reacted with H_2S gas and trimethlylsilylchloride in acetonitrile. The reaction was neutralized with sodium bicarbonate to give the tripod in very low yields (<4%). Because the acetal was in a cyclized form, the reaction apparently did not proceed as had expected and that incorporation of sulfur into the acetal may not have occurred at a fast enough rate to produce the tripod in decent yields.

3.3.3.2 Ethylene glycol protection

The next synthesis examined utilized ethylene glycol as the alcohol source to form a cyclic acetal of the trialdehyde in a procedure adapted from Ireland and Walba,[74] and Chan *et al*.[94] This reaction sequence is outlined in Scheme 3.14. In this synthesis, the triallyl methyl acetate (**23**) was first subjected to ozonolysis and reduction, using dimethyl sulfide at -78°C. Next, a mixture of ethylene glycol and *p*-toluenesulfonic acid were added along with sodium sulfate, to remove any water, and the reaction was allowed to warm to ambient temperature. The reaction was monitored via FTIR, and completion was reached when the spectrum showed a reduction in the carbonyl peak at 1731 cm^{-1}, and a large peak, corresponding to the C-O stretch of the acetal, appeared at 1120 cm^{-1}.

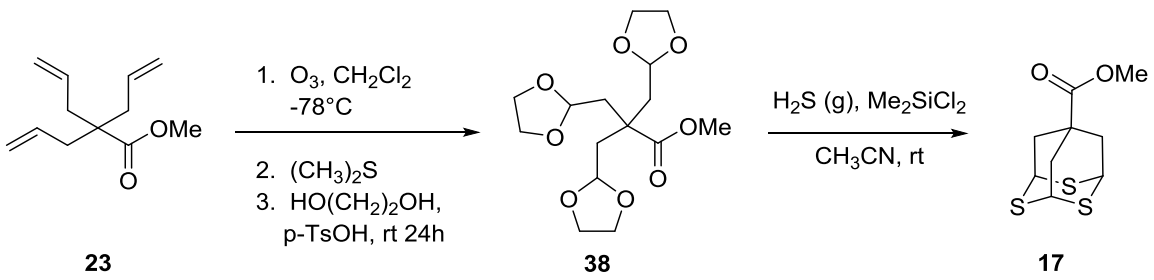

Scheme 3.14: Second reaction using an acetal intermediate (**38**) to form the tripod (**17**).[74,94]

In the ^{1}H NMR spectrum, the peak at 2.14 ppm corresponds to the methylene of the aliphatic shoulder, and the peak at 2.59 ppm is most likely residual ethylene glycol. The singlet at 3.71 ppm is characteristic of the OC*H*$_3$ of the ester, and the peaks at 3.73 ppm correlate to the acetal OC*H*$_2$C*H*$_2$O linkage. The peak at 5.33 ppm is representative of the hydrogen atoms α to both oxygen atoms of the acetal (CH$_2$C*H*-O$_2$). Also, the absence of the aldehyde peak usually present at ~7.2 ppm, indicates the reaction proceeded. The FTIR spectrum and the ^{1}H NMR spectrum are shown in Figures 3.9 and 3.10, respectively.

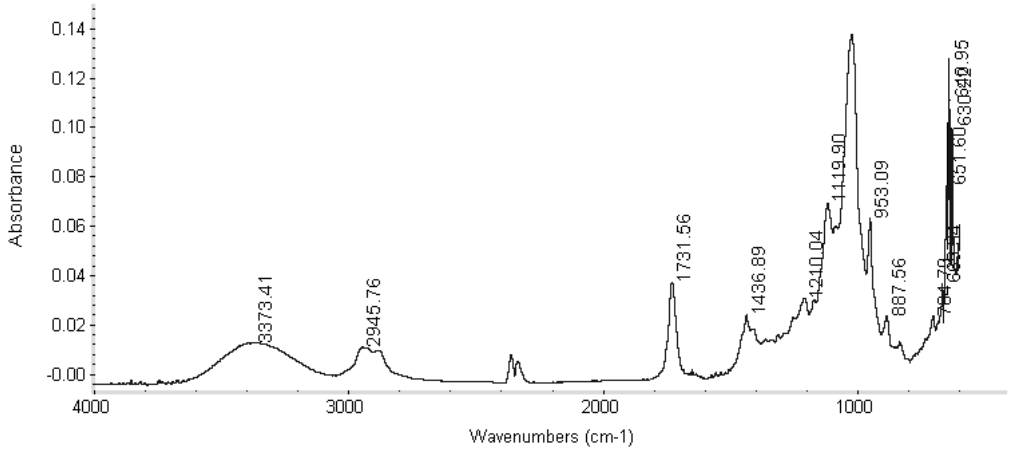

Figure 3.9: The FTIR spectrum of the reaction of triallyl methylacetate (**23**) with ethylene glycol.

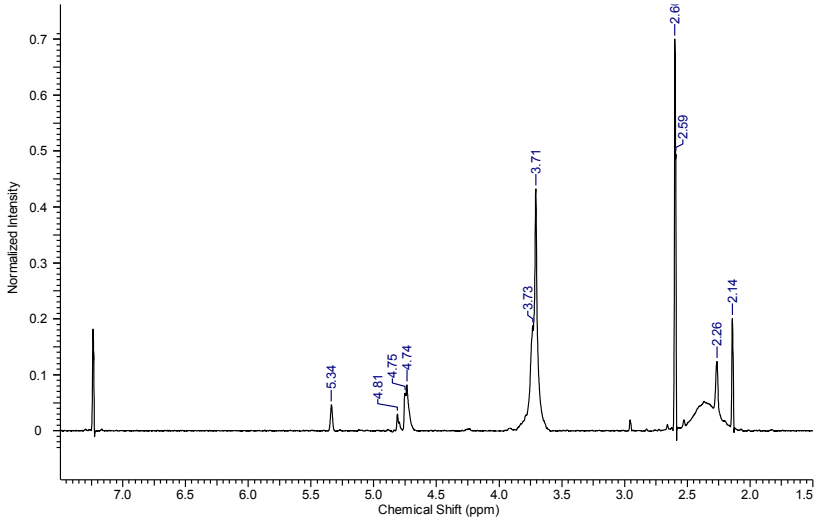

Figure 3.10: The ^{1}H NMR spectrum of the reaction of triallyl methylacetate (**23**) with ethylene glycol.

This acetal intermediate was dissolved in freshly distilled CH_2Cl_2 and further reacted with H_2S gas in the presence of dichlorodimethylsilane. This reaction was performed using a pressure vessel to ensure enough H_2S was dissolved in the solution. The reaction was stirred at room temperature for 24 h and showed formation of tripod product had

occurred, as shown by TLC analysis. Upon work-up with sodium bicarbonate and extraction with methylene chloride, the product was produced in 15% yield, a slight increase in yield compared to previous reactions and no oxygenated product was observed in the analysis of this reaction.

3.3.4 Triallyl carbinol to tripod reaction

The ideal starting material for the synthesis of tripod derivatives would be a molecule that has an easily manipulated functional group present at what will be the 7-position of the tripod. Another ideal property would have the triallyl moiety already present on the starting compound. One such compound is 4-allyl-1,6-heptadien-4-ol, or triallyl carbinol (**45**). In

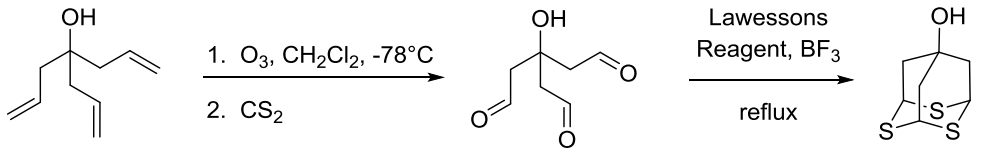

45 **53** **46**

Scheme 3.15: Attempted synthesis of 7-hydroxy-2,4,9-trithiaadamantane (**46**).[33]

the standard synthesis of tripod, the triallylmethyl acetate is subjected to ozonolysis and reduction, followed by thionation and cyclization.[33,34] This same synthetic sequence was applied to the triallyl carbinol (**45**) (Scheme 3.15). The triallyl carbinol was dissolved in CH_2Cl_2 and subjected to ozonolysis. It took an unusually long amount of time for the

persistent blue color to appear, indicating the solution has become saturated with ozone. The ozonide was reduced using dimethyl sulfide, and after stirring for 15 min, Lawesson's reagent and BF_3 were added and the reaction refluxed for 24 h. It was noted that the reaction mixture was extremely viscous and sticky when samples were taken out for TLC and NMR analysis. The reaction turned a blue/black color and no product or starting material could be detected by TLC. One reason this reaction was not successful could be from polymerization of the hydroxyl group from one molecule and an aldehyde group of another, similar to the proposed mechanism for the cyclization of the oxygenated tripod (**51**), as illustrated in Figure 3.3. To prevent polymerization from occurring, future syntheses may involve manipulating the alcohol group to the desired functionality prior to ozonolysis.

3.3.5 Attempt towards 2,4,9-trithiaadamantane-methylketone

Although the conversion of the triallyl carbinol to 2,4,9-trithiaadamantane-7-hydroxy was not successful, the methyl ketone derivative is still an ideal starting point for creating **18** and other novel amine drug analogs via reductive amination. An attempt to convert the methylester of the tripod to a methyl ketone was performed, in a procedure proposed by Evans and Morken, where a carbon nucleophile is added to the ester.[88] In this reaction, illustrated in Scheme 3.15, the tripod was dissolved in dry THF, and (trimethylsilyl)methyllithium was added dropwise under an inert atmosphere. After the addition of dry methanol, the reaction was analyzed using TLC. It appeared that a mixture of products and starting material was present. ^{1}H NMR analysis of the reaction

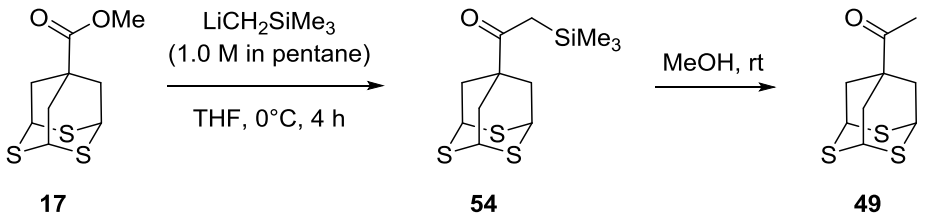

Scheme 3.16: Attempted synthesis of tripod methyl ketone (**49**).[88]

was carried out, and the spectrum shows a mixture of the ketone (**49**), the silane intermediate (**54**), and residual starting material (**17**). Based on the spectrum, namely the peak at 5.37 ppm, it appears that the base of the tripod is mostly in the oxygenated form (Figure 3.11). The peak at 0.10 ppm corresponds to the methyl groups of the silane. The peaks at 1.56 and 2.28 ppm may result from the methylene groups of the tripod from two different molecules: the silane-substituted **54** and the ketone **49**. The peaks at 3.75 and 3.84 ppm may also be indicative of the two products formed, correlating to the C*H*$_3$ of the ketone, or the α-methylene of the silane.

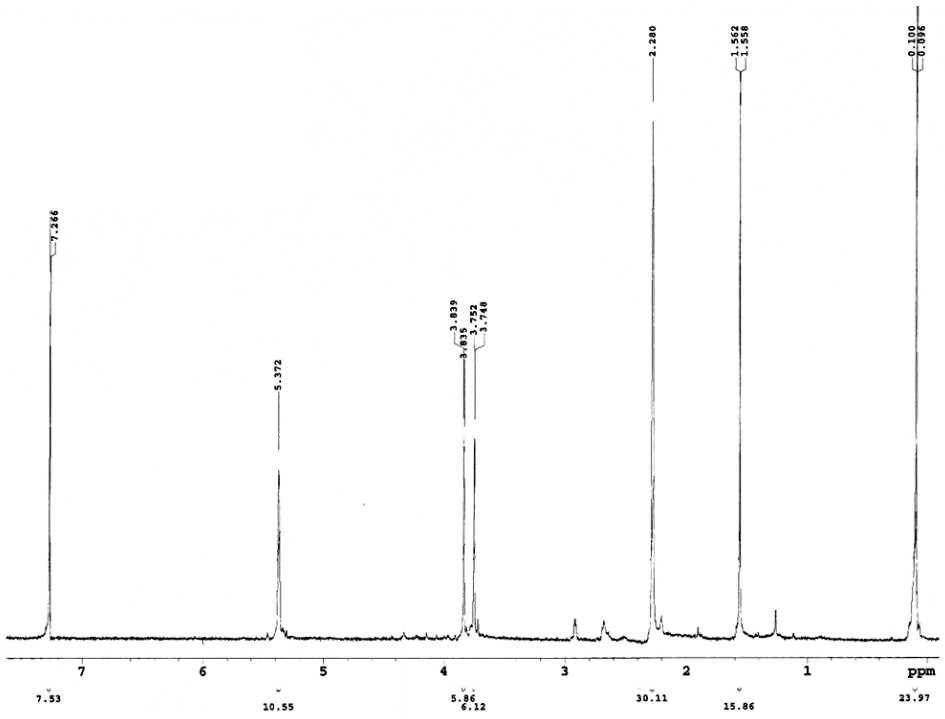

Figure 3.11: ^{1}H NMR spectrum of the reaction of **17** with (trimethylsilyl)methyllithium.

3.4 Conclusions and Future Work

As described in this chapter, the syntheses of methyl-2,4,8-trithiaadamantane-7-carboxylate are very low-yield, with the formation of several by-products especially during the key thionation and cyclization steps. Some of the attempts at improving the reaction yield were successful, but there is still room for optimization. The yields were slightly increased when using H_2S gas as the sulfur source, but this introduces a new set of issues, including the inconvenience of using a toxic gas, especially when considering commercial applications. Future studies may investigate new reactions to introduce sulfur during cyclization of the triallyl methylacetate.

The investigations into new starting compounds have opened doors for new derivative possibilities. If the hydroxy-tripod can be successfully synthesized, several pathways, previously discussed, could lead to the amantadine and rimantadine analogs in fewer steps. It would also be possible to introduce substituted amines during reductive amination to give unique molecules.[95] Once the hydroxy-tripod could be obtained, the manipulation to a nitrile could further the scope of reactions. Ritter-type reactions, where the nitrile is reacted with an electrophilic alkene to give N-alkyl amides, could be useful for creating a set of novel derivatives.[96] Also of importance is the conversion of the methyl ester to a methyl ketone. The attempts at this reaction, using (trimethylsilyl)methyllithium, gave a mixture of products. Further investigation of this transformation would be beneficial when synthesizing the rimantadine analog, which can be obtained from the ketone in one step rather than the multi-step syntheses outlined in Chapter 1. A synthesis, such as the Weinreb synthesis, could be investigated where the methyl ketone could be formed from the acid chloride.[97]

The use of a protecting group and a silane to prevent the cyclization of the trialdehyde intermediate proved to be successful. When using either methanol or ethylene glycol to form a tri-acetal intermediate and adding a silane during thionation, the incorporation of oxygen atoms in the ring was diminished. When employing this reaction, the tripod was synthesized with no detectable amounts of mono-, di-, or tri-oxygenated rings in the molecule. In a serendipitous reaction, the trioxaadamantane methyl ester, previously thought to be a nuisance in the tripod reaction, was created almost exclusively. It has been fully characterized, including high resolution mass

spectrometry analysis and a crystal structure was obtained. This compound could be used as the starting material to create new amine derivatives, which could also be evaluated as novel antiviral candidates for influenza A.

Although many obstacles must still be overcome in the synthesis of the tripod molecule, the reactions accomplished or attempted in this work have provided much insight into future directions of this project.

REFERENCES

1. Kawaoka, Yoshihiro. *Influenza Virology: Current Topics*. England: Caister Academic Press, 2006.

2. Hollenback, J.E. *Indian J Microbiol* **2009**, *49*, 348-351.

3. Neumann, G.; Noda, T.; Kawaoka, Y. *Nature* **2009**, *459*, 931-935.

4. Von Itzstein, M. *Nature Reviews. Drug Design* **2007**, *6(12)*, 967-971.

5. Chan, J.; Lewis, A.R.; Gilbert, M.; Karwaski, M.; Bennet, A.J. *Nature Chem Biol* **2010**, *6*, 405-411.

6. Stouffer, A.L.; Acharya, R.; Salom, D.; Levine, A.S.; Costanzo, L.D.; Soto, C.S.; Tereshko, V.; Nanda, V.; Stayrook, S.; DeGrado, W.F. *Nature* **2008**, *451*, 596-599.

7. Schnell, J.R.; Chou, J.J. *Nature* **2008**, *451*, 591-595.

8. Cady, S.D.; Schmidt-Rohr, K.; Wang, J.; Soto, C.S.; DeGrado, W.F.; Hong, M. *Nature* **2010**, *463*, 689-693.

9. Simonsen, L.; Viboud, C.; Grenfell, B.T.; Dushoff, J.; Jennings, L.; Smit, M.; Macken, C.; Hata, M.; Gog, J.; Miller, M.A.; Holms, E.C. *Mol. Biol. Evol*. **2007**, *24(8)*, 1811-1820.

10. Lindgren, G. *Chem. Scrip*. **1976**, *9*, 220-226.

11. Stetter, H.; Mayer, J.; Schwarz, M.; Wulff, K. *Chem. Ber*. **1960**, *93(1)*, 226.

12. Paulshock, M.; Watts, J.C. Pharmaceutical compositions and methods utilizing 1-aminoadamantane and its derivatives. E.I. Du Pont de Nemours and Company (Wilmington, DE) United States Patent 3,310,469 (Mar. 21, 1967).

13. Moiseev, I.K.; Doroshenko, R.I.; Ivanova, V.I. *Pharm. Chem. J*. **1976**, *10(4)*, 450.

14. Prichard, W.W. Adamantanes and tricyclo[4.3.1.1$^{3.8}$] undecanes. E.I. Du Pont de Nemours and Company (Wilmington, DE) *United States Patent* 3,352,912 (Nov. 14, 1967).

15. Prichard, W.W. Pharmaceutical compositions and methods of controlling influenza a virus infection utilizing substituted adamantanes and tricyclo[4.3.1.1$^{3.8}$] undecanes. E.I. Du Pont de Nemours and Company (Wilmington, DE) *United States Patent* 3,592,934 (July 13, 1971).

16. Brake, L.D. Preparations of α-methyl-adamantane-methylamine and α,4-dimethyl-1-bicyclo[2.2.2]octane methylamine. E.I. Du Pont de Nemours and Company (Wilmington, DE) *United States Patent* 3,489,802 (Jan. 13, 1970).

17. Liu, J.J. Process for preparing rimantadine. E.I. Du Pont de Nemours and Company (Wilmington, DE) *United States Patent* 4,551,552 (Nov. 5, 1985).

18. Liu, J.J. Process for preparing rimantadine. E.I. Du Pont de Nemours and Company (Wilmington, DE) *European Patent Application* 178668 (Oct. 17, 1985).

19. Bright, R.A.; Medina, M.; Xu, X.; Perez-Oronoz, G.; Wallis, T.R.; Davis, X.M.; Povinelli, L.; Cox, N.J. *Lancet* **2005**, *366*, 1175-1181.

20. Astrahan, P.; Kass, I.; Cooper, M. A.; Arkin, I. T. *Proteins* **2004**, *55*, 251–257.

21. Leonov, H.; Astrahan, P.; Krugliak, M.; Arkin. I.T. *J. Am. Chem. Soc.* **2011**, *133*, 9903-9911.

22. Stamatiou, G.; Foscolos, G.B.; Fytas, G.; Antonios, K.; Kolocouris, N.; Pannecouque, C.; Witvrouw M.; Padalko, E.; Neyts, J.; De Clercq, E. *Bioorg. Med. Chem.* **2003**, *11*, 5485–5492.

23. Kurtz, S.; Luo, G.; Hahnenberger, K.M.; Brooks, C.; Gecha, O.; Ingalls, K.; Numata, K.; Krystal, M. *Antimicrob. Agents Chemother*. **1995**, *39*, 2204-2209.

24. Tu, Q.; Pinto, L.H.; Luo, G.; Shaughnessy, M.A.; Mullaney, D.; Kurtz, S.; Krystal, M.; Lamb, R.A. *J. Virol*. **1996**, *70*, 4246-4252.

25. Wang, J.; Cady, S.D.; Balannik, V.; Pinto, L.H.; DeGrado, W.F.; Hong, M. *J. Am. Chem. Soc*. **2009**, *131,* 8066–8076.

26. Balanik, V.; Wang, J.; Ohigashi, Y.; Jing, X.; Magavern, E.; Lamb, R.A.; DeGrado, W.F.; Pinto, L.H. *Biochem*. **2009**, *48*, 11872-11882.

27. DeGrado, W.F. and Wang, J. Spiro-piperidine Inhibitors. Woodcock Washburn LLP (Philadelphia, PA) *United States Patent* 2010/0069420 (Mar. 18, 2010).

28. Zoidis, G.; Kolocouris, N.; Naesens, L.; De Clercq, E. *Bioorg. Med. Chem*. **2009**, *17*, 1534–1541.

29. Kolocouris, N.; Zoidis,G.; Foscolos, G. B.; Fytas, G.; Prathalingham, R. S.; Kelly, J. M.; Naesens, L.; De Clercq, E. *Bioorg. Med. Chem. Lett*. **2007**, 17, 4358.

30. Kittredge, K.W.; Minton, M.A.; Fox, M.A.; Whitesell, J.K. *Helv. Chim. Acta* **2002**, *85*, 788.

31. Lindgren, G. *Chem. Scrip*. **1976**, *9*, 220-226.

32. Hu, J. Liu, Y.; Khemtong, C.; El Khoury, J.M.; McAfoos, T.J.; Taschner, I.S. *Langmuir* **2004**, *20*, 4933–38.

33. Khemtong, C.; Hu, J. *J. Sulfur Chem.* **2005**, *26*, 105-109.

34. Khemtong, C.; Banerjee, D.; Liu, Y.; El Khoury, J.M.; Rinaldi, P.L.; Hu, J. *Supramol. Chem.* **2005**, *17(4)*, 335.

35. Tabushi, I.; Kuroda, Y.; Yokota, K. *Tetrahedron Letters* **1982**, *23* (44), 4601.

36. "Bond lengths in crystalline organic compounds", in *CRC Handbook of Chemistry and Physics, Internet Version 2005,* David R. Lide, ed., <http://www.hbcpnetbase.com>, CRC Press, Boca Raton, FL, 2005 (p. 1381-1388).

37. Hadad, C.M.; Rablen, P.R.; Wiberg, K.B. *J. Org. Chem*. **1998**, *63*, 8668-8681.

38. Kaefer, V.; Semedo, J.G.; Silva Kahl, V.F.; Von Borowsky, R.G.; Gianesini, J.; Kist, T.B.L.; Pereira, P.; Picada, J.N. *J. Appl. Toxicol.* **2010**, *30*, 745–753.

39. Koza, G.; Özcan, S.; Sahin, E.; Balci, M. *Tetrahedron* **2009**, *65*, 5973.

40. Pielak, R.M.; Chou, J.J. *Biochem. Biophys. Res. Commun*. **2010**, *401(1),* 58-63.

41. "Strengths of chemical bonds", in *CRC Handbook of Chemistry and Physics, Internet Version 2005,* David R. Lide, ed., <http://www.hbcpnetbase.com>, CRC Press, Boca Raton, FL, 2005 (p. 1446).

42. McGeary, R.P.; Bennett A.J.; Tran, Q.B.; Prins, J.; Ross, B.P. *Tetrahedron* **2009**, *65*, 3994.

43. Munch-Petersen. *J. Org. Syn*. **1953**, 33, 53-55.

44. Stieglitz, J. *Am. Chem. J*. **1896**, *18*, 751.
45. Linke, S.; Tissue, G.T.; Lwowski, W. *J. Am. Chem. Soc*. **1967**, *89*, 6308.

46. Lwowski, W. *Angew. Chem. Int. Ed*. **1967**, *6*, 897.

47. Capson, T.L.; Poulter, C.D.; *Tet. Lett*. **1984**, *25*(33), 3515.

48. Schulze, Matthias. *Syn. Comm*. **2010**, *40*, 1461.

49. Smith, P.A.S. *Org. React*. **1946**, *3*, 337.

50. Huang, A.; Moretto, A.; Janz, K.; Lowe, M.; Bedard, P.W.; Tam, S.; Di, L.; Clerin, V.; Sushkova, N.; Tchernychev, B.; Tsao, D.H.H.; Keith, J.C.; Shaw, G.D.; Schaub, R.G.; Wang, Q.; Kaila, N. *J. Med. Chem*. **2010**, *53*(16), 6003.

51. Zakharkin, L.I.; Khorlina, I.M. *Tet. Lett*. **1962**, 619-620.

52. Ireland, R.E.; Norbeck, D.W. *J. Org. Chem*. **1985**, *50(12)*, 2198.

53. Dessrosiers, J.; Côtè, A.; Boezio, A.A.; Charette, A.B. *Org. Synth*. **2006**, *83*, 5.

54. Smith, N.L.; Sisler, H.H. *J. Org. Chem*. **1961**, *26*, 5145-5149.

55. Sisko, J.; Mellinger, M.; Sheldrake, P.W.; Baine, N.H. *Org. Synth*. **2004**, *77*, 198.

56. Modhu, S.M.; Fröhlich, R.; Studer, A. *Org. Lett*. **2008**, *10*, 1847-1850.

57. Han, Z.; Busch, R.; Fandrick, K.R.; Meyer, A.; Xu, Y.; Krishnamurthy, D.K.; Senanayake, C.H. *Tetrahedron* **2011**, *67*, 7035-7041.

58. Han, Z.; Krishnamurthy, D.K.; Pflume, D.; Grover, P.; Wald, S.A.; Senanayake, C.H. *Org. Lett*. **2002**, *4*, 4025-4028.

59. Lesma, G.; Landoni, N.; Pilati, T.; Sacchetti, A.; Silvani, A. *J. Org. Chem.* **2009**, *74*, 4537-4541.

60. Mecozzi, T.; Petrini, M. *J. Org. Chem*. **1999,** *64,* 8970-8972.

61. Miyashita, M.; Yoshikoshi, A.; Grieco, P.A. *J. Org. Chem.* **1977**, *42(23)*, 3772.

62. Weinreb ref Nahm, S.; Weinreb, S.M.; *Tet. Lett*. **1981**, *22(39)*, 3815-3818.

63. Bost, R.W.; Constable, E.W. *Org. Synth.* **1936**, *16*, 81.

64. Grubbs, R.H.; Miller, S.J.; Fu, G.C. *Acc. Chem. Res.* **1995**, 28, 446-452.

65. Polshettiwar, V.; Varma, R.S. *J. Org. Chem.* **2008**, *73(18)*, 7417.

66. Olah, G.A.; Husain, A.; Balaram Gupta, B.G.; Narang, S.C. *Angew. Chem. Int. Ed.* **1981**, *20*, 690.

67. Aida, T.; Chan, T.H.; Harpp, D.N. *Angew. Chem. Int. Ed.* **1981**, *20*, 690.

68. Jung, M.E.; Andrus, W.A.; Orstein, P.L. *Tet. Lett.* **1977**, *48*, 4175.

69. Jarowiski, K.; Kocienski, P. *J. Chem. Soc. Perkin Trans. 1,* **1998**, *1*, 4005.

70. Meth-Cohn, O. *Org. Synth.* **1990**, *68*, 155.

71. Bevington, J.C.; Norrish, R.G.W. *Proc. R. Soc. Lond. A.* **1949**, *196*, 363-378.

72. Claus, R.E.; Schrieber, S.L. *Org. Synth.* **1986**, *64*, 150.

73. Bailey, P.S. J. *Org. Chem.* **1957**, *22(12)*, 1548.

74. Ireland, R.E.; Walba, D.M. *Org. Synth.* **1977**, *56*, 44.

75. Stowell, J.C.; Keith, D.R.; King, B.T. *Org. Synth.* **1984**, *62*, 140.

76. Kopka, I.E.; Fataftah, Z.A.; Rathke, M.W. *J. Org. Chem.* **1980**, *45*, 4616-4622.

77. Larock, R.C. *Comprehensive Organic Transformations*, 2nd ed., Wiley-VCH, New York **1999**, p 689-697.

78. Smith, M.B.; March, J. Advanced Organic Chmeistry: Reactions, Mechanisms, and Structure, 6th ed., John Wiley & Sons, Hoboken, New Jersey, p 556-557.

79. Reetz, M.T.; Chatziiosifidis, I. *Angew. Chem Int.Ed.* **1981**, *20*, 1017.

80. Zieger, H.E.; Wo, S. *J. Org. Chem.* **1994**, *59*, 3838.

81. Okada, I.; Kitano, Y. *Synthesis.* **2011**, *24*, 3997.

82. Canonne, P.; Foscolos, G.B.; Lemay, G. *Tet. Lett.* **1980**, 155.

83. Klyuev, M.V.; Khidekel, M.L. *Russ. Chem. Rev*. **1980**, *49*, 14.

84. Kadyrov, R.; Riermeier, T.H.; Dingerdissen, U.; Tararov, V.; Borner, A.J. *J. Org. Chem*. **2003**, *68*, 4067.

85. Chi, Y.; Zhou, Y.G.; Zhang, X. *J. Org. Chem*. **2003**, *68*, 4120.

86. Miller, A.E.G.; Biss, J.W.; Schwartzman, L.H. *J. Org. Chem*. **1959**, *24*, 627.

87. Marshall, J.A.; Andersen, N.H.; Schlicher, J.W. *J. Org. Chem*. **1970**, *35*, 858.

88. Evans, M.A.; Morken, J.P. *J. Am. Chem. Soc.* **2002**, *124*, 9020.

89. Mulzer, J.; Mantoulidis, A.; Ohler, E. *J. Org. Chem*. **2000**, *65*, 7456.

90. Nguyen, S.T.; Johnson, L.K.; Grubbs, R.H.; Ziller, J.W. *J. Am. Chem. Soc*. **1992**, *114(10)*, 3974.

91. Cullen, E.R.; Guziec, F.S. *J. Org. Chem*. **1986**, *51*, 1212-1216.

92. Whitesell, J.K.; Minton, M.A. *J. Am. Chem. Soc*. **1986**, *108*, 6802.

93. Samour, C.M.; Daskalakis, S. Preparation of aliphatic-substituted 1,3-dioxacycloalkanes as pharmaceutical skin penetration enhancers. Macrochem corporation (Woburn, MA) *European Patent Appl.* EP0268460 (May 25, 1988).

94. Chan, T.H.; Brook, M.A.; Chaly, T. *Synthesis*, **1983**, 203.

95. Abdel-Magid, A.F.; Carson, K.G.; Harris, B.D.; Maryanoff, C.A; Shah, R.D. *J. Org. Chem.,* **1996**, *61*, 3849-3862.

96. Ritter, J.J.; Kalish, J. *J. Am. Chem. Soc*. **1948**, *70*, 4048.

97. Nahm, S.; Weinreb, S.M. *Tet. Lett*. **1981**, *22(39)*, 3815.

APPENDICIES

APPENDIX A

^{1}H and ^{13}C NMR SPECTRA OF SELECTED COMPOUNDS

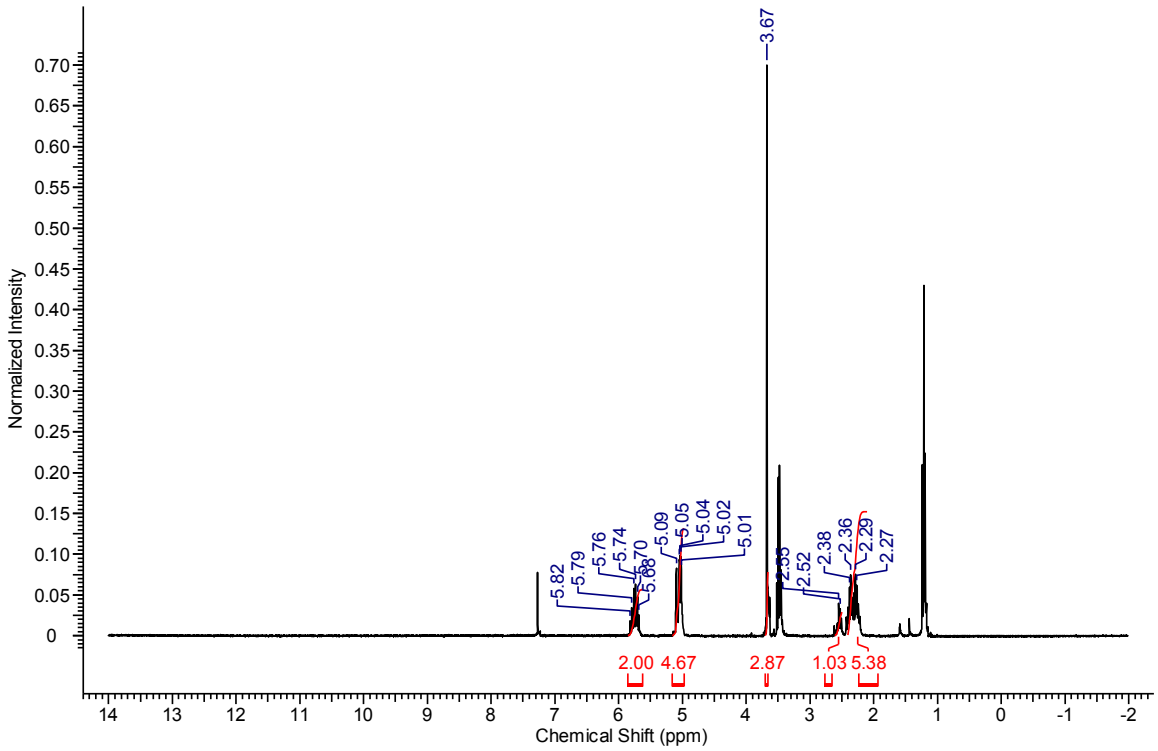

Figure A1: ^{1}H NMR spectrum of diallyl methylacetate (**22**).

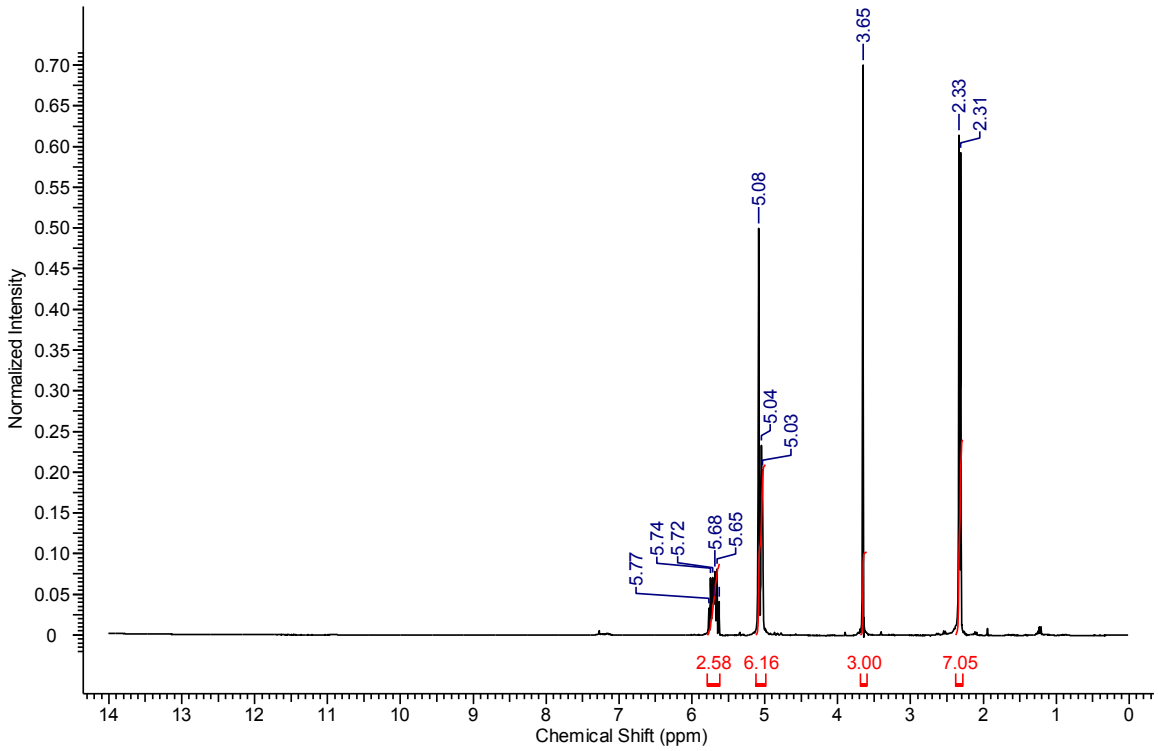

Figure A2: ^{1}H NMR spectrum of triallyl methylacetate (**23**).

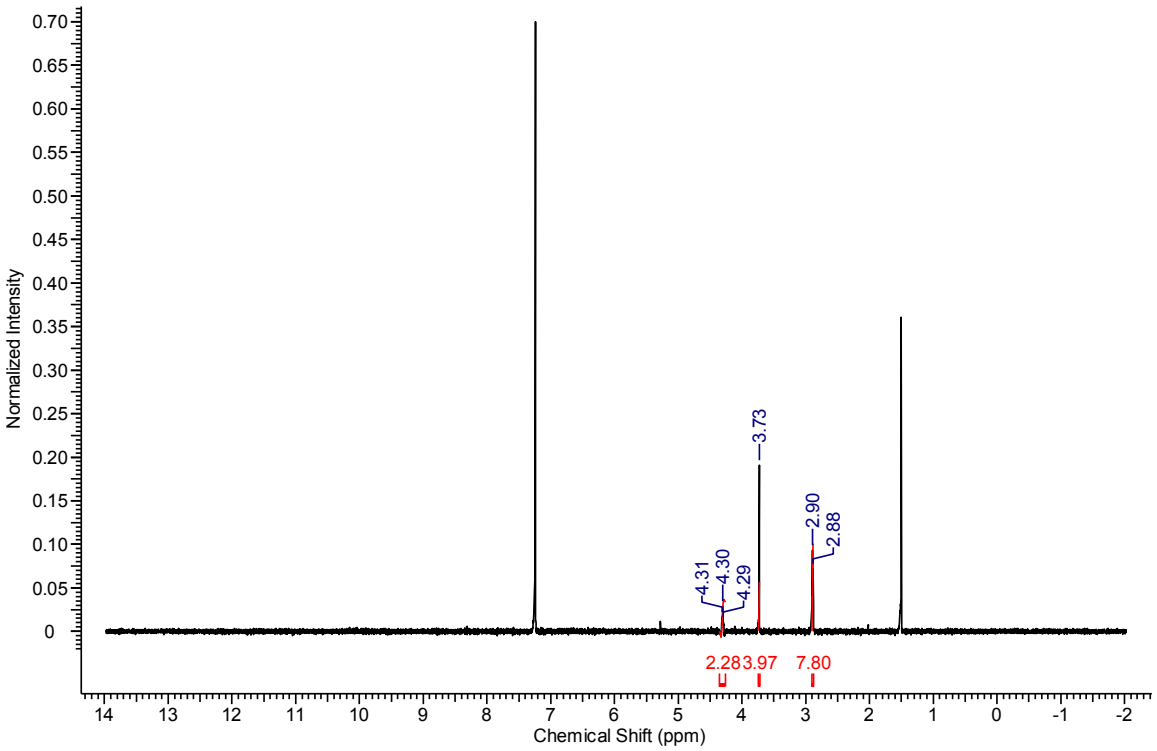

Figure A3: ^{1}H NMR spectrum of methyl-2,4,9-trithiaadamantan-7-carboxylate (**17**).

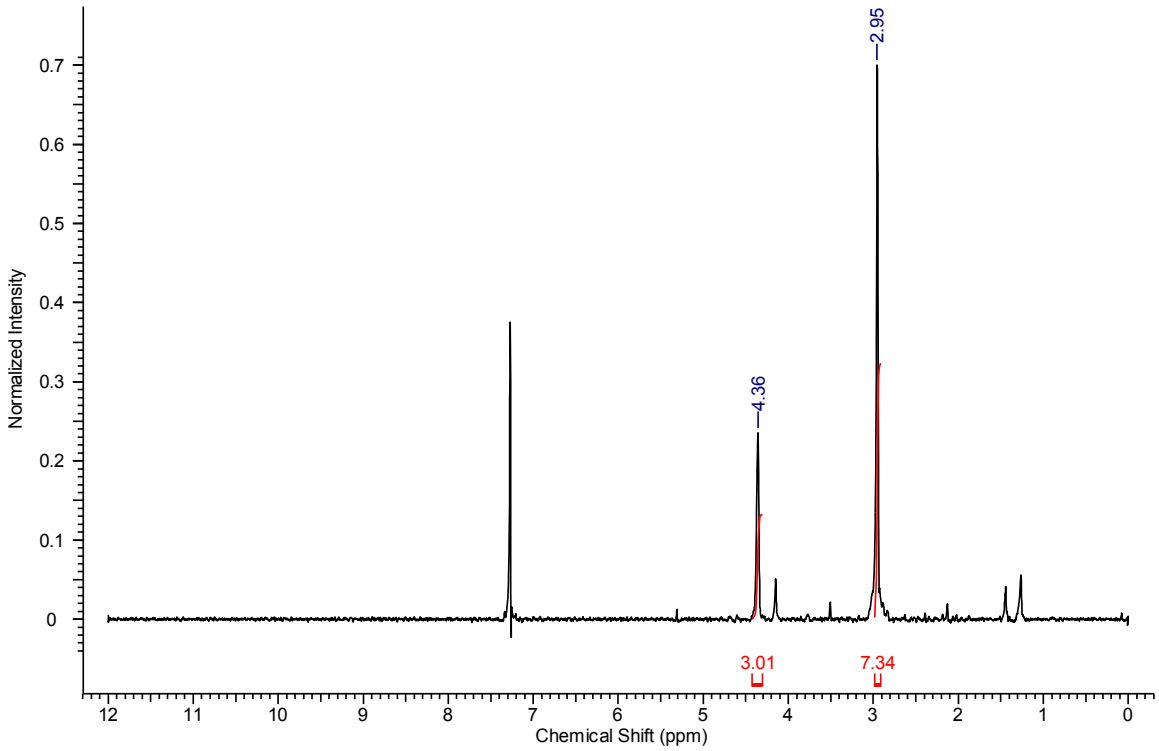

Figure A4: ^{1}H NMR spectrum of 2,4,9-trithiaadamantan-7-carboxylic acid (**26**).

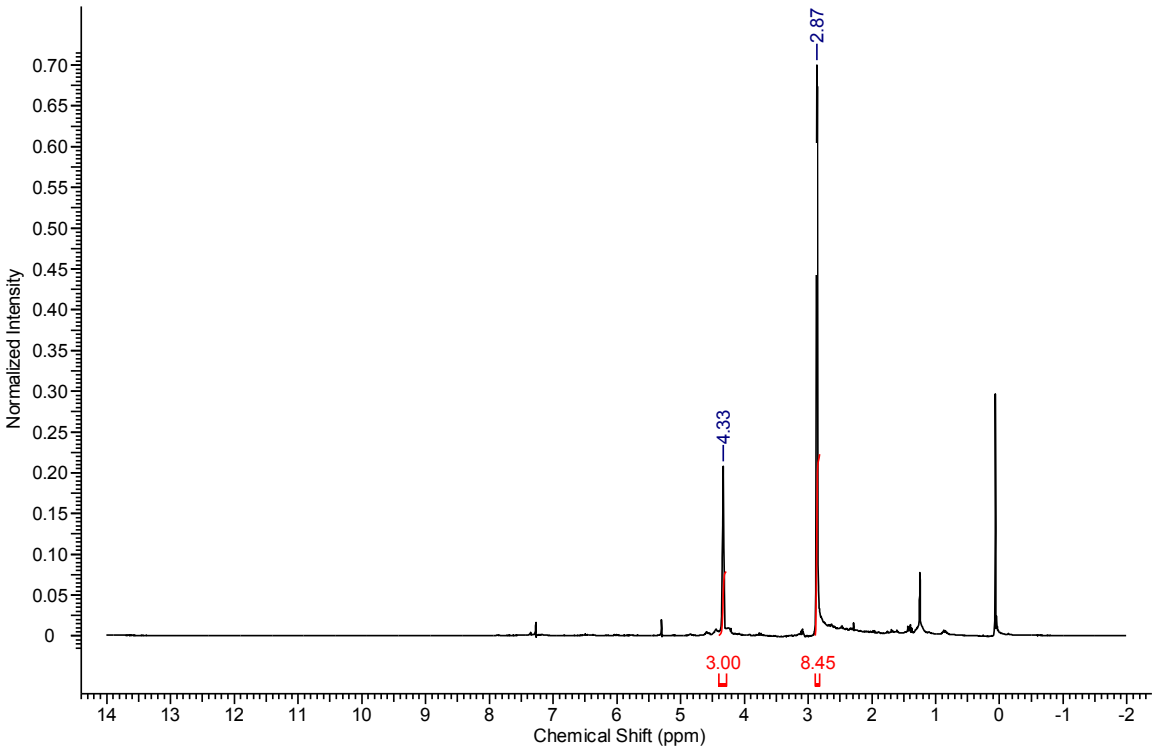

Figure A5: ^{1}H NMR spectrum of 2,4,9-trithiaadamantan-7-acyl azide (**27**).

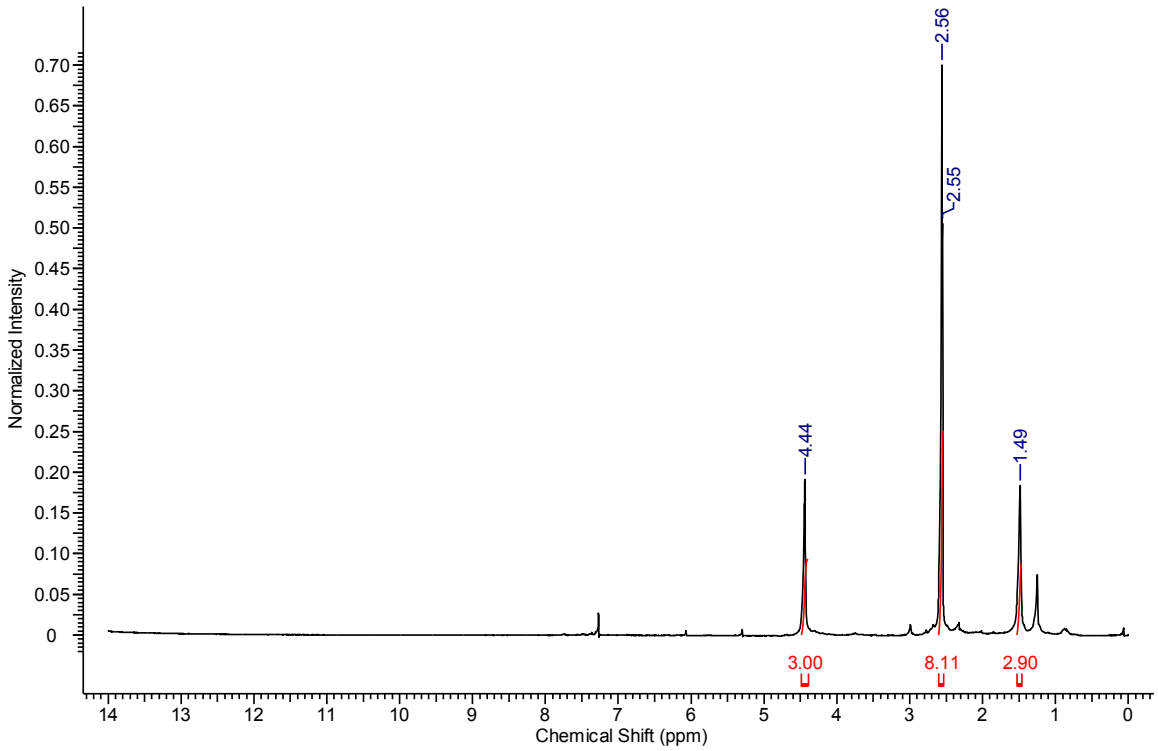

Figure A6: ^{1}H NMR spectrum of 2,4,9-trithiaadamantan-7-amine (**18**).

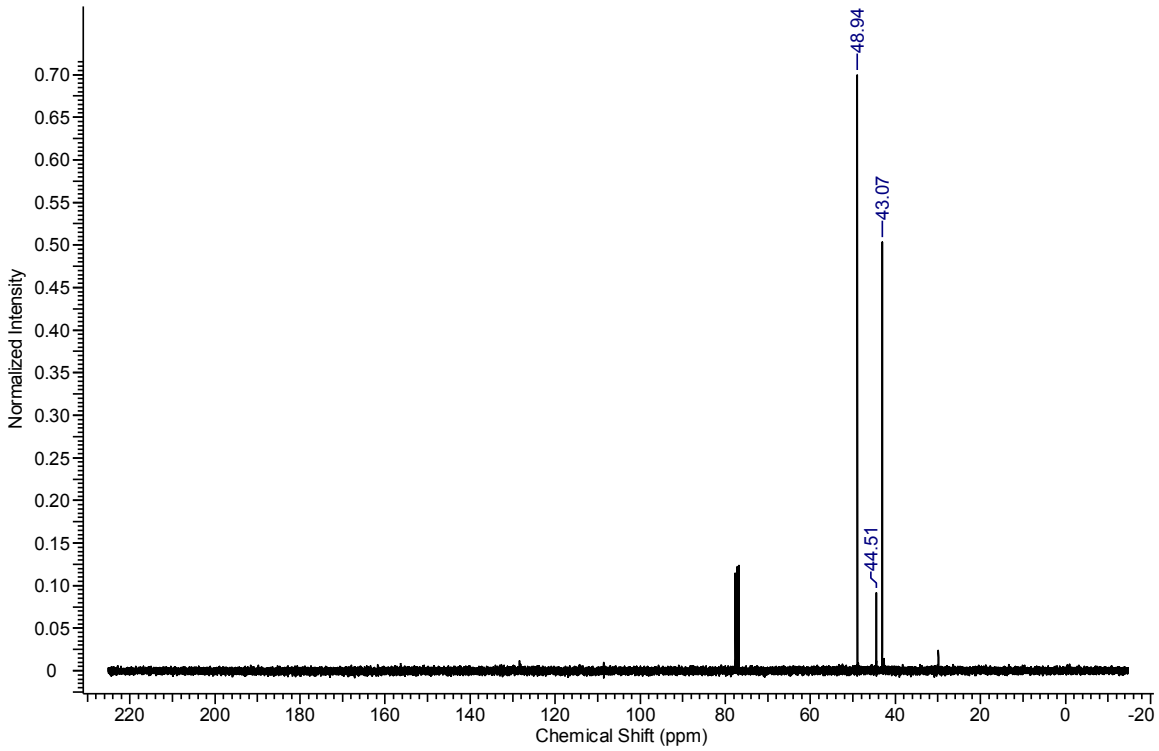

Figure A7: ^{13}C NMR spectrum of 2,4,9-trithiaadamantan-7-amine (**18**).

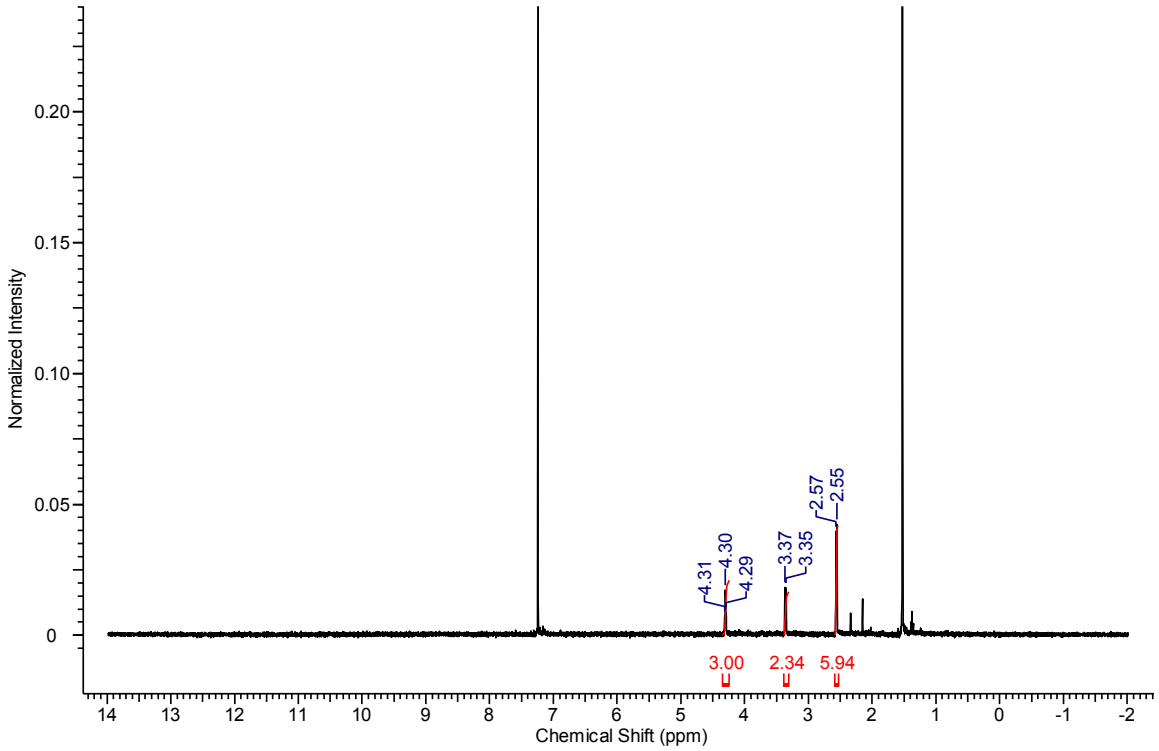

Figure A8: ^{1}H NMR spectrum of 2,4,9-trithiaadamantan-7-methanol (**29**).

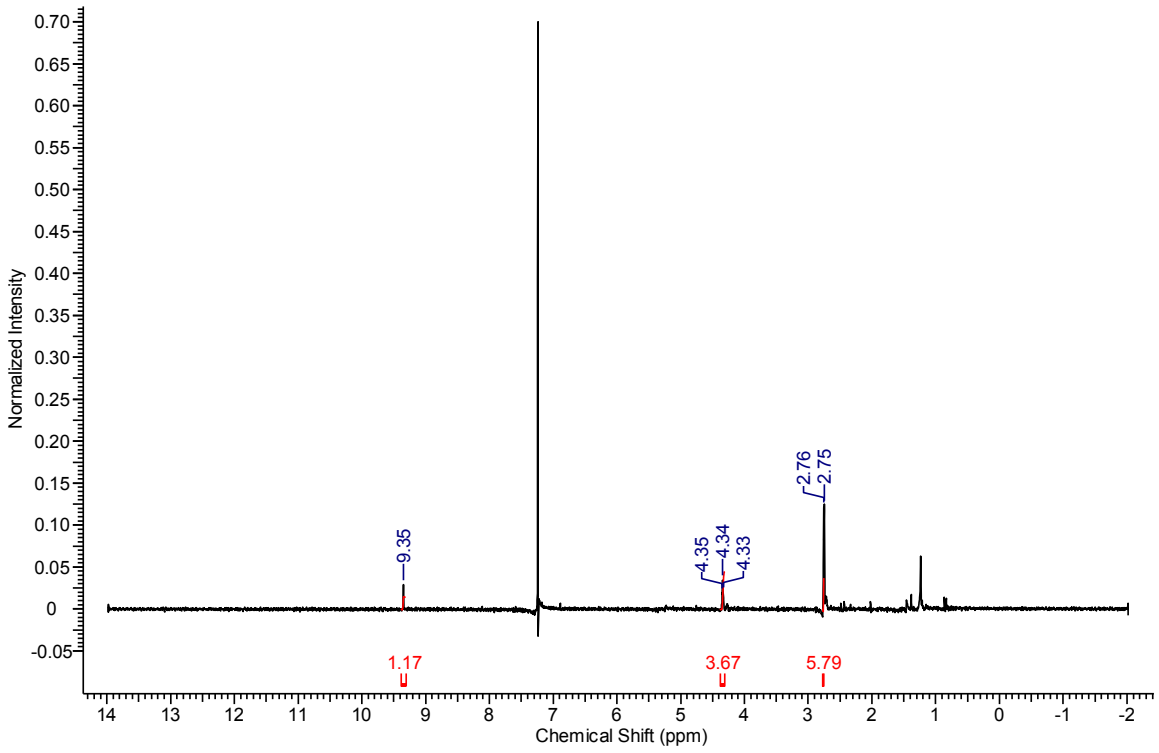

Figure A9: ^{1}H NMR spectrum of 2,4,9-trithiaadamantan-7-carbaldehyde (**30**).

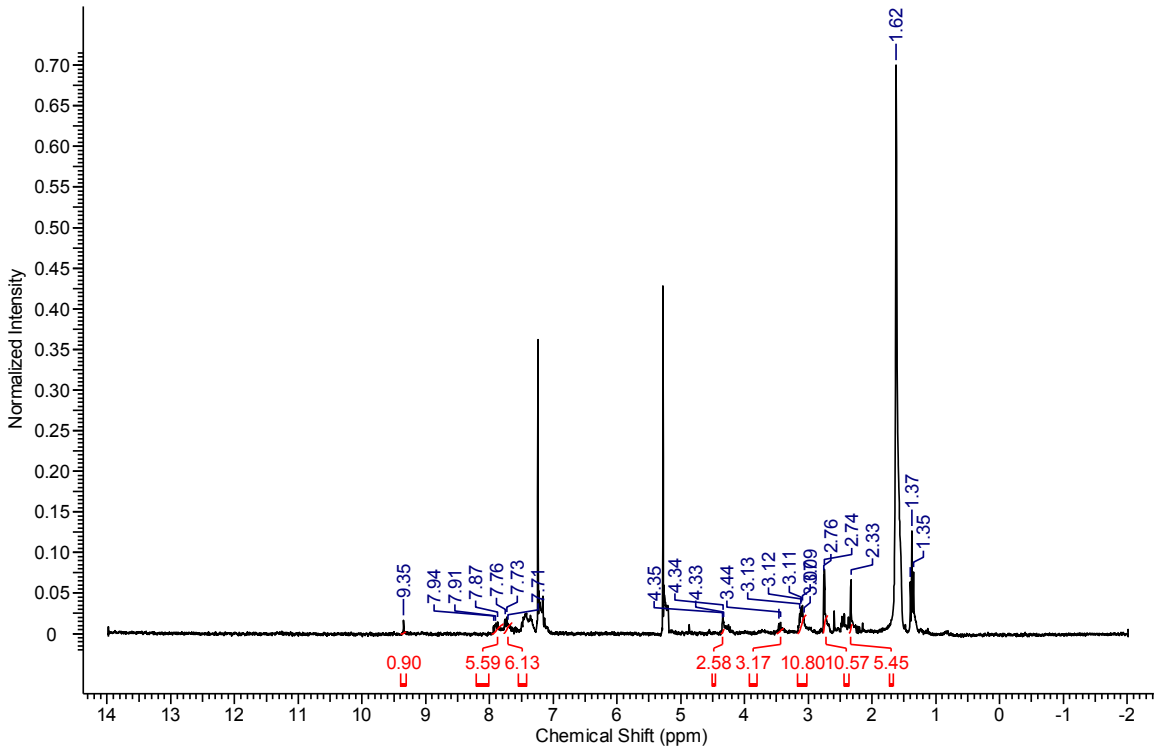

Figure A10: ^{1}H NMR spectrum of crude mixture of **16** with *P,P*-diphenylphosphinic amide and PTSA.

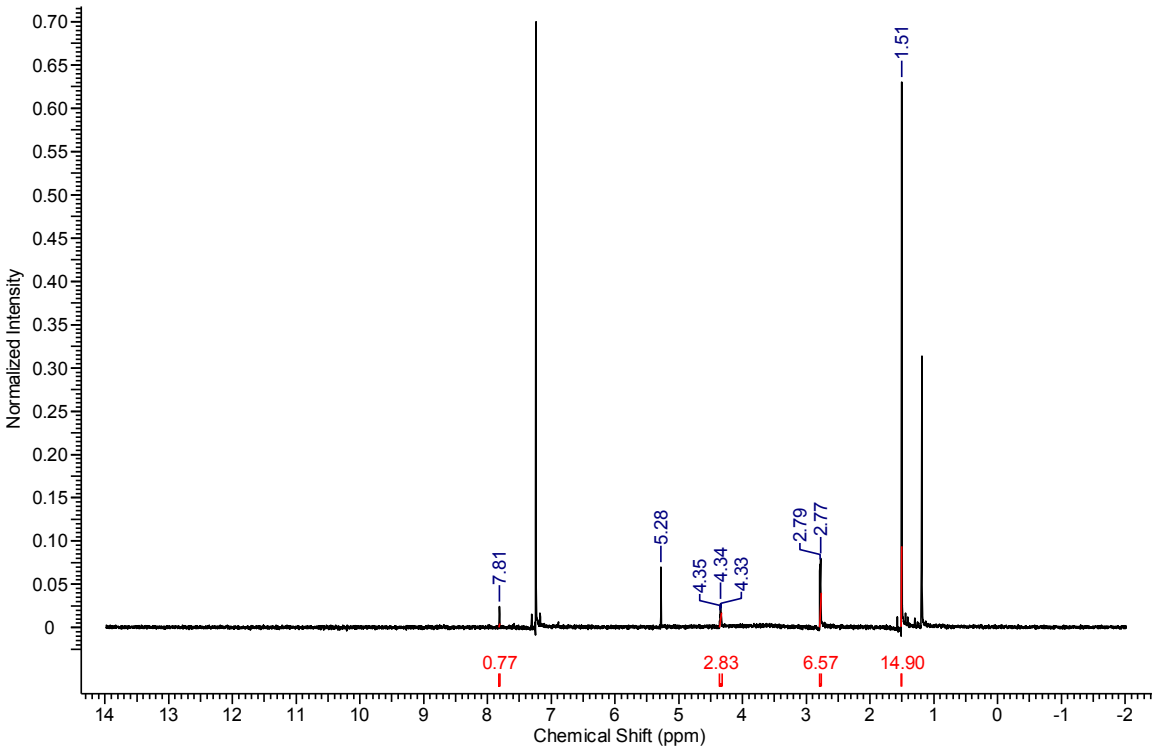

Figure A11: ^{1}H NMR spectrum of the tripod *tert*-butylsulfinylimine intermediate (**32**).

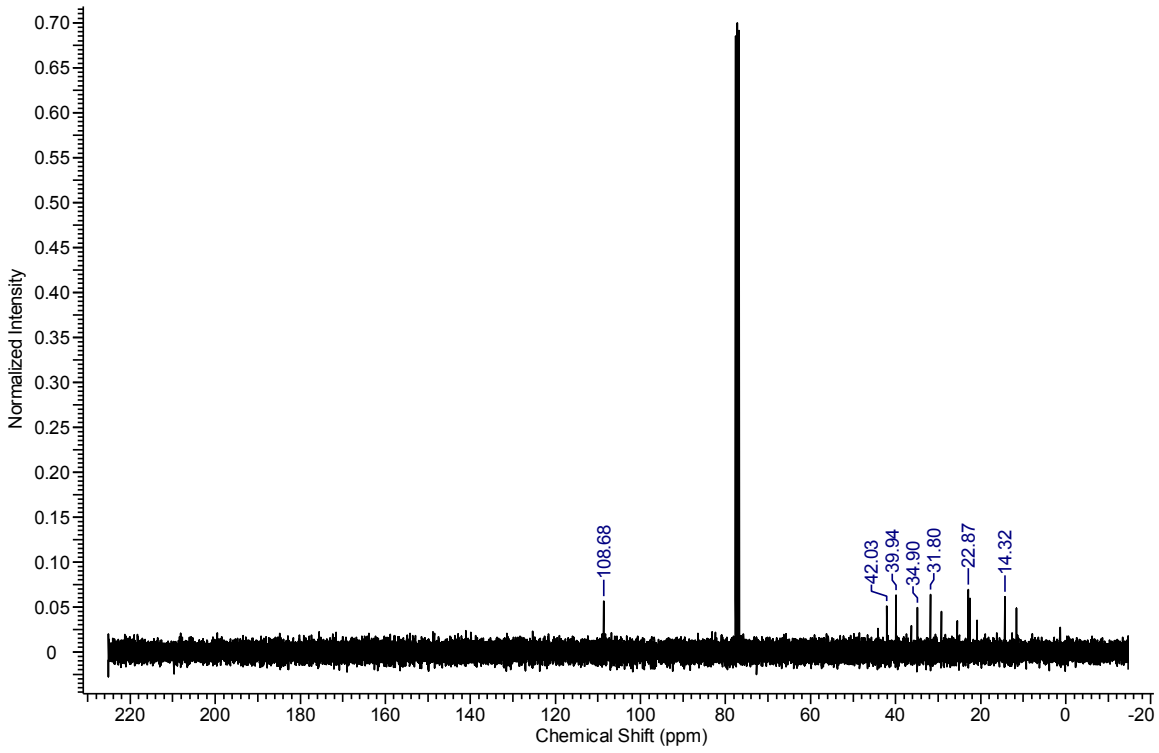

Figure A12: ^{13}C NMR spectrum of the tripod *tert*-butylsulfinylimine intermediate (**32**).

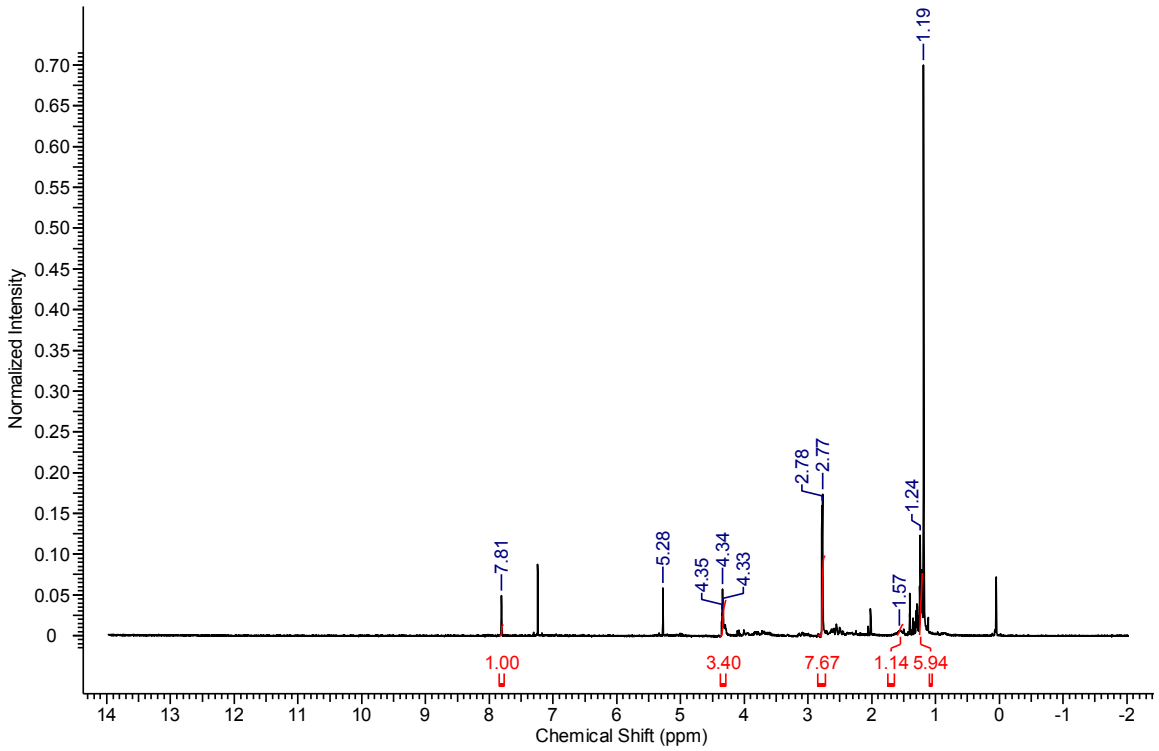

Figure A13: ^{1}H NMR spectrum of methylated tripod *tert*-butylsulfinylimine (**35**).

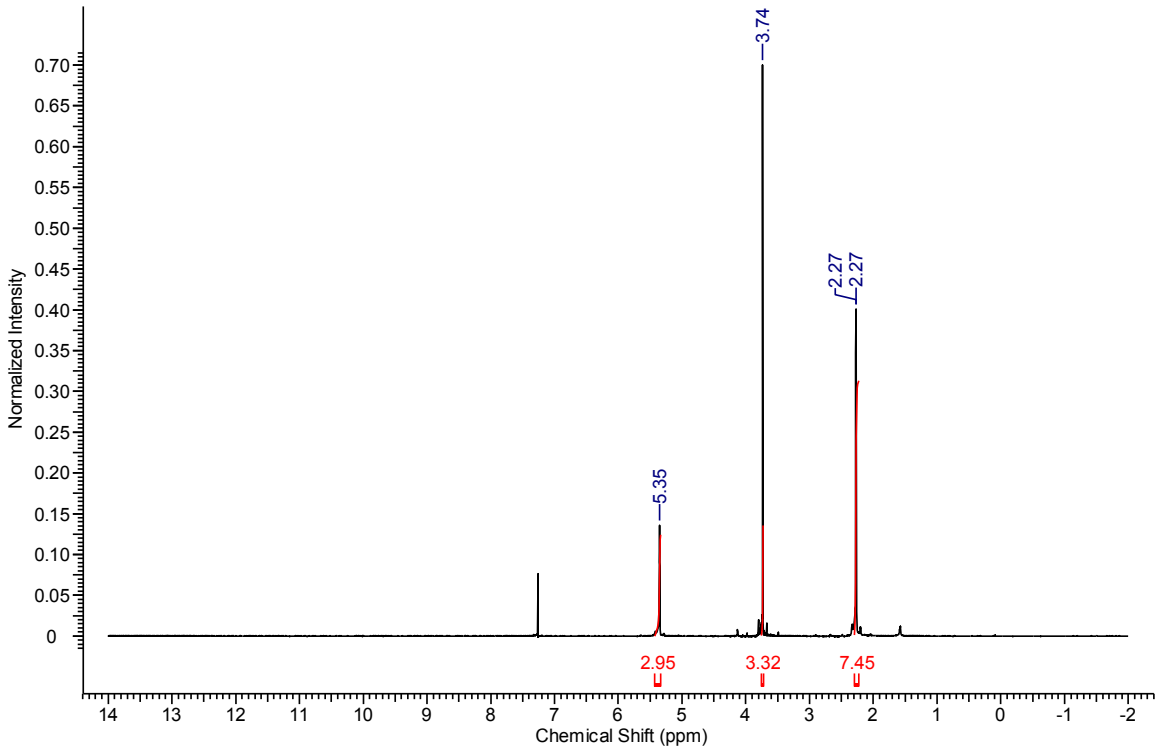

Figure A14: ^{1}H NMR spectrum of methyl-2,4,9-tritoxaadamantan-7-carboxylate (**51**).

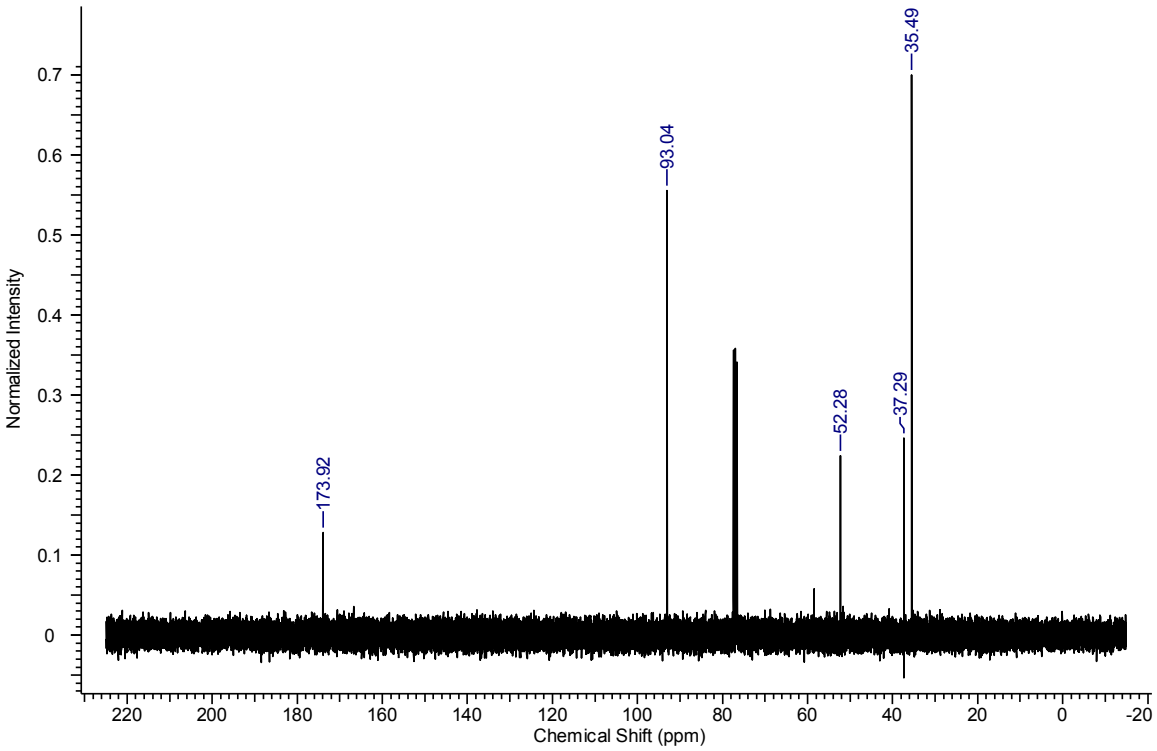

Figure A15: ^{13}C NMR spectrum of methyl-2,4,9-tritoxaadamantan-7-carboxylate (**51**).

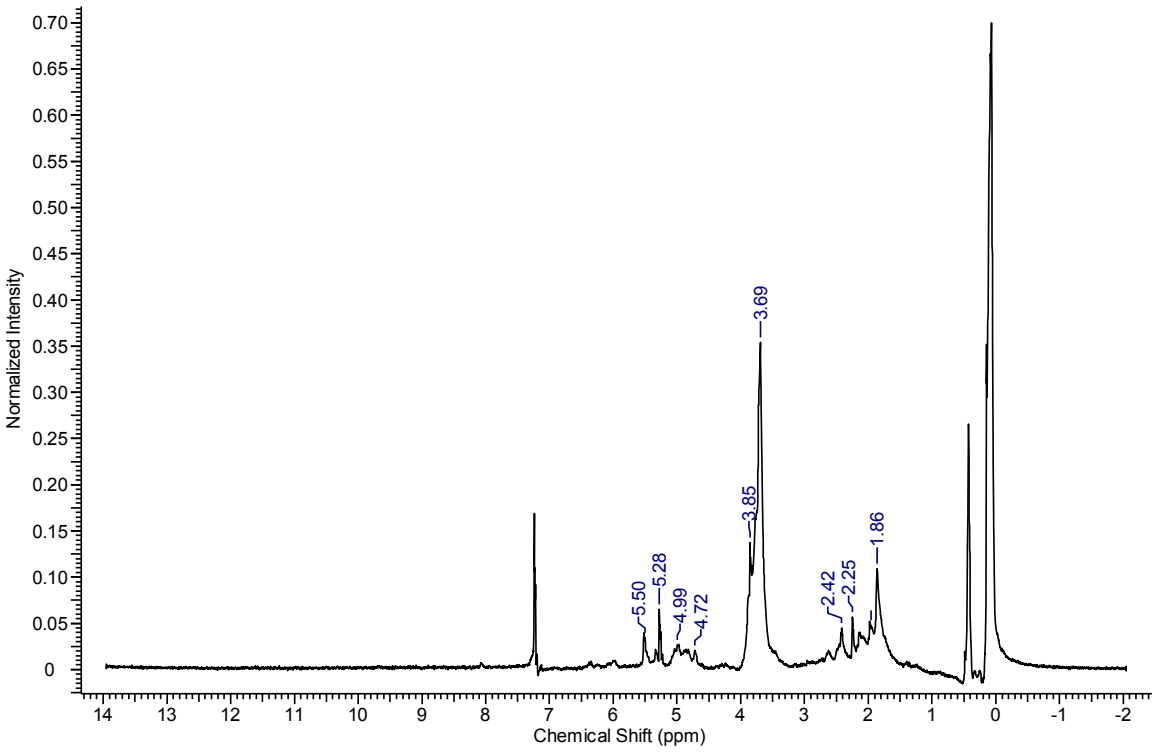

Figure A16: ^{1}H NMR spectrum of acetal **52** (methoxy protected triallyl methylacetate).

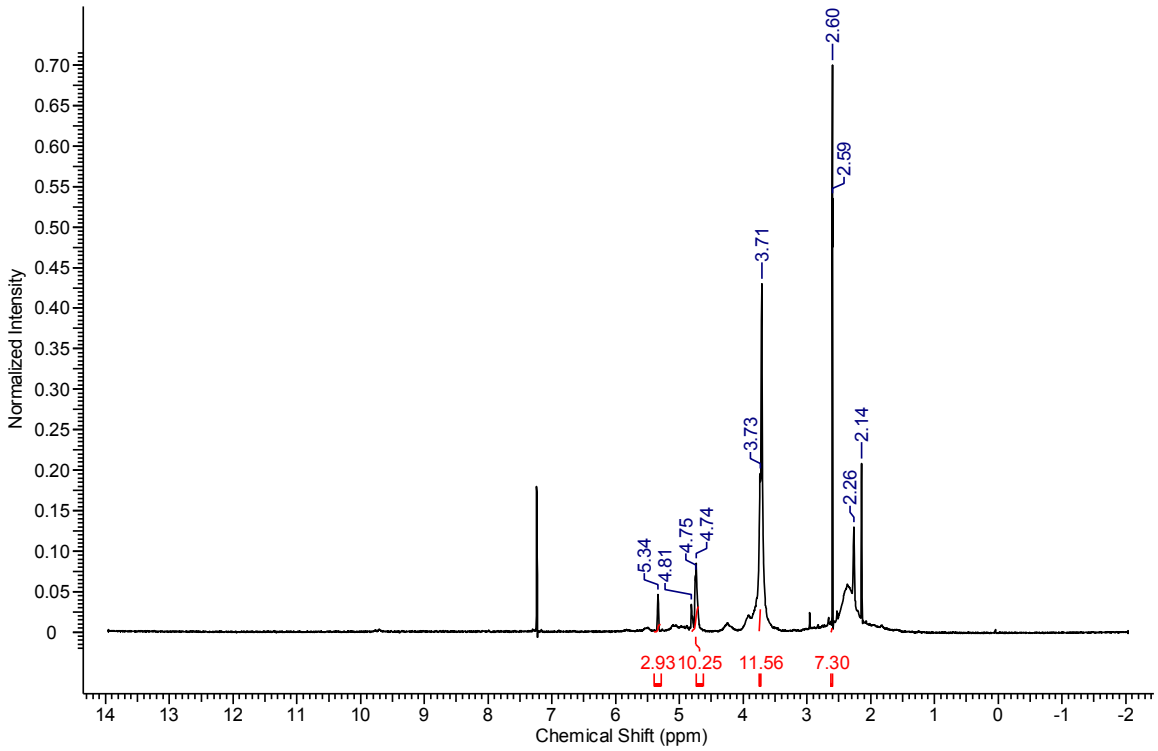

Figure A17: ^{1}H NMR spectrum of acetal **38** (ethylene glycol protected triallyl methylacetate).

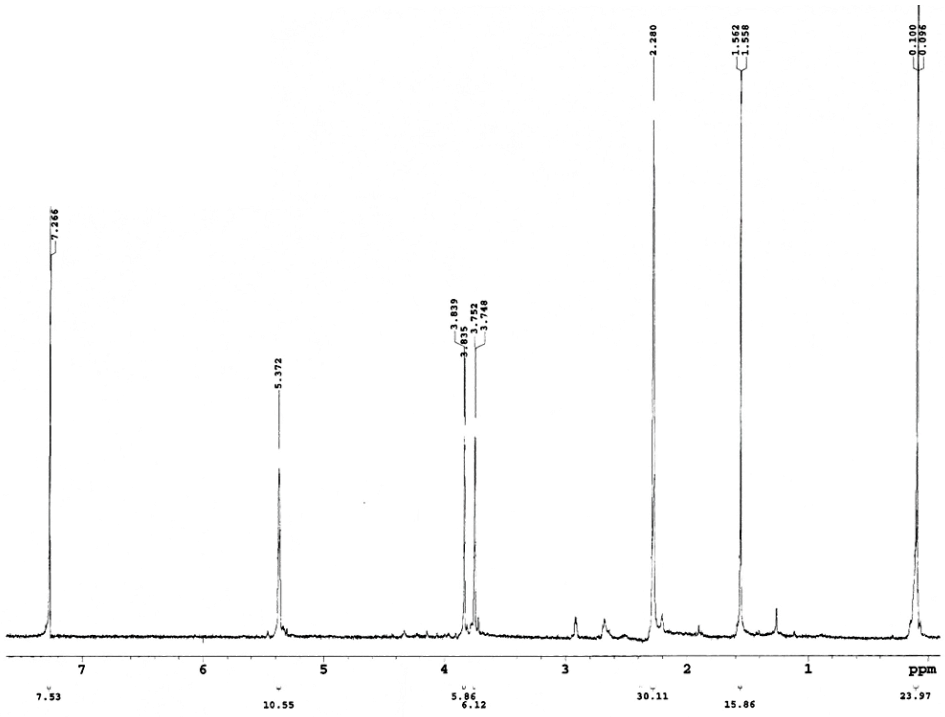

Figure A18: ^{1}H NMR spectrum of tripod methylketone (**54**) and tripod methylketone substituted trimethyl silane (**49**).

APPENDIX B

FTIR SPECTRA OF SELECTED COMPOUNDS

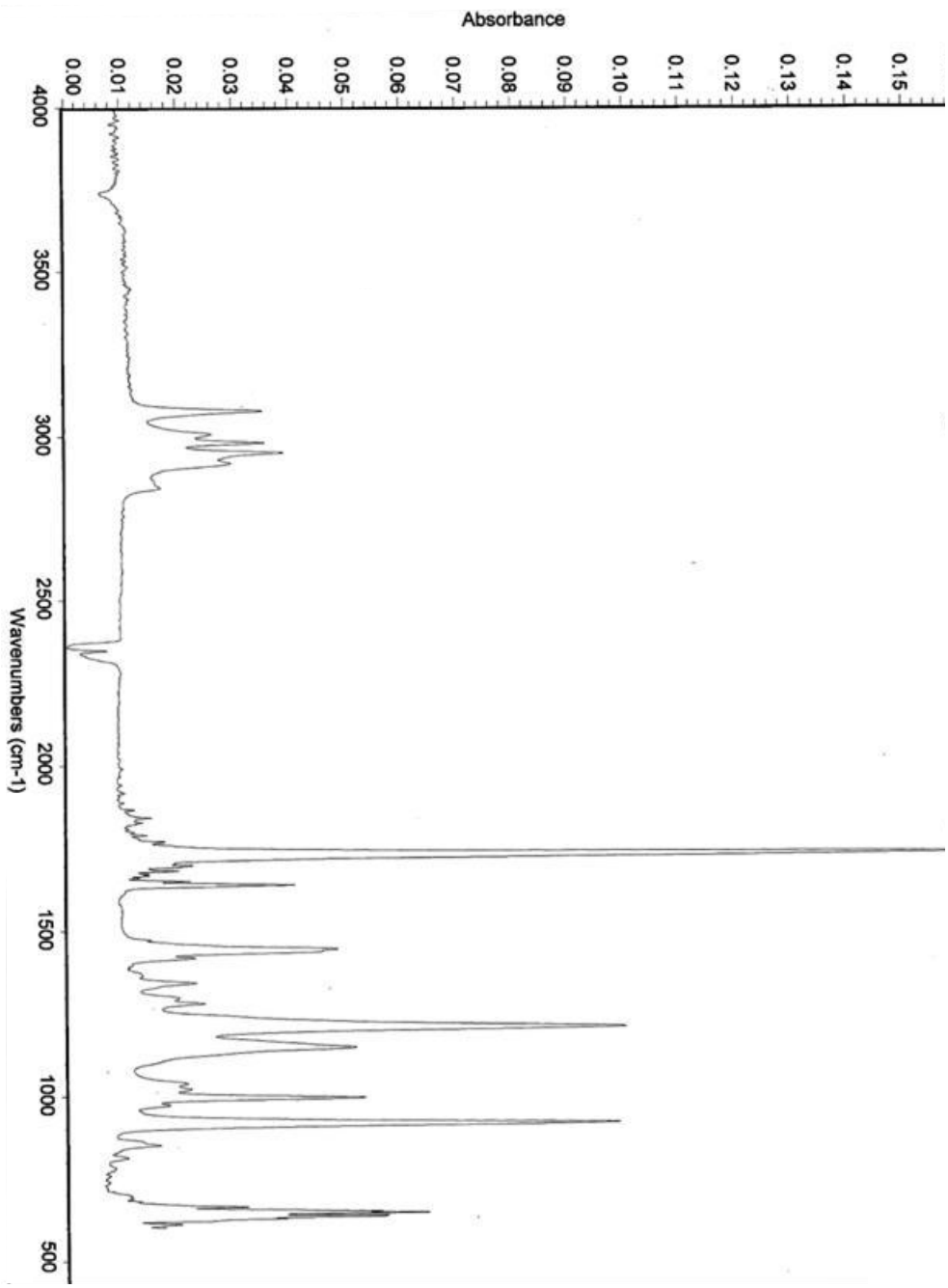

Figure A19: FTIR spectrum of triallyl methylacetate (**23**).

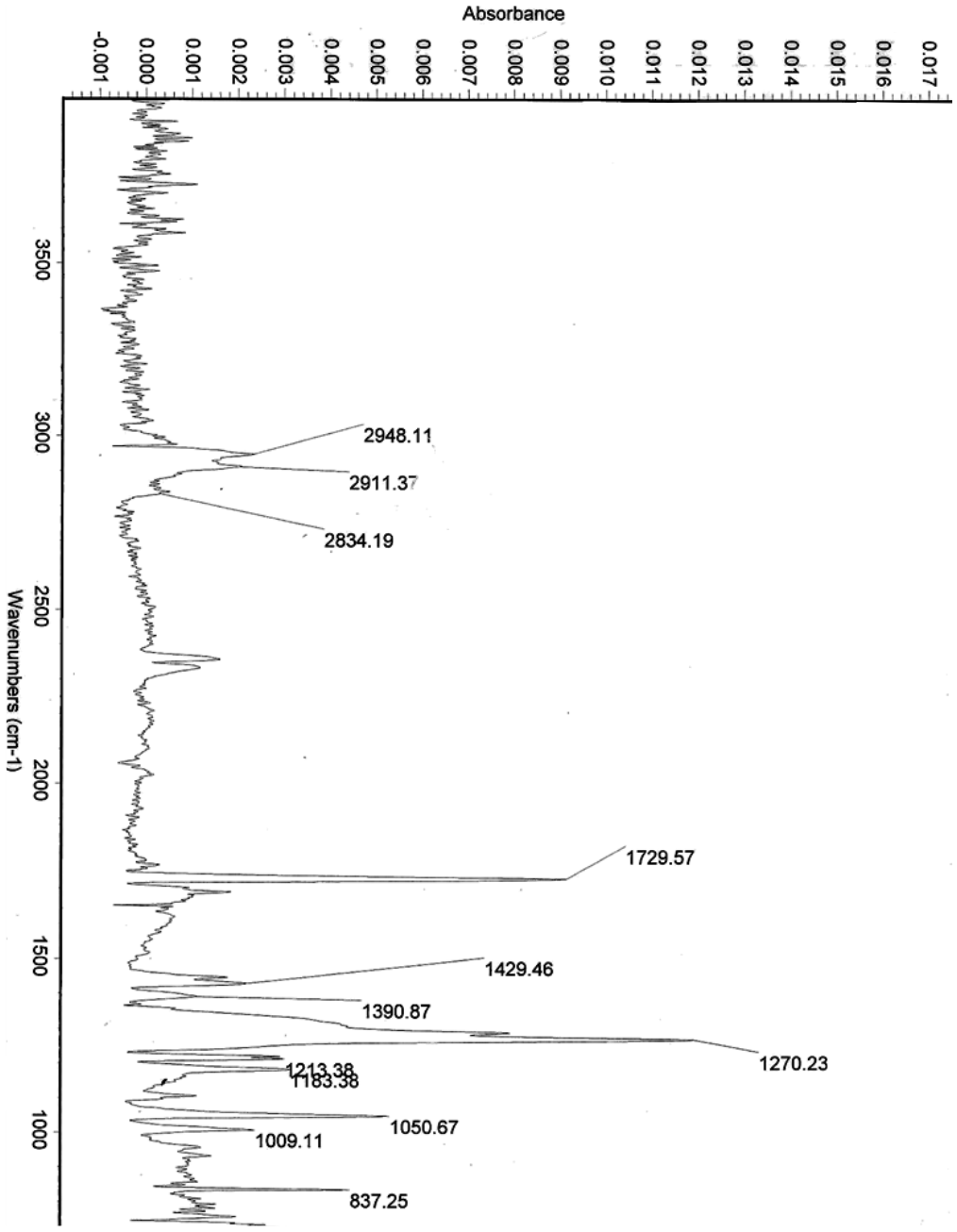

Figure A20: FTIR spectrum of methyl-2,4,9-trithiaadamantan-7-carboxylate (**17**).

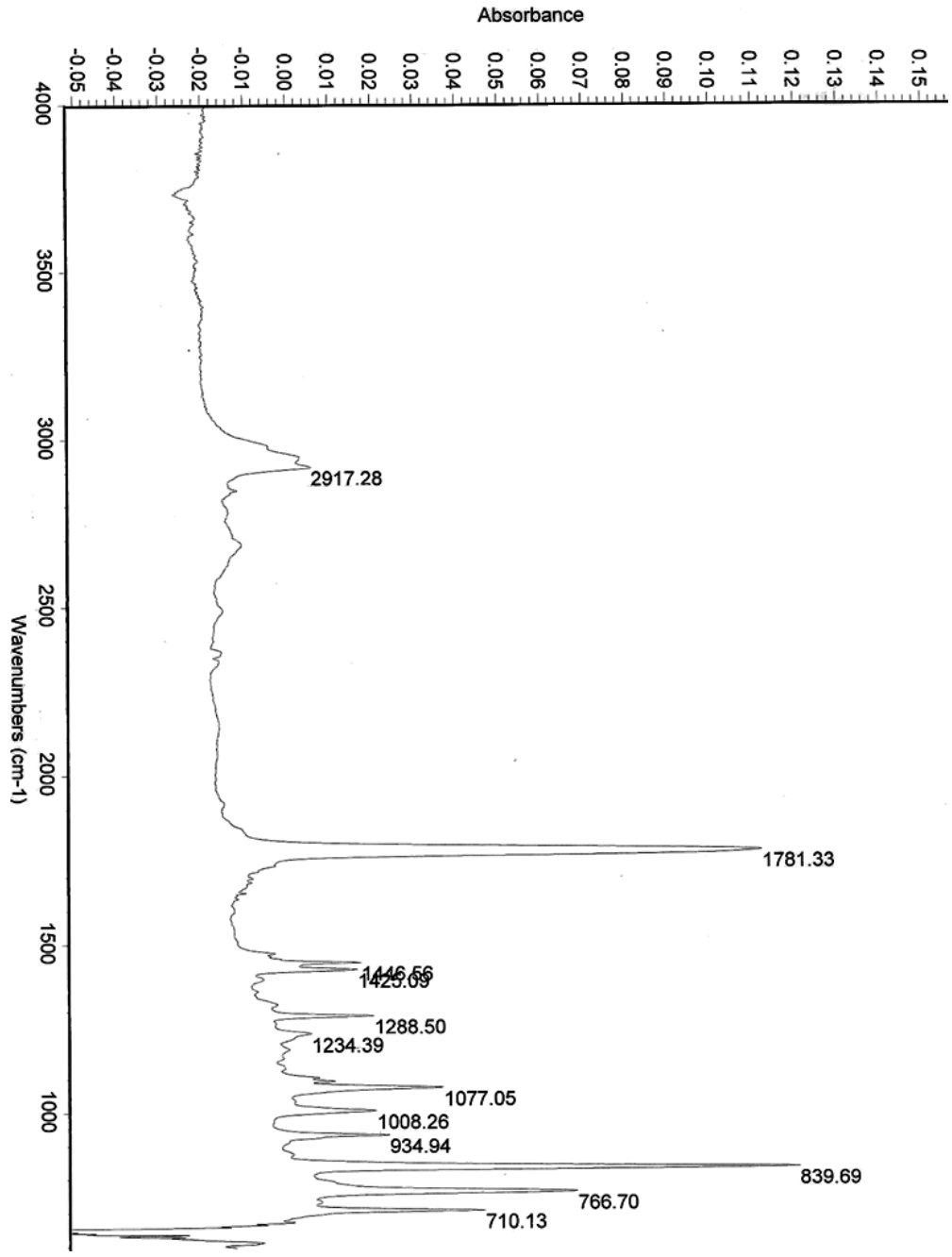

Figure A21: FTIR spectrum of 2,4,9-trithiaadamantan-7-acylchloride (**27**).

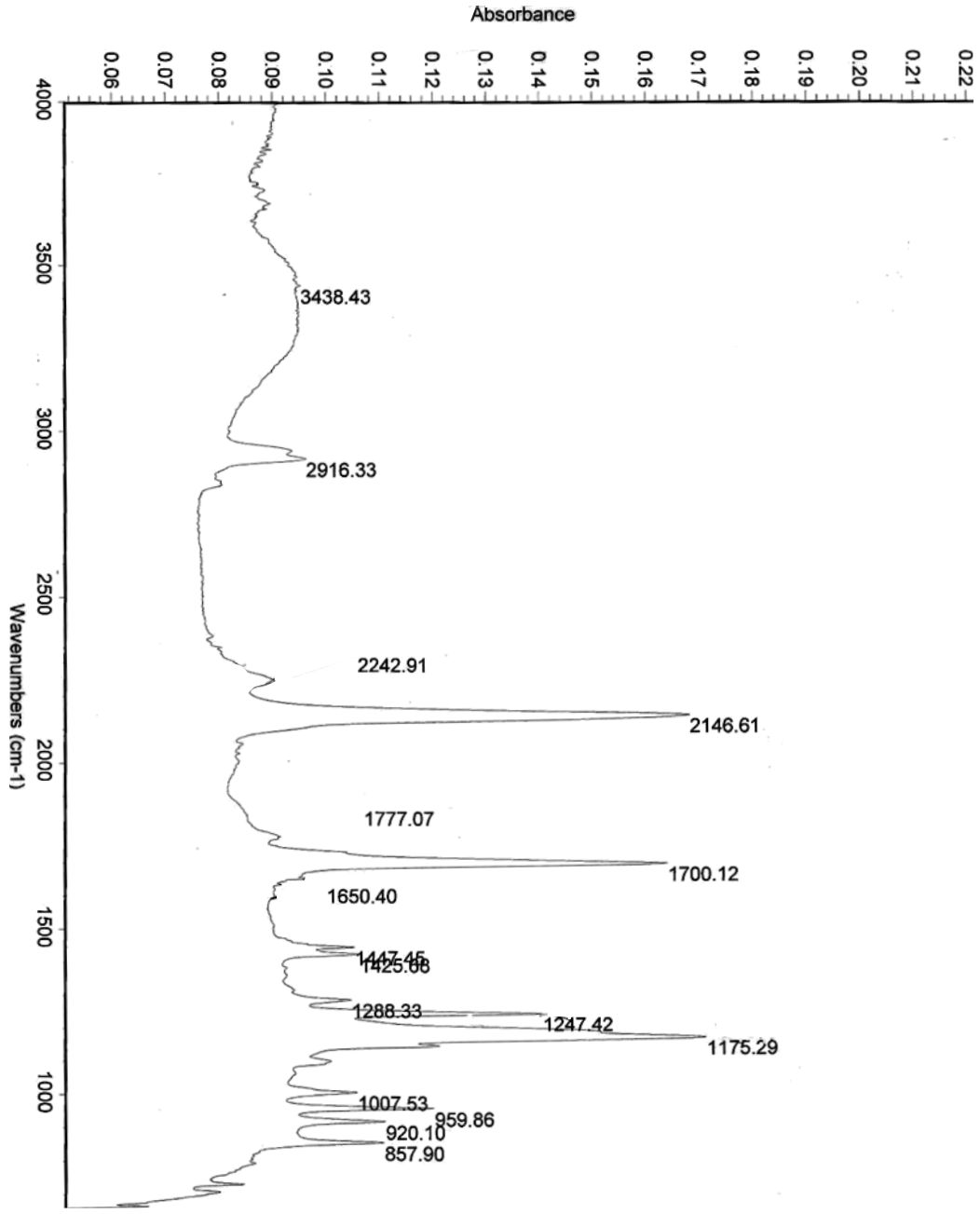

Figure A22: FTIR spectrum of 2,4,9-trithiaadamantan-7-acylchloride (**28**).

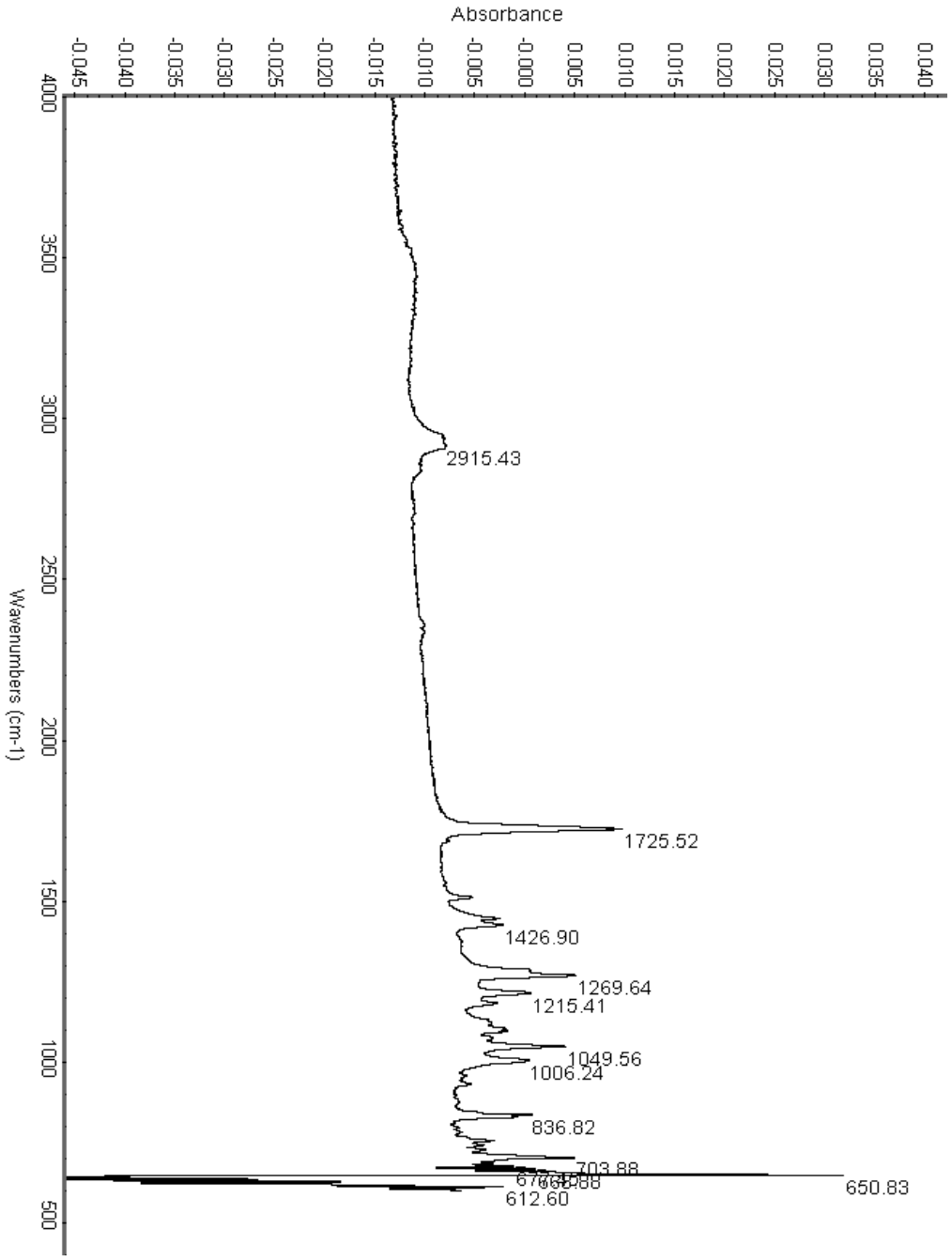

Figure A23: FTIR spectrum of 2,4,9-trithiaadamantan-7-yl-methanol (**29**).

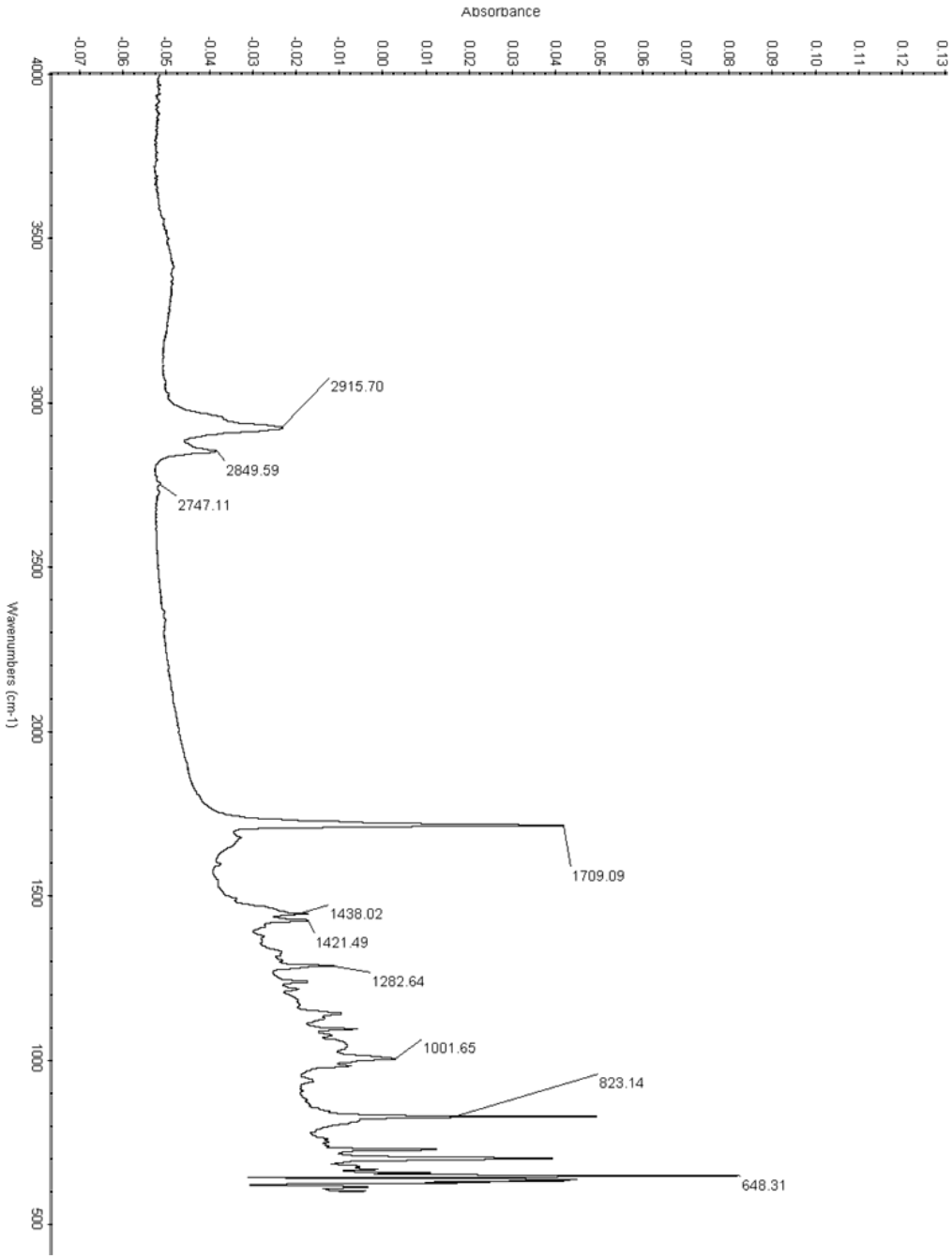

Figure A24: FTIR spectrum of 2,4,9-trithiaadamantan-7-carbaldehyde (**30**).

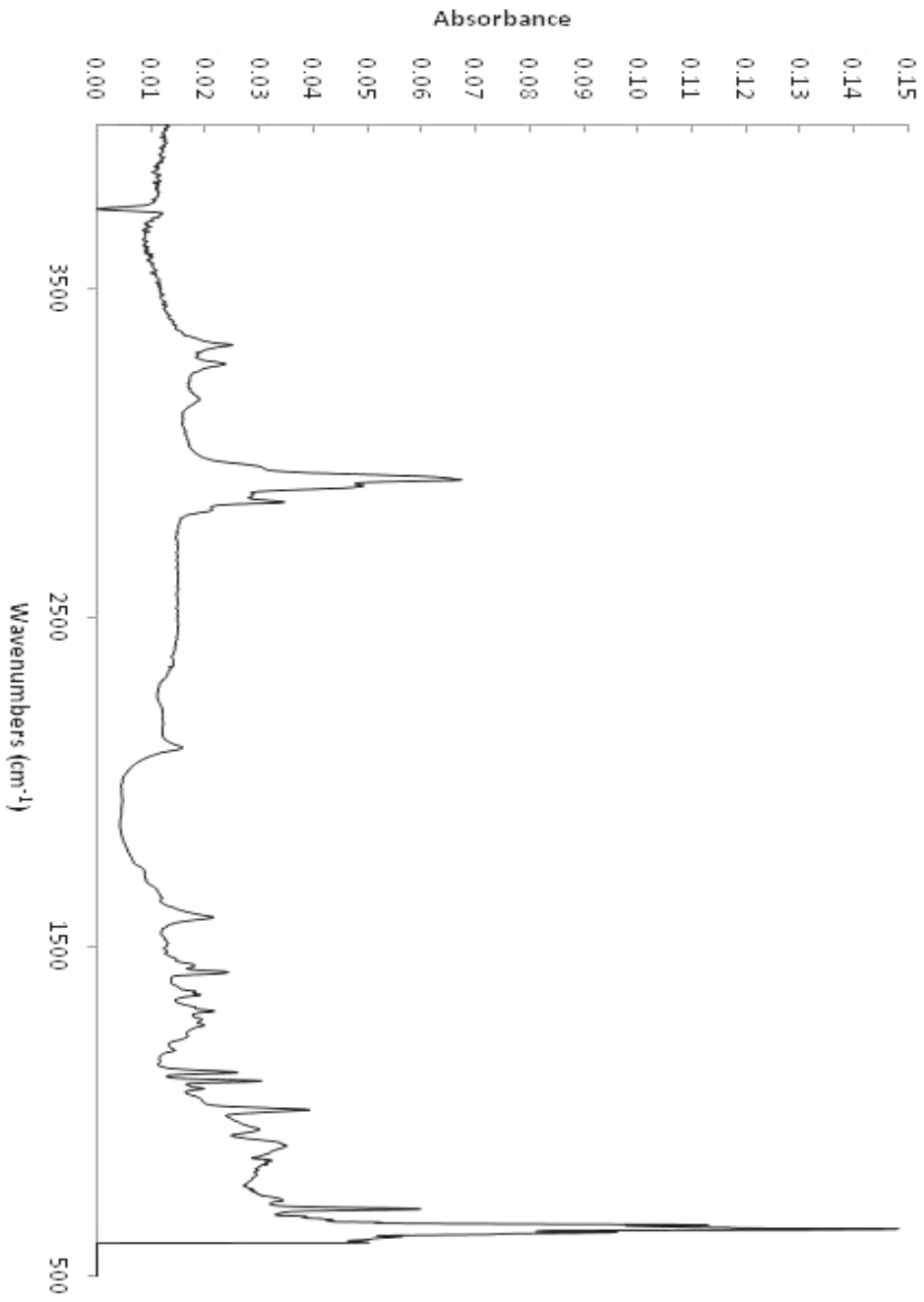

Figure A25: FTIR spectrum of 2,4,9-trithiaadamantan-7-amine (**17**).

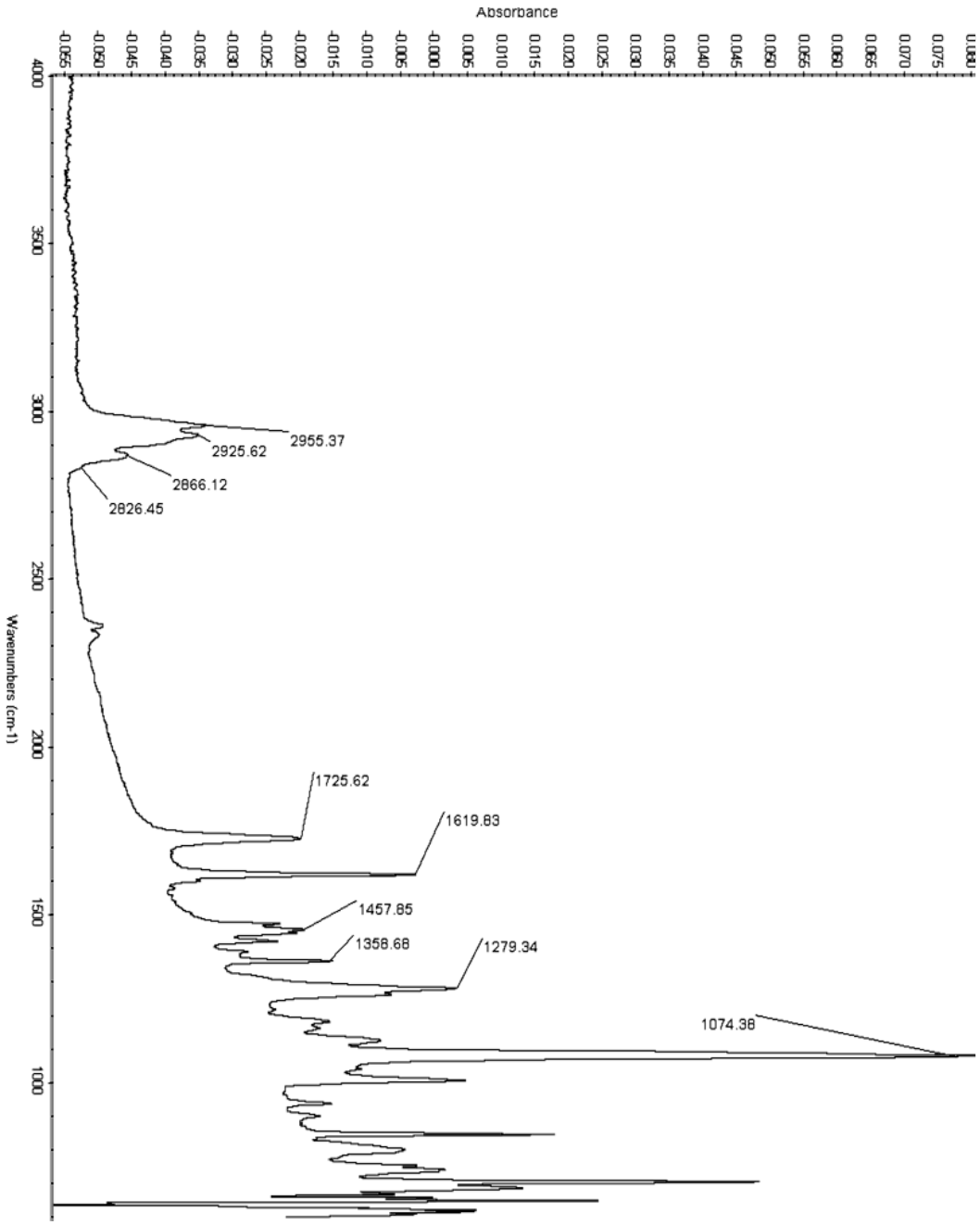

Figure A26: FTIR spectrum of tripod *tert*-butylsulfinylimine intermediate (**32**).

APPENDIX C

COPYRIGHT PERMISSIONS

Copyright Clearance Center

Print this page

Confirmation Number: 11131167
Order Date: 10/17/2013

Customer Information

Customer: Trcy Olin
Account Number: 3000708593
Organization: Trcy Olin
Email: tracy647@netzero.com
Phone: +1 (330)6470467
Payment Method: Invoice

This not an invoice

Order Details

Nature

Billing Status: **N/A**

Order detail ID: 64082785
ISSN: 0028-0836
Publication Type: Journal
Volume:
Issue:
Start page:
Publisher: Nature Publishing Group

Permission Status: Granted
Permission type: Republish or display content
Type of use: Republish in a thesis/dissertation
Order License Id: 3251401148583

Requestor type	Not-for-profit entity
Format	Print, Electronic
Portion	image/photo
Number of images/photos requested	2
Title or numeric reference of the portion (s)	Figure 4: SSNMR structure of Amt-bound M2 in lipid bilayers, Figure 5: Comparison of the high-pH...of Amt-bound M2.
Title of the article or chapter the portion is from	Structure of the amantadine binding site of influenza M2 proton channels in lipid bilayers
Editor of portion(s)	N/A
Author of portion(s)	Sarah D. Cady, et. al.
Volume of serial or monograph	463
Page range of portion	689-693
Publication date of portion	February 4, 2010
Rights for	Main product
Duration of use	Life of current edition
Creation of copies for the disabled	no
With minor editing privileges	no

For distribution to	Worldwide
In the following language(s)	Original language of publication
With incidental promotional use	no
Lifetime unit quantity of new product	0 to 499
Made available in the following markets	education, professional
The requesting person/organization	Tracy Olin
Order reference number	
Author/Editor	Tracy C. Olin
The standard identifier	not yet sure
The proposed price	0
Title	DESIGN AND SYNTHESIS OF 2,4,9-TRITHIAADAMANTANE DERIVATIVES AS ANTI-INFLUENZA A DRUG CANDIDATES
Publisher	ohiolink
Expected publication date	Dec 2013
Estimated size (pages)	150

Note: This item was invoiced separately through our **RightsLink service.** More info **$ 0.00**

Total order items: 1 **Order Total: $0.00**

Copyright Clearance Center

Print this page

Confirmation Number: 11131343
Order Date: 10/17/2013

Customer Information

Customer: Trcy Olin
Account Number: 3000708593
Organization: Trcy Olin
Email: tracy647@netzero.com
Phone: +1 (330)6470467
Payment Method: Invoice

This not an invoice

Order Details

Nature

Billing Status: **N/A**

Order detail ID: 64085694
ISSN: 0028-0836
Publication Type: Journal
Volume:
Issue:
Start page:
Publisher: Nature Publishing Group

Permission Status: Granted
Permission type: Republish or display content
Type of use: Republish in a thesis/dissertation
Order License Id: 3251570532665

Requestor type	Not-for-profit entity
Format	Electronic
Portion	image/photo
Number of images/photos requested	3
Title or numeric reference of the portion (s)	Figure 1: Structure of the M2 ion channel, Figure 3: Low pH-induced....Trp 41 gate. Figure 4: schematic illustration of M2 channel activation.
Title of the article or chapter the portion is from	Structure and mechanism of the M2 ion channel of influenza A virus
Editor of portion(s)	n/a
Author of portion(s)	Jason Schnell and James Chou
Volume of serial or monograph	451
Page range of portion	591-596
Publication date of portion	January 31, 2008
Rights for	Main product
Duration of use	Life of current edition
Creation of copies for the disabled	no
With minor editing	no

For distribution to	Worldwide
In the following language(s)	Original language of publication
With incidental promotional use	no
Lifetime unit quantity of new product	0 to 499
Made available in the following markets	education, professional
The requesting person/organization	Tracy Olin
Order reference number	
Author/Editor	Tracy Olin
The standard identifier	n/a
Title	DESIGN AND SYNTHESIS OF 2,4,9-TRITHIAADAMANTANE DERIVATIVES AS ANTI-INFLUENZA A DRUG CANDIDATES
Publisher	Ohiolink
Expected publication date	Dec 2013
Estimated size (pages)	150

Note: This item was invoiced separately through our **RightsLink service.** More info **$ 0.00**

Total order items: 1 **Order Total: $0.00**

Copyright Clearance Center

Print this page

Confirmation Number: 11147524
Order Date: 12/30/2013

Customer Information

Customer: Trcy Olin
Account Number: 3000708593
Organization: Trcy Olin
Email: tracy647@netzero.com
Phone: +1 (330)6470467
Payment Method: Invoice

This not an invoice

Order Details

Nature

Billing Status: **N/A**

Order detail ID:	64244141
ISSN:	1476-4687
Publication Type:	e-Journal
Volume:	
Issue:	
Start page:	
Publisher:	Nature Publishing Group

Permission Status: **Granted**
Permission type: Republish or display content
Type of use: Republish in a thesis/dissertation
Order License Id: 3299001066845

Requestor type	Not-for-profit entity
Format	Print, Electronic
Portion	image/photo
Number of images/photos requested	4
Title or numeric reference of the portion (s)	Figure 1: Crystal structure of the M2...from the influenza A virus, Figure 2: Asymmetric structure of the C-terminal His/Trp gate of M2TM, Figure 3: Superposition of the crystallographic tetramer....gating region of the channel, Figure 4: Minimal mechanism of activation and conductance through the channel.

Title of the article or chapter the portion is from	Structural basis for the function and inhibition of an influenza virus proton channel
Editor of portion(s)	N/A
Author of portion(s)	Amanda L. Stouffer, et al.
Volume of serial or monograph	451
Page range of portion	596-600
Publication date of portion	January 31, 2008
Rights for	Main product
Duration of use	Life of current edition
Creation of copies for the disabled	no
With minor editing privileges	no
For distribution to	Worldwide
In the following language(s)	Original language of publication
With incidental promotional use	no
Lifetime unit quantity of new product	0 to 499
Made available in the following markets	education, professional
The requesting person/organization	Tracy Olin
Order reference number	
Author/Editor	Tracy Olin
The standard identifier	not yet sure
The proposed price	0
Title	design and synthesis of 2,4,9-trithiaadamantane derivatives as anit-influenza A drug candidates
Publisher	ohiolink
Expected publication date	May 2014
Estimated size (pages)	150

Note: This item was invoiced separately through our **RightsLink service.** More info **$ 0.00**

Total order items: 1 **Order Total: $0.00**